ARPHA Preprints

PREPRINT

Author-formatted, not peer-reviewed document posted on 15/04/2025

DOI: https://doi.org/10.3897/arphapreprints.e155798

Fungal Frontiers in Toxic Terrain: Revealing Culturable Fungal Communities in Taiwan's Serpentine Paddy Fields

Kai-Wen Cheng, Jiue-in Yang, Piroonporn Srimongkol, Marc Stadler, Aphichart Karnchanatat, Hiran Ariyawansa

Fungal Frontiers in Toxic Terrain: Revealing Culturable Fungal communities in Taiwan's Serpentine Paddy Fields

Kai-Wen Cheng[1+], Jiue-in Yang[2+], Piroonporn Srimongkol[3], Marc Stadler[4] , Aphichart Karnchanatat[5, 6] and Hiran A. Ariyawansa[1, 3*]

[1] Department of Plant Pathology and Microbiology, National Taiwan University, Taiwan
[2] Department of Nematology, University of California, Riverside, USA
[3] The Institute of Biotechnology and Genetic Engineering, Chulalongkorn University, Thailand
[4] Department Microbial Drugs, Helmholtz Centre for Infection Research GmbH (HZI), Braunschweig, Germany
[5] Center of Excellence in Bioconversion and Bioseparation for Platform Chemical Production, The Institute of Biotechnology and Genetic Engineering, Chulalongkorn University, 254 Phayathai Road, Pathumwan, Bangkok, 10330, Thailand
[6] High-Value Food from Mushrooms and Bioactive Plants in the Green Economy Value Chain Research Group, The Institute of Biotechnology and Genetic Engineering, Chulalongkorn University, 254 Phayathai Road, Pathumwan, Bangkok, 10330, Thailand
[+] **contributed equally to this study**
Corresponding author: Hiran A. Ariyawansa (ariyawansa44@ntu.edu.tw)

Abstract

Serpentine soils are predominantly distributed along the Circum-Pacific margin and the Mediterranean, including eastern Taiwan. These soils are characterized by high levels of heavy metals, including nickel and chromium, and a low calcium-to-magnesium ratio, creating a unique environment that fosters microorganisms with specialized traits. In this study, culture-dependent isolation methods were used to elucidate the composition of culturable fungal communities in serpentine-characterized paddy fields in eastern Taiwan. A total of 154 fungal strains were isolated from serpentine paddy fields in eastern Taiwan. These strains were grouped into 79 morphotypes based on colony morphology and subsequently evaluated through morphological and multi-locus phylogenetic analyses. The results revealed that 60% of the strains belong to class Dothideomycetes, followed by 21% in Sordariomycetes and 19% in Eurotiomycetes. At the genus level, *Westerdykella* was the dominant genus, accounting for 35% of the total isolated strains, followed by *Pyrenochaetopsis* (20%), *Talaromyces* (19%), and *Pseudorhypophila* (8%). The study reports 11 novel species: *Dimorphiseta formosana* **sp. nov.**, *D. serpentinicola* **sp. nov.**, *Parasarocladium formosum* **sp. nov.**, *Phialoparvum formosanum* **sp. nov.**, *Poaceascoma serpentinum* **sp. nov.**, *Pseudorhypophila formosana* **sp. nov.**, *Reticulascus formosana* **sp. nov.**, *Sarocladium*

formosum **sp. nov.**, *S. serpentinicola* **sp. nov.**, *Talaromyces taiwanensis* **sp. nov.**, and *Westerdykella formosana* **sp. nov**. Additionally, 11 species are reported for the first time in Taiwan: *Pseudothielavia terricola*, *Pseudoxylomyces aquaticus*, *Pyrenochaetopsis oryzicola*, *Py. paucisetosa*, *Setophaeosphaeria microspora*, *Talaromyces adpressus*, *T. thailandensis*, *Westerdykella aquatica*, *W. capitulum*, *W. dispersa*, and *W. globosa*. In addition, this study presents the first documented asexual morph within the genus *Poaceascoma*, represented by *P. serpentinum*. These discoveries will be valuable for future evaluations of the potential uses and functions of these species as bioremediation agents.

Keywords
Heavy metal, 11-new species, phylogeny, serpentine soil, taxonomy

Introduction
Serpentinite is a metamorphic rock produced by the hydrothermal transformation of ultramafic rocks and contains serpentine minerals (Alexander 2004). Serpentine soils, despite covering only about 1% of the Earth's exposed surface, hold significant environmental and ecological importance for several reasons (Oze et al. 2008; Kumarathilaka et al. 2014). They are widespread across regions of the Circum-Pacific margin and the Mediterranean Sea (Kumarathilaka et al. 2014). Simultaneously, these environments exhibit low levels of essential plant nutrients, including calcium, potassium, nitrogen, and phosphorus (Cheng et al. 2009). Furthermore, during serpentinization (i.e., the hydration of originally anhydrous ultramafic rocks), calcium content decreases, which leads to a low calcium-to-magnesium ratio (McGahan et al. 2008; Cheng et al. 2009). Collectively, these conditions impose significant stress on most plant life. Serpentines are generally unstable types of soils (Bonifacio et al. 1997) and has the potential to release significant amounts of heavy metals, particularly chromium and nickel, into the environment during the weathering process (Hseu et al. 2015).

The toxicity caused by high concentrations of nickel and chromium in serpentinite soils, referred to as the “serpentine syndrome,” results in low productivity and high levels of floral and microbial endemism (Oze et al. 2008). Serpentine sites are ecologically significant due to their exceptionally high proportion of endemic species uniquely adapted to these extreme conditions (Daghino et al. 2012). A recent study conducted in Italy demonstrated that the fungal genera *Aspergillus*, *Penicillium*, and *Cladosporium* are dominant in serpentine soils (Daghino et al. 2012). Notably, fungal groups such as *Aspergillus* and *Penicillium*, classified within Eurotiomycetes, are frequently reported from environments with high levels of heavy metals (Gadd 2007; Roccotiello et al. 2010). Microbial communities vary according to precipitation, soil

texture, and weathering processes. For instance, it has been reported that fungal community structure differs between high and low precipitation conditions, with fungal diversity being lowest in drier environments. (Solano-Arguedas et al. 2022; Botha et al. 2024). Additionally, microbes such as fungi in serpentine environment generally exhibit stronger resistance to heavy metal, showing their adaptability to extreme conditions (Gonçalves and Martins-Loução 2009). Therefore, researchers have shown great interest in exploring the acclimation and survival strategies of microorganisms in serpentine environments, aiming to use these microbes as bioremediators for reducing heavy metal concentrations in agricultural fields (Hou et al. 2020).

In Taiwan, serpentinites and serpentine soils are mainly found in Yilan County (Nan'ao), Hualien County (Fonglin, Ruisui, Shoufeng, Wanrung, Yuli), and Taitung County (Beinan, Chishang, Donghe, Guanshan) (Liu et al. 2007; Cheng et al. 2009; Hsieh 2020). Their elevated chromium and nickel content may pose potential risks to local crops, the environment, and groundwater (Hseu and Lai 2017). The mean total Ni concentration in the serpentine fields was 472 mg/kg, significantly exceeding the natural background levels and soil control standards in Taiwan (Hseu and Lai 2017). Recent studies have repeatedly reported the remarkable diversity of mycobiota of Taiwan including the discovery of novel species (Ariyawansa et al. 2020; Chuang et al. 2024; Hsu et al. 2024). Although several studies have been carried out on the bacterial community' s structure in these soil type in Taiwan (Koner et al. 2023; Kumar et al. 2023), no comprehensive studies have focused on the culturable fungal communities in serpentine environments. Hence, the present work aimed at chraterization of the culturable fungal communities in serpentine-characterized paddy fields in eastern Taiwan using polyphasic taxonomic approach.

Materials and methods

Sample collection and fungal isolation

A total six serpentine soil sampling sites from a previous study (Hsieh 2020) were surveyed from rice fields in eastern Taiwan during November 2022, as listed in Table 1. From each site, 50 soil samples were randomly collected at depths of 5 to 15 cm. For each sample, 10 g of soil was mixed with 50 ml of sterilized water in a 50 ml centrifuge tube (LabServ®). The tubes were thoroughly vortexed and subjected to serial dilution. Finally, 10^{-4} dilution solutions were plated onto three different culture media in 9-cm Petri dishes. To obtain the various fungi with different nutrients requirements, three types of culture media: half-strength potato dextrose agar (½ PDA), half-strength malt extract agar (½ MEA), and 1.5% water agar (1.5% WA). In total, five plates were used for each type of medium (Khan et al. 2019; Latz et al. 2020). The media were prepared at half-strength concentrations to prevent the overly rapid growth of certain fungi (Su

et al. 2012). Additionally, 100 mg/L ampicillin was added to inhibit the growth of non-fungal organisms (Ellegaard-Jensen et al. 2013). Fungal mycelial growth was observed at 36 hours, and single hyphal tip isolation was performed twice using a 27G×½" needle (Terumo AGANI™). The isolated single colonies were then maintained at room temperature (25°C ± 1°C) for further studies.

Morphological examination of fungal colonies and reproductive structures

Morphological characterization was based on the colony size, colony color, the direction of fungal hyphal growth, and any changes or deformities in the color of the culture medium. PDA and 1.5 % WA supplemented with sterile carnation leaves were used to induce sporulation of selected fungal isolates (Fisher et al. 1982). Microscopic characteristics were observed under a dissecting microscope (Leica SAPO, Germany) and a compound microscope (Olympus BX51, Japan). Photographs were captured using a Leica MC190 HD camera (Leica Microsystems, Wetzlar, Germany) equipped with a microscope. Sexual and asexual stages of fungal isolates observed in culture were imaged using differential interference contrast and measured using cellSense Standard software (Olympus).

DNA extraction, PCR amplification and sequencing

Genomic DNA was extracted from the 7- to 10-day-old mycelium using the EasyPure Genomic DNA Spin kit (Bioman Scientific Co., LTD., Taiwan) following the manufacturer's protocol. PCR amplification was performed in 25 µl reaction mixture containing 12.5 µl of 2X Taq PCR Mix-RED (Bioman Scientific Co., LTD., Taiwan), 9.5 µl of dH_2O, 1 µl of each forward and reverse primer, and 1 µl of fungal DNA template. PCR reactions for amplification of each locus along with their respective primer pairs, are listed in Table 2. The PCR products were examined on 1 % agarose electrophoresis gel stained with BioGreen™ Safe DNA Gel buffer (Bioman Scientific Co., LTD., Taiwan). Purification and sequencing were performed at Genomics Inc (New Taipei City, Taiwan) by Sanger sequencing technology.

Strain selection and Phylogenetic analyses

NCBI BLASTn was initially used to identify the closest matches per each strain, using ITS region to determine the family/genus level classification. Based on the BLASTn results, additional loci were sequenced, as listed in Table 2. Furthermore, for each strain, additional related sequences and DNA sequences from ex-type and additional verified strains were retrieved according to their genus by following recently published research articles. Key references and GenBank accession numbers for each locus are detailed in Table X. The multiple Sequence alignments were obtained using MAFFT version 7

(https://mafft.cbrc.jp/alignment/server/) and manually adjusted in MEGA version 7 (Tsai et al. 2021). To understand the evolutionary relationships of the isolates obtained in this study, phylogenetic analyses were performed using maximum likelihood (ML) for both individual and multi-locus datasets and Bayesian inference (BI) for multi-locus analyses. ML analysis with 1000 bootstraps was conducted using W-IQ-TREE (http://iqtree.cibiv.univie.ac.at/) (Trifinopoulos et al. 2016). For BI, the best evolutionary model for each partition determined using MrModeltest version 2.3 (Nylander 2004), and details were provided in supplementary Table S1. Bayesian phylogenetic trees were generated using MrBayes version 3.2.7 (Ronquist et al. 2012). The Bayesian analysis ran for ten million generations in total, automatically stopping once the mean standard deviation of split frequencies dropped below 0.01. Tree samples were recorded at intervals of one thousand generations. The MCMC heated chain was configured at a temperature of 0.15. To confirm when each run reached stationarity and evaluate the need for additional runs, the distribution of log-likelihood values was examined in Tracer v1.5 (http://beast.community/tracer). ML bootstrap values (MLB) of 70% or higher and Bayesian posterior probabilities (BPPs) of 0.95 or higher were provided at each node, whereas nodes with bootstrap values below 70% or BPPs below 0.95 were considered unresolved. FigTree v. 1.4.0 (http://tree.bio.ed.ac.uk/software/figtree/) was used to visualize the resulting phylogenetic trees and modified by using Adobe Illustrator v. 2021.

Table 1. Details of the Sampling locations.

Sample name	Location	GPS coordination
SR1	Wanrung Township, Hualien County	23°42'40.3"N, 121°24'48.2"E
SR2	Wanrung Township, Hualien County	23°42'41.2"N, 121°24'41.8"E
SR3	Guanshan Township, Taitung County	23°02'18.2"N, 121°11'25.0"E
SR4	Guanshan Township, Taitung County	23°02'17.6"N, 121°11'26.3"E
SR5	Guanshan Township, Taitung County	23°02'14.8"N, 121°11'22.6"E
SR6	Guanshan Township, Taitung County	23°02'12.8"N, 121°11'22.0"E

Table 2. List of primers used in this study.

Region	Primer pairs	Sequence (5' to 3')	References
LSU	LROR	ACCCGCTGAACTTAAGC	Vilgalys and Hester 1990;
	LR5	TCCTGAGGGAAACTTCG	Rehner and Samuels 1994
tef-1	EF1-983F	GCYCCYGGHCAYCGTGAYTTYAT	Rehner and Buckley 2005

	EF1-2218R	ATGACACCRACRGCRACRGTYTG	Rehner and Buckley 2005
rpb2	RPB2-5f	GAYGAYMGWGATCAYTTYGG	Liu et al. 1999
	RPB2-7cR	CCCATRGCTTGYTTRCCCAT	Liu et al. 1999
SSU	NS1	GTAGTCATATGCTTGTCTC	White et al. 1990
	NS4	CTTCCGTCAATTCCTTTAAG	White et al. 1990
ITS	ITS1	TCCGTAGGTGAACCTGCGG	White et al. 1990
	ITS 4	TCCTCCGCTTATTGATATGC	White et al. 1990
tub2	BT1819R	TTCCGTCCCGACAACTTCGT	Miller and Hundorf 2005
	BT2916	CTCAGCCTCAGTGAACTCCAT	Miller and Hundorf 2005
	Bt2a	GGTAACCAAATCGGTGCTGCTTTC	Glass and Donaldson 1995
	Bt2b	ACCCTCAGTGTAGTGACCCTTGGC	Glass and Donaldson 1995
	TUB2Fd	GTBCACCTYCARACCGGYCARTG	Woudenberg et al. 2009
	TUB4Rd	CCRGAYTGRCCRAARACRAAGTTGTC	Woudenberg et al. 2009
***cmd*A**	CAL-228F	GAGTTCAAGGAGGCCTTCTCCC	Carbone and Kohn 1999
	CAL2Rd	TGRTCNGCCTCDCGGATCATCTC	Groenewald et al. 2013
	CMD5	CCGAGTACAAGGAGGCCTTC	Hong et al. 2006
	CMD6	CCGATAGAGGTCATAACGTGG	Hong et al. 2006

Large subunit ribosomal RNA (LSU); translation elongation factor 1-alpha (*tef*-1); small subunit ribosomal RNA (SSU); ribosomal internal transcribed spacer (ITS); RNA polymerase II second largest subunit (*rpb2*); *β-tubulin* (*tub2*); calmodulin (*cmd*A)

Results

The fungal communities of serpentine soils in Taiwan

Using the soil suspension-plating method on ½ PDA, ½ MEA, and 1.5% water agar, a total of 154 fungal strains were isolated. These strains were grouped into 79 morphotypes based on colony morphology, then identified through molecular methods. Among the three media, ½ PDA yielded the highest number of isolates. All strains identified in this study were classified in Ascomycota, with 60% categorized in Dothideomycetes, 21% in Sordariomycetes, and 19% in Eurotiomycetes. *Westerdykella* was identified as the most abundant fungal genus accounting for 35% of the total strains, followed by *Pyrenochaetopsis* (20%), *Talaromyces* (19%), and *Pseudorhypophila* (8%). In addition to these main genera, the study also identified several other fungal genera, including, *Dimorphiseta*, *Parasarocladium*, *Phialoparvum*, *Poaceascoma*, *Pseudothielavia*, *Pseudoxylomyces*, *Reticulascus*, *Sarocladium*, and *Setophaeosphaeria.*

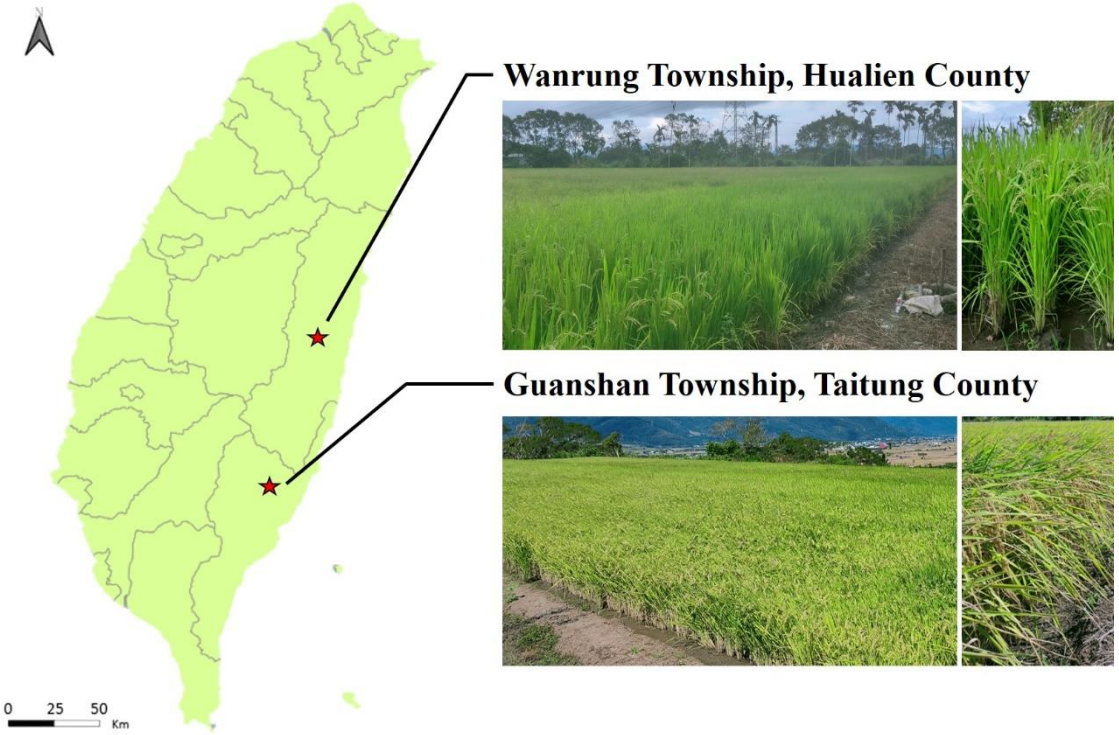

Figure 1. Sampling site location.

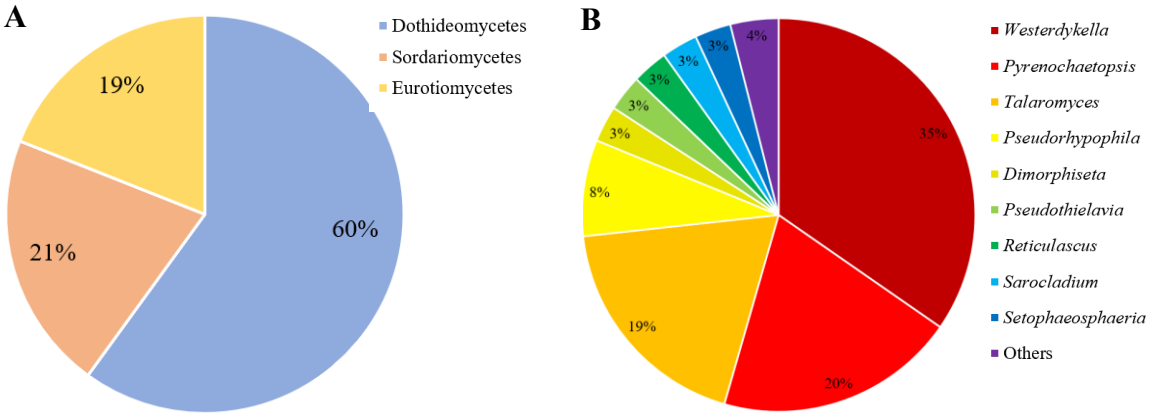

Figure 2. Fungal communities in six serpentine paddy soil samples (A) relative abundance at class level (B) relative abundance at genus level.

Taxonomy

The phylogenetic placement and comprehensive descriptions of all novel species, as well as new records of fungal genera in Taiwan or in serpentine environments, are provided below.

Dothideomycetes

Dothideomycetes strains (48) identified in this study classified into one order, five families, five genera, and 10 species.

Poaceascoma

The genus *Poaceascoma*, first introduced by Phookamsak and Hyde (2015) in Phookamsak et al. (2015), as saprobic fungal group on Poaceae and *P.helicoides* was designated as the generic type of the genus. Currently, 14 species are recognized in MycoBank (Accession date: February 15, 2025) for *Poaceascoma*. *Poaceascoma* species are usually characterized by semi-immersed to erumpent, globose to subglobose ascomata with short to long papillae, often surrounded by a turf-like structure (Phookamsak et al. 2015). Ascus fissitunicate, bitunicate, elongate-cylindrical usually contain eight filiform, hyaline, multi-septate ascospores. *Poaceascoma* species mainly reported from Thailand but recently also have been recorded from Australia, China, Hungary, and Taiwan (Hyde et al. 2018; Imrefi et al. 2024). These species are mainly reported from dead stems or roots of herbaceous plants (Poaceae) or submerged wood in freshwater ecosystems (Phookamsak et al. 2015; Luo et al. 2016; Crous et al. 2020; Boonmee et al. 2021; Zang et al. 2023).

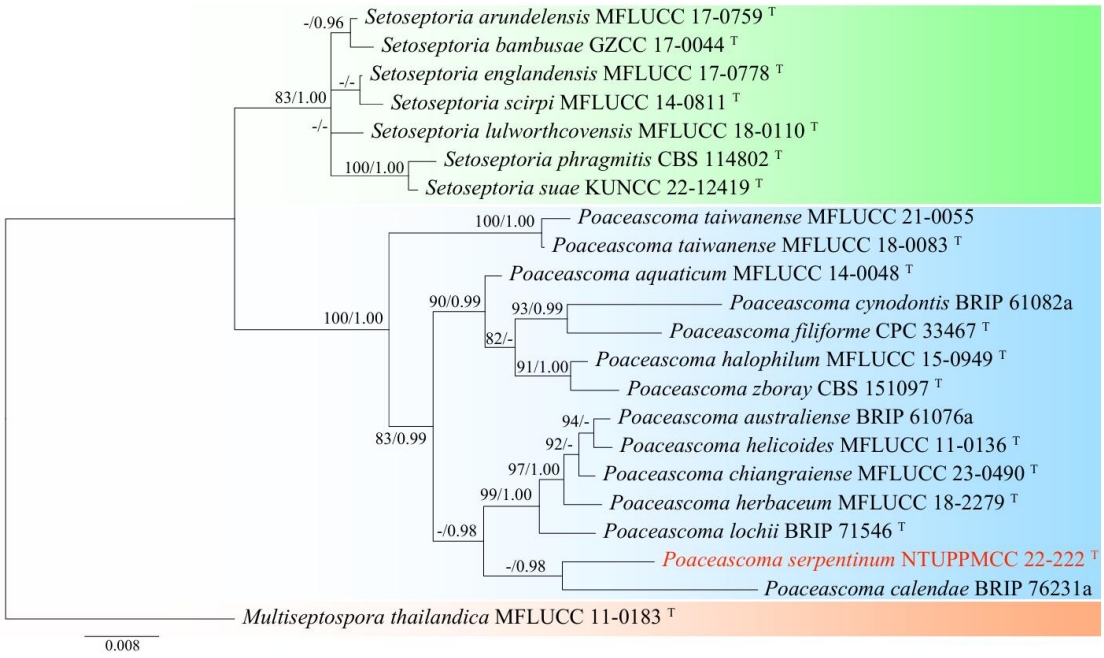

Figure 3. Maximum-likelihood phylogenetic tree based on concatenated sequences of ITS, LSU, SSU, and *tef-1* for the genus *Poaceascoma*. The tree was rooted with *Multiseptospora thailandica* MFLUCC 11-0813. MLB ≥ 70% and BPPs ≥ 0.95 were shown at each node; values lower than these thresholds are indicated by a hyphen (–). The scale bar indicates the number of estimated substitutions per site. The new strain is shown in red. The type strains are marked with ^{T}.

Poaceascoma serpentinum K.W. Cheng & H.A. Ariyawansa, sp. nov.

MycoBank: MB858705

Typification: Guanshan Township, Taitung County, Taiwan, 23°02'17.6"N, 121°11'26.3"E, serpentine soil in rice field, 3rd November 2022, K.W. Cheng, holotype, NTUPPMH 22-216 (Permanently preserved in a metabolically inactive state), ex-holotype NTUPPMCC 22-222.

Etymology: Named after the serpentine soil from which the species was isolated.

Description: On carnation leaves (*Dianthus caryophyllus*) supplanted on WA (NTUPPMCC 22-222). *Sexual morph*: undetermined. *Asexual morph*: Sporulation difficult on PDA and MEA, conidia produced on carnation leaves and on the surface or submerged in WA after 10 days. *Conidia* smooth-walled, 3–4-distoseptate, ellipsoid to oblong, occasionally slightly curved, pale brown to subhyaline when immature, dark brown when mature. Aggregated in varying sizes, 12–15.7 µm × 31.3–48.6 µm ($\bar{x}$=14 × 37.8 µm, L/W ratio=2.72, n=30) (Fig. 4C–G).

Culture characteristics: NTUPPMCC 22-222 on PDA medium exhibit slow growth, reaching 35 mm diam after 14 days at 25°C, with pale gray, fluffy to floccose surface and smooth margins. Reverse side of the colony showed a central brownish color that gradually fades into a lighter beige ring toward the edges (Fig. 4A–B).

Notes: This study describes *Poaceascoma serpentinum* as a novel fungal species based on a single strain isolated from serpentine soil. While it is ideal to examine multiple strains when introducing a new species, isolating additional strains of this fungus proved challenging, likely due to its ecological niche and low abundance in the sampled environment. However, the species is well-supported as distinct based on comprehensive morphological and phylogenetic evidence (Fig. 3). Phylogenetic analysis across multiple loci clearly separates *P. serpentinum* from its closest relatives, *P. calendae* (BRIP 76231a) with significant genetic divergence in ITS sequences (identities = 418/472, 88.6% including gaps). Previously, species in this genus have been described solely based on their sexual stage, with no documented asexual stage (Zang et al. 2023). However, in the present study, we observed only the asexual stage of NTUPPMCC 22-222 but did not observe any sexual stage of the fungus even when carnation leaves were used as the substrate. As a result, morphological comparisons between NTUPPMCC 22-222 and its closely related species are not possible. While this study establishes *P. serpentinum* as a distinct species, future studies should aim to recover additional isolates from similar environments to further validate its phenotypic variation and ecological distribution. Notably, this study is also the first to document the asexual morphology of a *Poaceascoma* species.

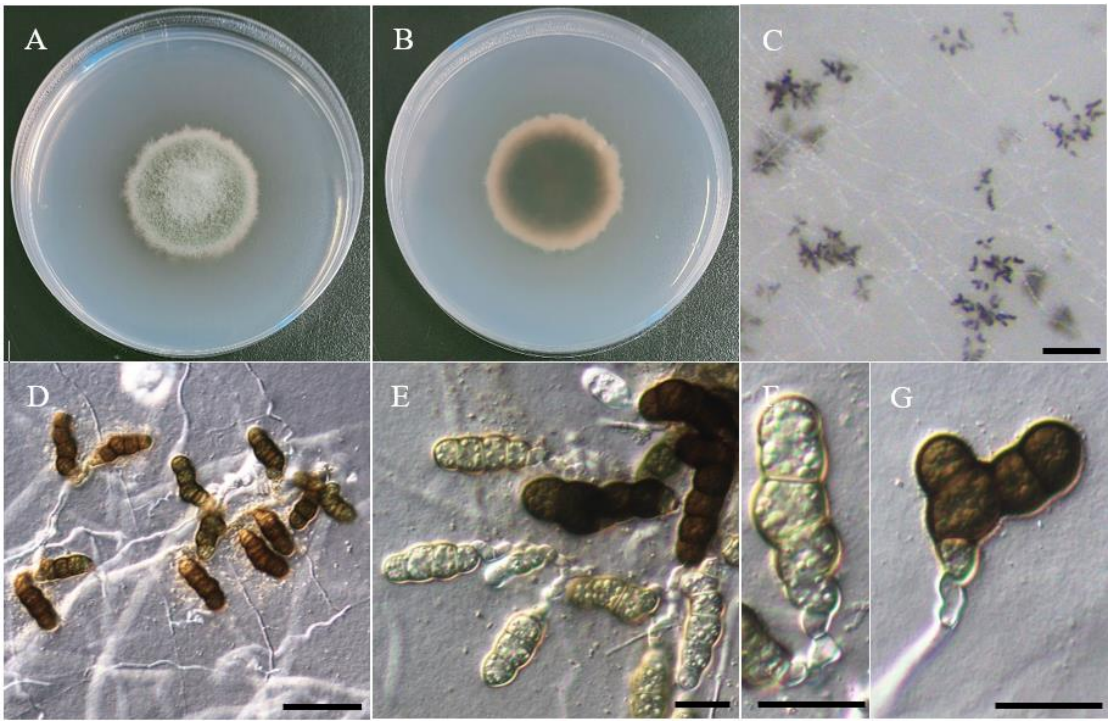

Figure 4. Morphology of *Poaceascoma serpentinum* NTUPPMCC 22-222 (A)(B) 14-days-old colony on PDA (C–G) Immature and mature conidia. Scale bars: C = 0.2 mm; D = 50 µm; E–G = 20 µm.

Pseudoxylomyces

The genus *Pseudoxylomyces* was introduced by Tanaka and Hiray (2015) as a saprobic species in habitat on submerged wood and typified with *P. elegans* (Goh et al. 1997; Tanaka et al. 2015). Currently, only two species are recognized in MycoBank (Accession date: February 15, 2025) for *Pseudoxylomyces*. However, this group has a wide distribution and has been reported from Australia, Brazil, Hong Kong, India, Japan, Seychelles, Thailand and USA (Dong et al. 2020). The majority of the isolates reported for this genus were derived from the submerged wood in aquatic environment (Dong et al. 2020).

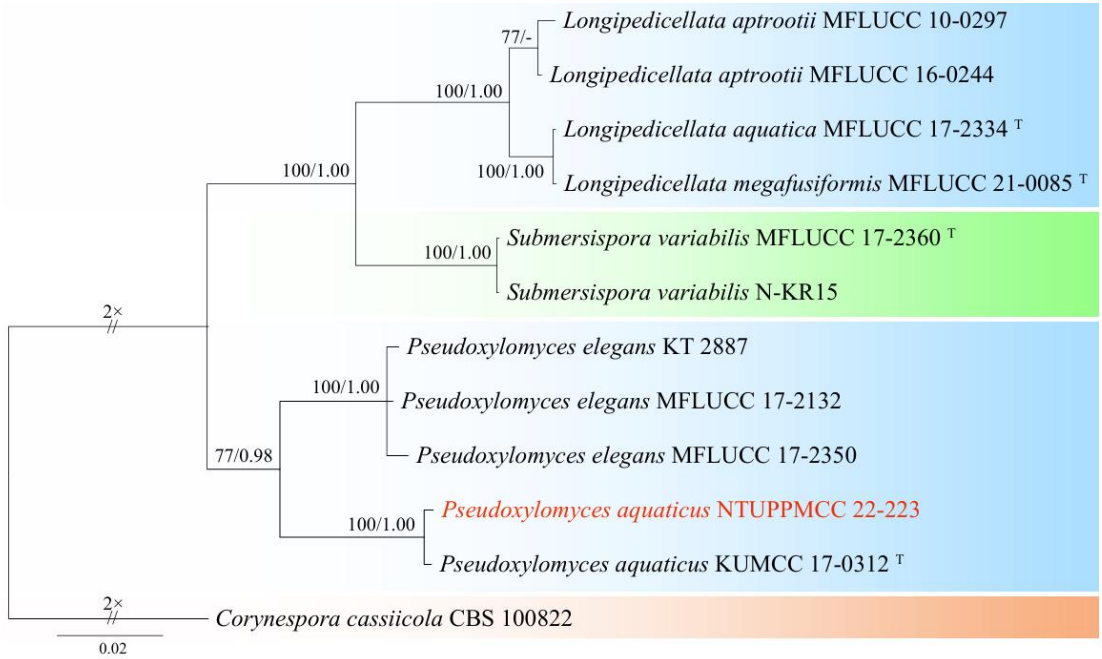

Figure 5. Maximum-likelihood phylogenetic tree based on concatenated sequences of ITS, LSU, SSU, and *tef-1* for the genus *Pseudoxylomyces*. The tree was rooted with *Corynespora cassiicola* CBS 100822. MLB ≥ 70% and BPPs ≥ 0.95 were shown at each node; values lower than these thresholds are indicated by a hyphen (–). The scale bar indicates the number of estimated substitutions per site. The new strain is shown in red. The type strains are marked with ^{T}.

Pseudoxylomyces aquaticus W. Dong, H. Zhang & K.D. Hyde (2020)

MycoBank: MB557916

Description: On carnation leaves (*Dianthus caryophyllus*) supplanted on WA (NTUPPMCC 22-223). *Sexual morph*: undetermined. *Asexual morph*: *Conidiophores* short (7–13.5 µm) or absent. *Conidiogenesis* holoblastic. *Conidia* solitary, pale brown to brown, broadly fusiform, most 5 thick and obvious septa (few 2–4 septa), rough, thick-walled, 37.6–50 µm × 11.8–17 µm ($\bar{x}$=44 x 14.5 µm, L/W ratio=3.05, n=20) (Fig. 6C–F).

Culture characteristics: NTUPPMCC 22-223 on PDA medium reaching 30 mm diam after 14 days at 25°C, with dark grayish-brown in the center, pale brown to gray in margin, velvety, rough surface, entire edge, and similar to reverse side of the colony (Fig. 6A–B).

Material examined: Wanrung Township, Hualien County, Taiwan, 23°42'40.3"N, 121°24'48.2"E, serpentine soil in rice field, 2nd November 2022, K.W. Cheng, living culture NTUPPMCC 22-223.

Notes: *Pseudoxylomyces* aquaticus was previously documented on submerged wood in Thailand. Our study recovered a single isolate (NTUPPMCC 22-223) that

clustered in a strongly supported clade with the ex-type strain (KUMCC 17-0312) established by Dong et al. (2020), confirming its identity as *P. aquaticus* (Fig. 5). In addition, this is the first discovery of the *Pseudoxylomyces* species in Taiwan.

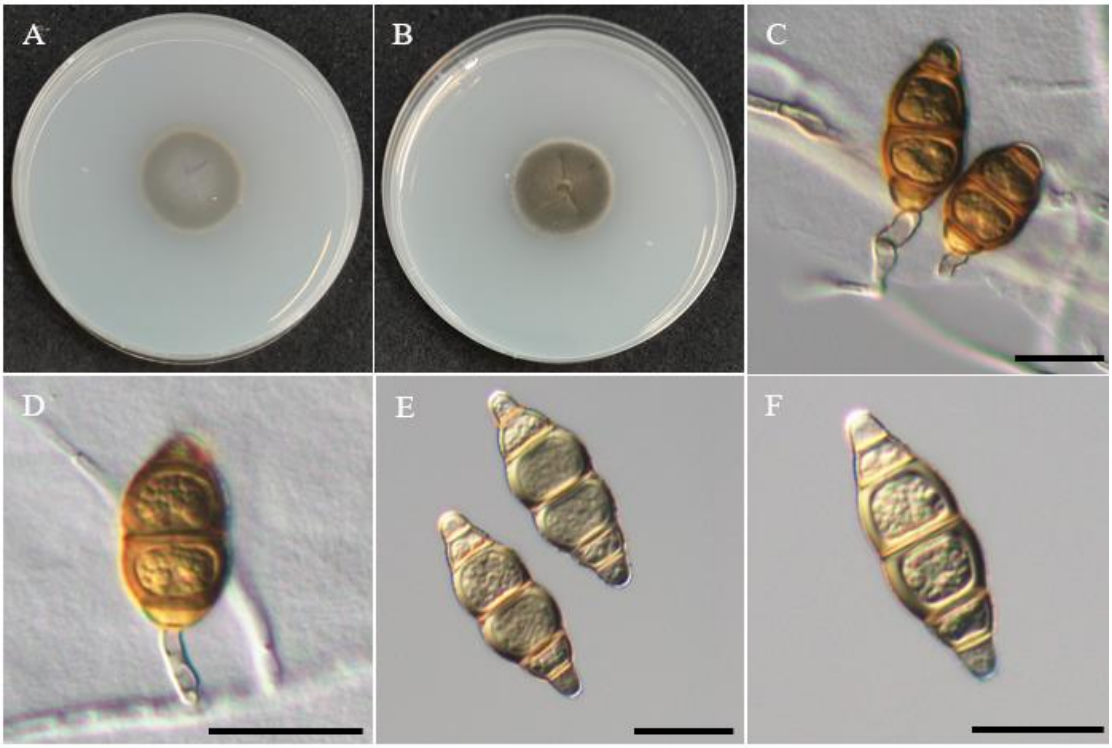

Figure 6. Morphology of *Pseudoxylomyces aquaticus* NTUPPMCC 22-223 (A)(B) 14-days-old colony on PDA (C)(D) Immature conidia and conidiophores (E)(F) Conidia. Scale bars: C–F = 20 µm.

Pyrenochaetopsis

The genus *Pyrenochaetopsis* was introduced by de Gruyter et al. (2010), as a saprobic species on Poaceae and typified with *P. leptospora*. Currently, 27 species are recognized in MycoBank (Accession date: February 15, 2025) for *Pyrenochaetopsis*. These species are widely distributed around the world and can be found in diverse ecological niches, functioning as saprobes, endophytes, or pathogens (de Gruyter et al. 2010; Surono et al. 2023). However, most of the species are associated with plant debris, soil, or dung some have also been discovered on opportunistic infections in nematode cysts or human tissues (Valenzuela-Lopez et al. 2018).

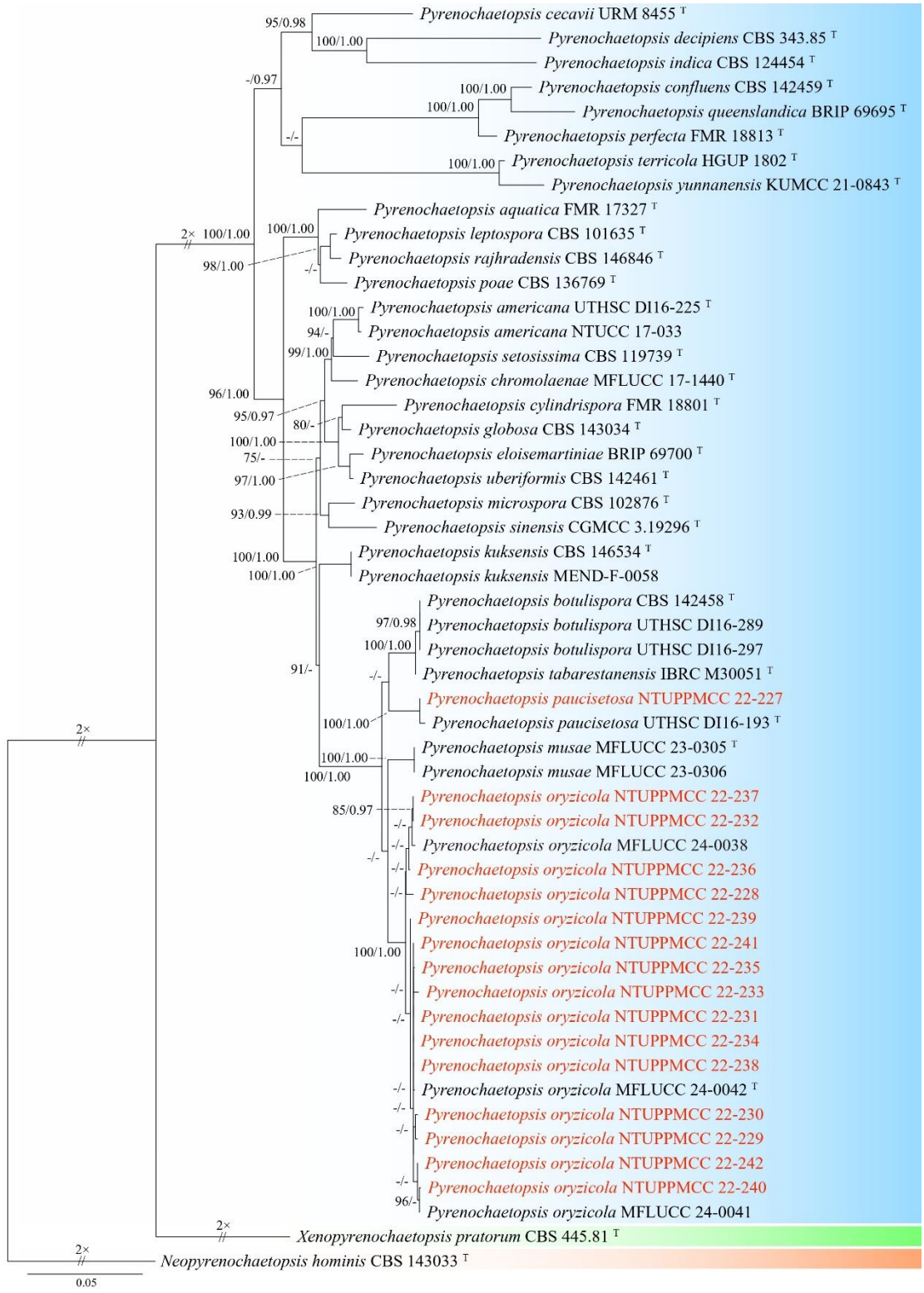

Figure 7. Maximum-likelihood phylogenetic tree based on concatenated sequences of ITS, LSU, *rpb2*, and *tub2* for the genus *Pyrenochaetopsis*. The tree was rooted with *Neopyrenochaetopsis hominis* CBS 143033. MLB ≥ 70% and BPPs ≥ 0.95 were shown at each node; values lower than these thresholds are indicated by a hyphen (–). The

scale bar indicates the number of estimated substitutions per site. The new strains are shown in red. The type strains are marked with ^{T}.

Pyrenochaetopsis paucisetosa N. Valenzuela-Lopez, J.F. Cano, J. Guarro, and A.M. Stchigel (2018)

MycoBank: MB819766

Description: On carnation leaves (*Dianthus caryophyllus*) supplanted on WA (NTUPPMCC 22-227). *Sexual morph*: undetermined. *Asexual morph*: *Conidiomata* 128–219 µm, pycnidial, globose to subglobose, dark brown, ostiolate, superficial on WA and carnation leaves, with dark brown, septate setae. *Pycnidial wall* composed of *textura angularis*, septate setae, brown, pseudoparenchymatous cells. *Conidiogenous cells* hyaline, phialidic, smooth-walled, 3.6–5.0 µm × 2.9–4.1 µm ($\bar{x}$=4.1 × 3.5 µm, n=30). *Conidia* hyaline, cylindrical to ellipsoidal, aseptate, with 2 small guttules, 3.7–4.7 µm × 1.5–2.1 µm ($\bar{x}$=4.2 × 1.8 µm, L/W ratio=2.4, n=30) (Fig. 8C–H).

Culture characteristics: NTUPPMCC 22-227 on PDA medium expanded slowly, reaching 28 mm diam after 14 days at 25°C, with pale gray, floccose surface, smooth margins, and medium-gray on the reverse side of the colony (Fig. 8A–B).

Material examined: Wanrung Township, Hualien County, Taiwan, 23°42'41.2"N, 121°24'41.8"E, serpentine soil in rice field, 2nd November 2022, K.W Cheng, living culture NTUPPMCC 22-227.

Notes: In the present study, strain NTUPPMCC 22-227 identified as *Pyrenochaetopsis paucisetosa,* clustering in the same clade with the type strain of *P. paucisetosa* (UTHSC DI16-193) in both single and multi-gene phylogeny analysis (Valenzuela-Lopez et al. 2018), thus verifying the identification of the studied species (Fig. 7). Previous reports indicate that *P. paucisetosa* has been isolated from a human toe nail in USA (Valenzuela-Lopez et al. 2018) and from freshwater sediment in Korea (Goh et al. 2020). The culture characteristics of NTUPPMCC 22-227 on PDA were similar to those of the ex-holotype of *P. paucisetosa* (UTHSC DI16-193). However, the conidia of *P. paucisetosa* NTUPPMCC 22-227 in our study were more elongated than previous reports ($\bar{x}$=4.2 × 1.8 µm versus 3–4 × 2–2.5 µm; 3.6 × 1.9 µm) (Valenzuela-Lopez et al. 2018; Goh et al. 2020). Furthermore, this is the first record of *P. paucisetosa* in Taiwan, as well as its first occurrence in paddy field soil.

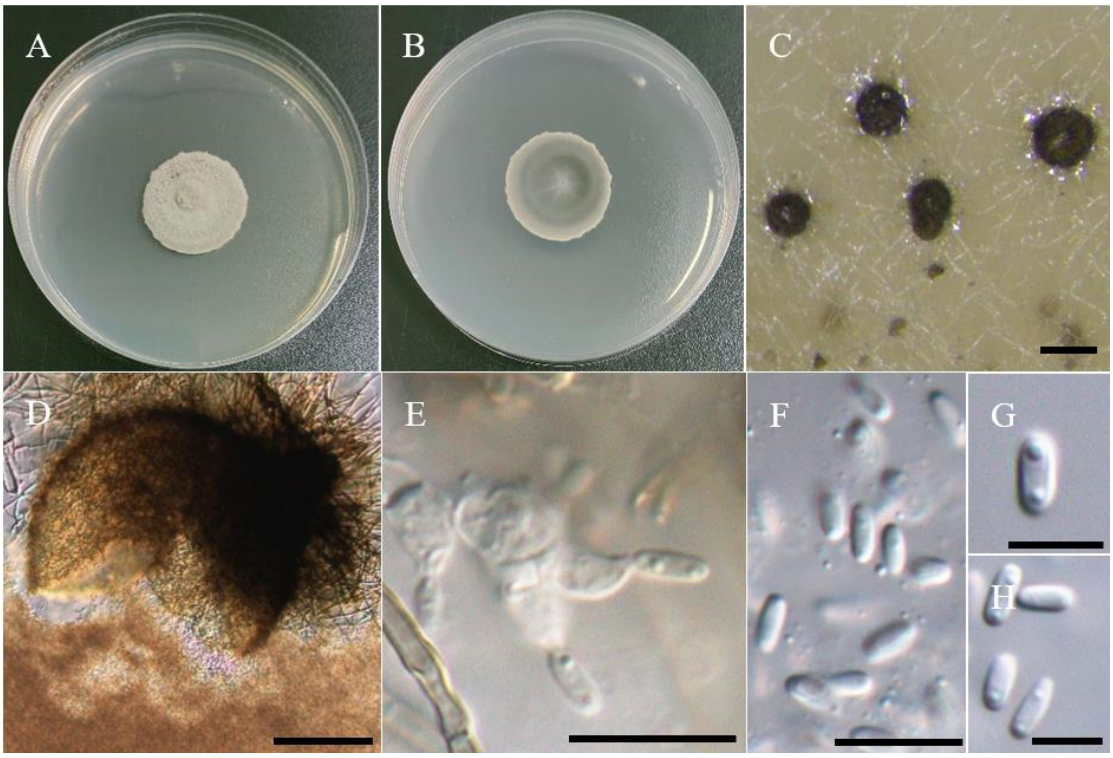

Figure 8. Morphology of *Pyrenochaetopsis paucisetosa* NTUPPMCC 22-227 (A)(B) 14-days-old colony on PDA (C) Conidiomata (D) Squashed conidiomata (E) Conidiogenous cells (F–H) Conidia. Scale bars: C = 0.2 mm; D = 0.1 mm; E–F = 10 µm; G–H = 5 µm

Pyrenochaetopsis oryzicola S. Absalan, S. Lumyong, and K.D. Hyde (2024)

MycoBank: MB902535

Description: On carnation leaves (*Dianthus caryophyllus*) supplanted on WA (NTUPPMCC 22-222). *Sexual morph*: undetermined. *Asexual morph*: *Pyrenochaetopsis oryzicola* NTUPPMCC 22-229 exhibited difficulty sporulating conidiomata in PDA medium after 21 days but was sporulate on water agar and when media supplement with carnation leaves. *Conidiomata* 140–196 µm, pycnidial, brown, globose to subglobose, ostiolate, superficial on WA and carnation leaves, with dark brown, septate setae. *Pycnidial wall textura angularis* to *globulosa*, brown, pseudoparenchymatous cells. *Conidiogenous cells* hyaline, phialidic, smooth-walled, and hard to distinguish from the pycnidial wall 3.3–5.6 µm × 3.0–4.6 µm ($\bar{x}$=4.4 × 3.5 µm, n=30). *Conidia* hyaline, cylindrical to ellipsoidal, aseptate, with 2 small but obvious guttules, 3.6–5.1 µm × 1.7–2.5 µm ($\bar{x}$=4.3 × 2.2 µm, L/W ratio=2.03, n=50) (Fig. 9C–F).

Culture characteristics: NTUPPMCC 22-229 on PDA medium reaching 45 mm diam after 14 days at 25°C, with greenish-gray, flat, velvety to floccose surface and smooth margins, and similar to reverse side of the colony (Fig. 9A–B).

Material examined: Wanrung Township, Hualien County, Taiwan, 23°42'40.3"N, 121°24'48.2"E, serpentine soil in rice field, 2nd November 2022, K.W Cheng, living culture NTUPPMCC 22-228 to 242.

Notes: *Pyrenochaetopsis oryzicola* was originally reported from dead panicles of *Oryza sativa* in paddy fields in Thailand (Absalan et al. 2024). In the present, in both single- and multi-gene phylogenetic analyses showed that strains from NTUPPMCC 22-228 to 242 isolated in this study, grouped with the clade containing the ex-type strain of *P. oryzicola* (MFLUCC 24-0042) (Fig. 7). Consequently, these strains were identified as *Pyrenochaetopsis oryzicola*. Their culture characteristics on PDA, along with conidial morphology, were consistent with those of the epitype of *P. oryzicola* (MFLU 24-0319). However, the conidiogenous cells of *P. oryzicola* NTUPPMCC 22-229 isolated in our study were larger than those reported in the previous study ($\bar{x}$ = 4.4 × 3.5 µm versus 1.5 × 1.0 µm) (Absalan et al. 2024).

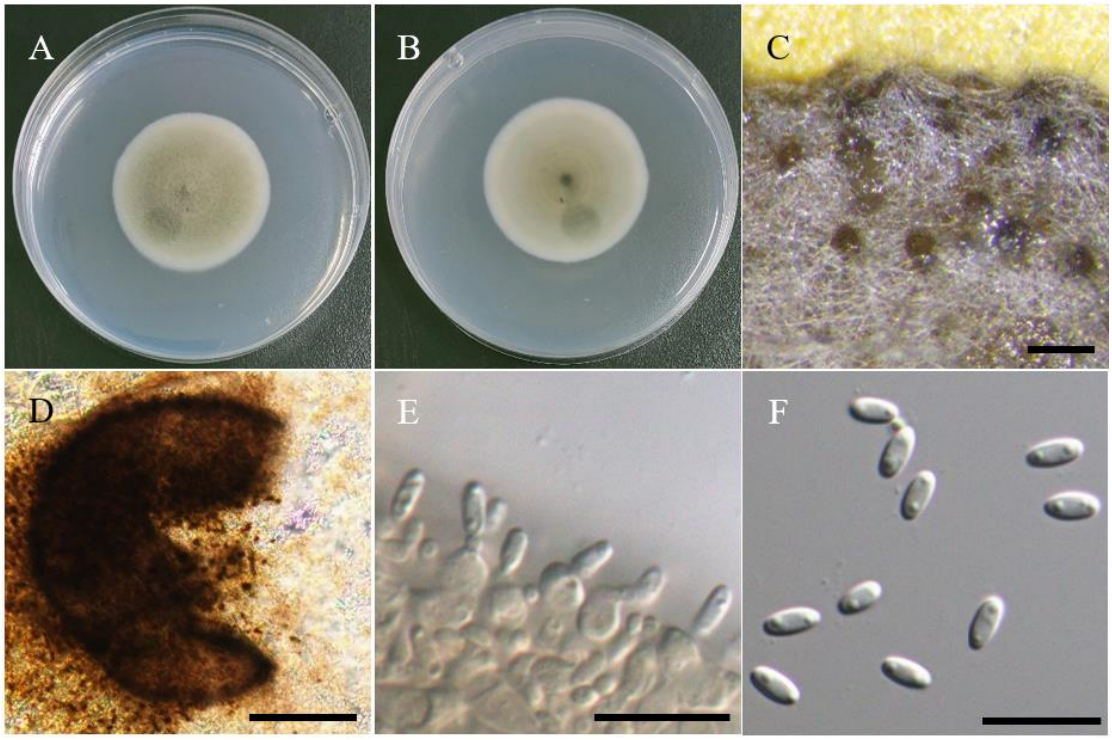

Figure 9. Morphology of *Pyrenochaetopsis oryzicola* NTUPPMCC 22-229 (A)(B) 14-days-old colony on PDA (C) Conidiomata (D) Squashed conidiomata (E) Conidiogenous cells (F) Conidia. Scale bars: C = 0.5 mm; D = 0.1 mm; E–F = 10 µm.

Setophaeosphaeria

Crous and Zhang (2014) introduced the genus *Setophaeosphaeria* to accommodate *S. hemerocallidis* isolated from leaf of *Hemerocallis fulva* (Crous et al. 2014). Currently, three species are recognized in MycoBank (Accession date: February 15, 2025) for *Setophaeosphaeria*. *Setophaeosphaeria* spp. are widely distributed and have been reported from Australia, Brazil, China, Italy, South Korea, and Netherlands, (Crous et al. 2017; Crous et al. 2018b; Choi et al. 2024; Liu et al. 2024). However, most of these strains were isolated from the leaf spots and branch dieback (Liu et al. 2024).

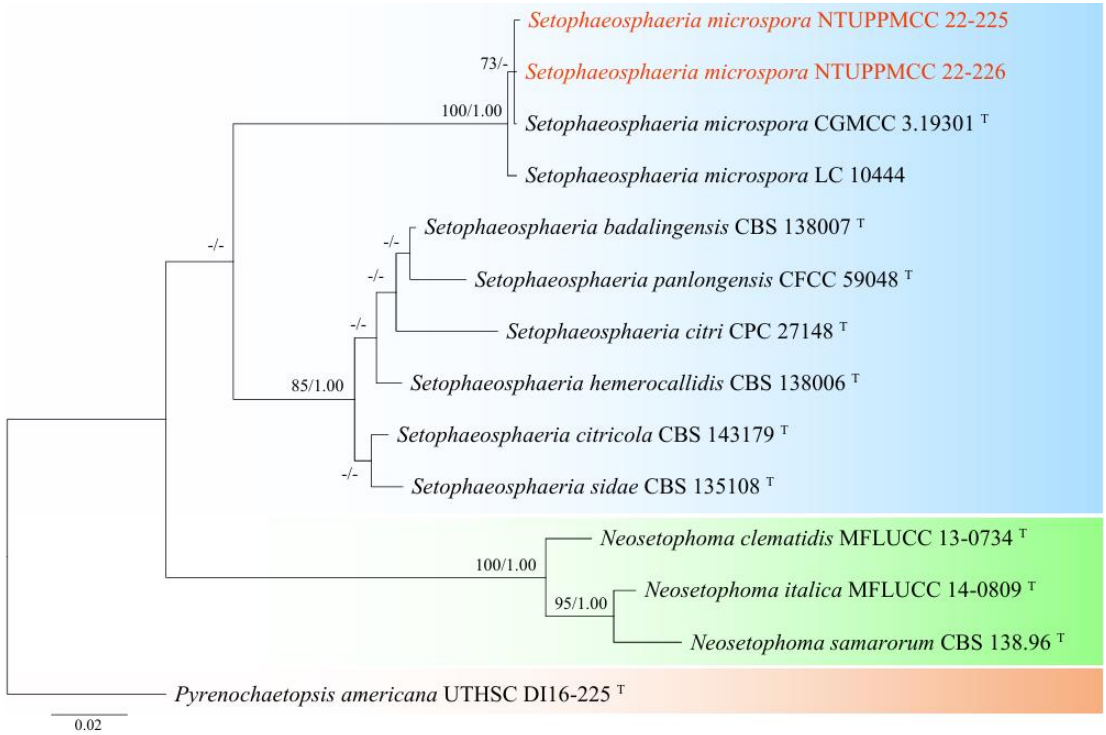

Figure 10. Maximum-likelihood phylogenetic tree based on concatenated sequences of ITS, LSU, and *tub2* for the genus *Setophaeosphaeria*. The tree was rooted with *Pyrenochaetopsis americana* UTHSC DI16-225. MLB ≥ 70% and BPPs ≥ 0.95 were shown at each node; values lower than these thresholds are indicated by a hyphen (–). The scale bar indicates the number of estimated substitutions per site. The new strains are shown in red. The type strains are marked with ^{T}.

Setophaeosphaeria microspora Z.F. Zhang & L. Cai (2020)

MycoBank: MB556393

Description: On carnation leaves (*Dianthus caryophyllus*) supplanted on WA (NTUPPMCC 22-225). *Sexual morph*: undetermined. *Asexual morph*: *Conidiomata* 170–240 µm, pycnidial, brown, globose, ostiolate, submerged or superficial on PDA. *Setae* brown, straight to slightly curved, thick-walled, smooth, septate, up to 160–250 µm long, 3.5–4.0 µm wide at broadest part. *Pycnidial wall textura angularis* to *globulosa*, brown to dark brown, multi-layers. *Conidiogenous cells* hyaline, cylindrical, smooth-walled, 3.3–4.5 µm × 2.3–3.5 µm ($\bar{x}$=3.9 × 2.9 µm, n=15). *Conidia* hyaline, cylindrical, obtuse ends, aseptate, with 2 small but obvious guttules, 3.2–4.0 µm × 1.3–1.7 µm ($\bar{x}$=3.7 × 1.4 µm, L/W ratio=2.54, n=30) (Fig. 11C–I).

Culture characteristics: NTUPPMCC 22-225 on PDA medium reaching 35 mm diam after 14 days at 25°C, with dark grayish-green in center, beige in margin, velvety, entire edge, and similar to reverse side of the colony (Fig. 11A–B).

Material examined: Guanshan Township, Taitung County, Taiwan, 23°02'12.8"N, 121°11'22.0"E, serpentine soil in rice field, 2nd November 2022, K.W Cheng, living culture NTUPPMCC 22-225 and NTUPPMCC 22-226.

Notes: The strains named NTUPPMCC 22-225 and NTUPPMCC 22-226 isolated in the present study clustered with ex-type strain *Setophaeosphaeria microspore* CGMCC 3.19301 with strong statistical support, confirming their identification as *S. microspora* (Fig. 10). However, *S. microspora* (NTUPPMCC 22-225) exhibited smaller conidiogenous cells than the type strain CGMCC 3.19301 (3.3–4.5 µm × 2.3–3.5 µm versus 7.0–10.0 µm × 2.5–4.0 µm) (Zhang et al. 2020). This study represents the first report of *Setophaeosphaeria* in Taiwan.

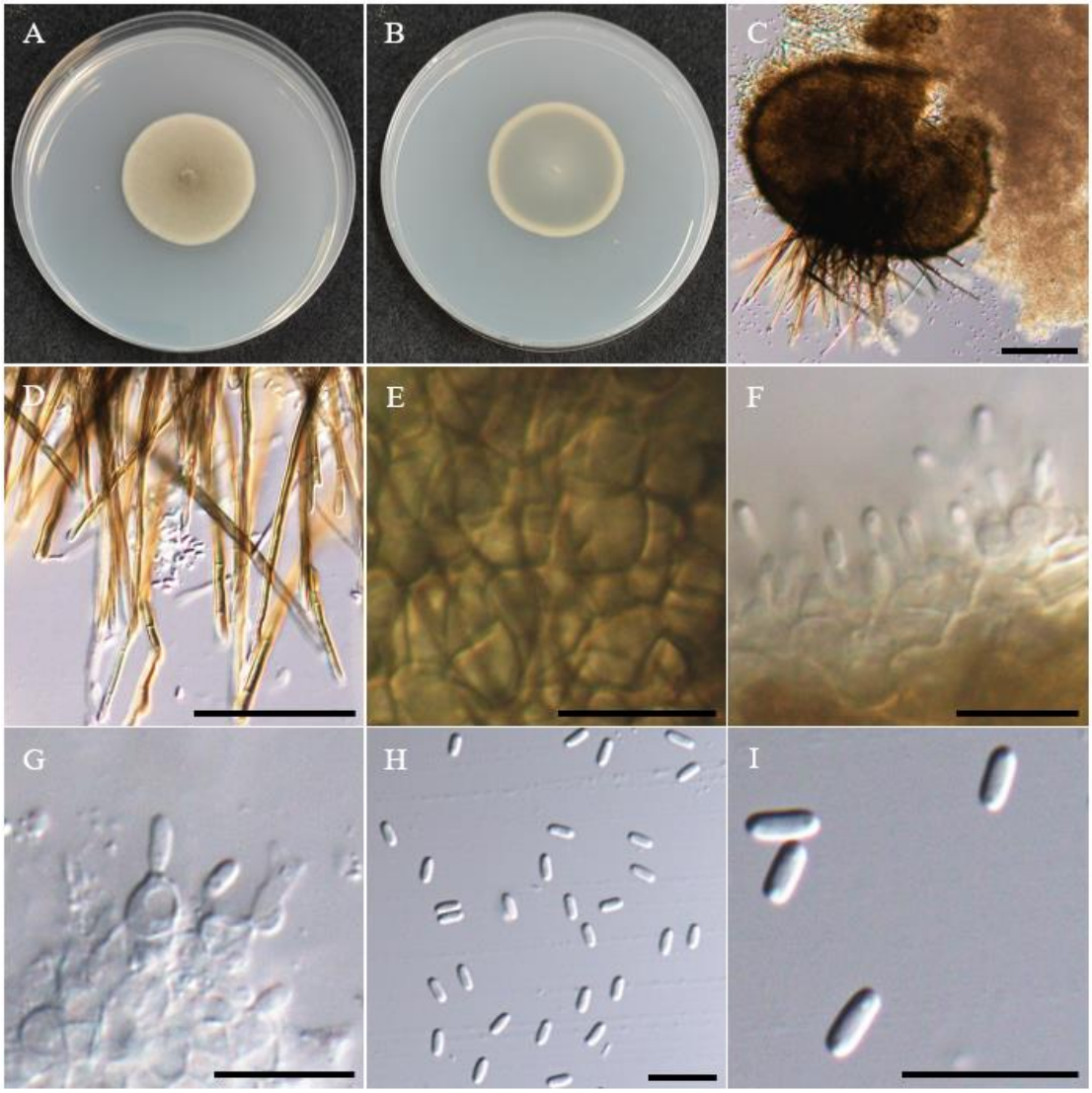

Figure 11. Morphology of *Setophaeosphaeria microspora* NTUPPMCC 22-225 (A)(B) 14-days-old colony on PDA (C) Squashed Conidiomata (D) Setae (E) Pycnidial wall (F)(G) Conidiogenous cells (H)(I) Conidia. Scale bars: C = 0.1 mm; D = 50 µm E–I = 10 µm.

Westerdykella

Stolk (1955) introduced *Westerdykella* and typified the genus with *W. ornata*, which was isolated from soil in Mozambique. Currently, 14 *Westerdykella* species are listed in MycoBank (Accession date: February 15, 2025), which have been recorded worldwide on a wide range of substrates including dung, plant debris, soil, and water (Chethana et al. 2021). However, there have also been rare reports of *W. dispersa* isolated from patients in hospitals (Sue et al. 2014; Lipovy et al. 2018). Most species in *Westerdykella* have been described based on the presence of the sexual morph, but some species, such as *W. dispersa*, formed both the sexual and asexual morphs in the same culture medium (Clum 1955).

In this study, 29 isolates were clustered within the genus *Westerdykella*. Among them, five strains (NTUPPMCC 22-243 to 247) grouped with the ex-type strain of *W. globosa* (IFO 32588) with strong statistical support. Additionally, DNA sequences of four strains (NTUPPMCC 22-248 to 251) were nested within the clade containing the ex-type strain of *W. aquatica* and other representative strains (JAUCC 1788 and P71). A single isolate (NTUPPMCC 22-252) clustered within the clade containing *W. purpurea* (MFLUCC 20-0140). Moreover, two strains (NTUPPMCC 22-253 and NTUPPMCC 22-254) grouped with the ex-type strain of *W. capitulum* (CBS 354.65). Furthermore, the majority of *Westerdykella* strains, including 11 isolates, were clustered within the clade corresponding to *W. dispersa*. Notably, five newly isolated strains (NTUPPMCC 22-255 to 259) in this study formed a distinct clade within the genus, separate from any known species. Therefore, this new lineage is introduced as *Westerdykella formosana* below.

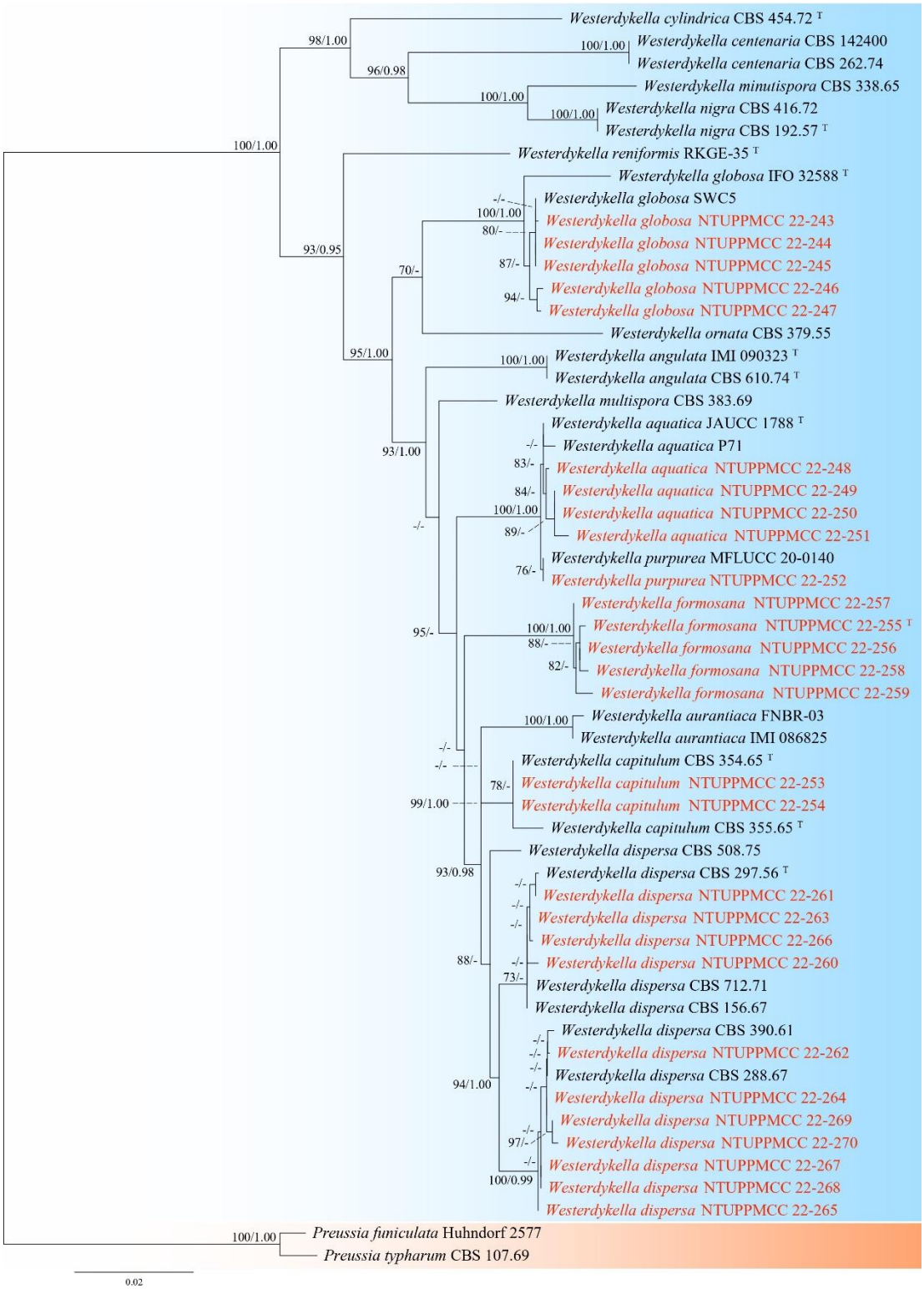

Figure. 12 Maximum-likelihood phylogenetic tree based on concatenated sequences of ITS, LSU, and *tub2* for the genus *Westerdykella*. The tree was rooted with *Preussia funiculata* Huhndorf 2577 and *P. typharum* CBS 107.69. MLB ≥ 70% and BPPs ≥ 0.95 were shown at each node; values lower than these thresholds are indicated by a hyphen (–). The scale bar indicates the number of estimated substitutions per site. The new strains are shown in red. The type strains are marked with ^{T}.

Westerdykella formosana K.W. Cheng & H.A. Ariyawansa, sp. nov.

MycoBank: MB858706

Typification: Wanrung Township, Hualien County, Taiwan, 23°42'40.3"N, 121°24'48.2"E, serpentine soil in rice field, 2nd November 2022, K.W Cheng, holotype, NTUPPMH 22-218 (Permanently preserved in a metabolically inactive state), ex-holotype NTUPPMCC 22-255, ex-isotype NTUPPMCC 22-256 to 259.

Etymology: Named after Formosa, the former name of Taiwan, where the type specimen was collected.

Description: On PDA medium (NTUPPMCC 22-255). *Sexual morph*: *Cleistothecia* 250–430 µm diam, non-ostiolate, globose, glabrous, mostly superficial, some submerged, dirty gray when immature, black when mature. *Peridium* single-layered, brown, translucent, membranous, angular cells. *Asci* subglobose to globose, hyaline when immature, 32-spored, 14.6–18.4 µm × 15.7–21.0 µm ($\bar{x}$=16.3 × 18.3 µm, L/W ratio=1.1, n=30). *Ascospores* ellipsoidal, smooth, subhyaline to light brown, 1 to 2 guttules, no germ-slits, 1.8–3.2 µm × 3.4–6.4 µm ($\bar{x}$=2.6 × 5.2 µm, L/W ratio=2.01, n=50) (Fig. 13C–J). *Asexual morph*: undetermined.

Culture characteristics: NTUPPMCC 22-255 on PDA medium reaching 80 mm diam after 14 days at 25°C, with flat, sparse aerial mycelium, creamy white, surface and margins smooth (Fig. 13A–B).

Notes: In both single- and concatenated locus phylogeny strains identified as *Westerdykella formosana* formed a distinct clade separate from the clades representing existing *Westerdykella* species (Fig. 12). The morphology of this new linage was typical of *Westerdykella* in having globose to subglobose cleistothecioid ascomata containing 32-spored asci and dark-colored ascospores (Ebead et al. 2012; Song et al. 2020; Goh et al. 2021). However, the ex-type strain of *Westerdykella formosa* NTUPPMCC 22-255 formed larger asci but smaller ascospores compared to its phylogenetically closely related species *W. aquatica* ($\bar{x}$=16.3 × 18.3 µm versus 15.3 × 14.1 µm; $\bar{x}$=5.2 × 2.6 µm versus 6.5 × 2.9 µm) (Song et al. 2020).

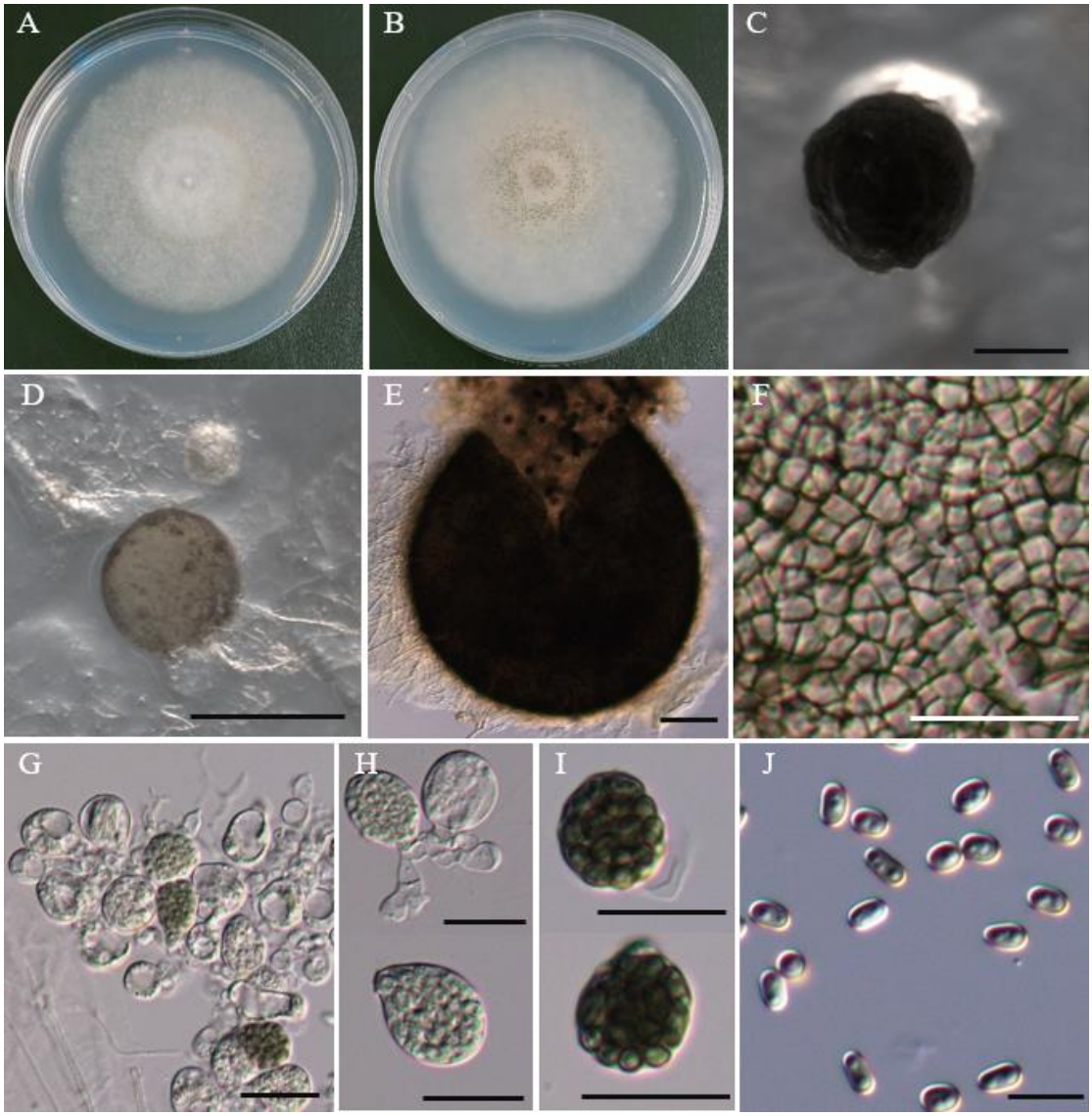

Figure 13. Morphology of *Westerdykella formosana* NTUPPMCC 22-255 (A)(B) 14-days-old colony on PDA (C) Ascomata (D) Immature ascoma (E) Squashed ascomata (F) Peridium (G)(H) Immature ascus (I) Ascus (J) Ascospore. Scale bars: C–D = 0.25 mm; E = 100 µm; F–I = 20 µm; J = 10 µm.

Westerdykella globosa T. Ito and A. Nakagiri (1995)

MycoBank: MB415330

Description: On PDA medium (NTUPPMCC 22-246). *Sexual morph*: *Cleistothecia* clustered in submerged regions, 106–185 µm diam, globose to subglobose, dirty gray when immature, dark brown to black when mature. *Asci* subglobose to ovoid, hyaline when immature, greenish brown when mature, 32-spored, edges slightly irregular due to crowding of mature ascospores, 20.8–29.8 µm × 26.9–40.2 µm ($\bar{x}$=24.5 × 32.7 µm, L/W ratio=1.35, n=30). *Ascospores* mostly globose, some subglobose, smooth, yellowish-brown, 1 to 2 guttules, 5.4–6.9 µm × 5.2–6.8 µm ($\bar{x}$=5.9 × 6.1 µm, L/W ratio=1.03, n=50) (Fig. 14C–I). *Asexual morph*: undetermined.

Culture characteristics: NTUPPMCC 22-246 on PDA medium attained a diameter of 50 mm after 14 days at 25°C. The growth was radial with a slightly diffused edge, predominantly creamy white and partly fluffy, with only the cleistothecia cluster region turning dark brown (Fig. 14A–B).

Material examined: Guanshan Township, Taitung County, Taiwan, 23°02'14.8"N, 121°11'22.6"E, serpentine soil in rice field, 3rd November 2022, K.W. Cheng, living culture NTUPPMCC 22-243 to 247.

Notes: *Preussia globosa* was synonymized under *Westerdykella globosa* by Ito (1995). This species has been reported from various environments, including soil from a stream bank and stored wheat grains in India (Rai and Tewari 1963; Kumari et al. 2019), paddy soil in Japan (Ito and Nakagiri 1995), and soil cultivated with *Ganoderma lucidum* in China (Zaheer et al. 2024). Our strains (NTUPPMCC 22-243–247) grouped with *W. globosa* in both single and multi-gene phylogeny (Fig. 12). The strains isolated in the present study shares similar morphologies with *W. globose* in producing globose, brown mature ascospores. Notbly, consistent with previous studies, only the sexual stage was observed for strains identified as *W. globosa* in the present study. However, it is worthy to note that the asci of our strains are larger than previously reported (21–30 µm × 27–40 µm versus 14–17 µm × 20–24 µm) (Ito and Nakagiri 1995). This is the first report of *Westerdykella globosa* in Taiwan.

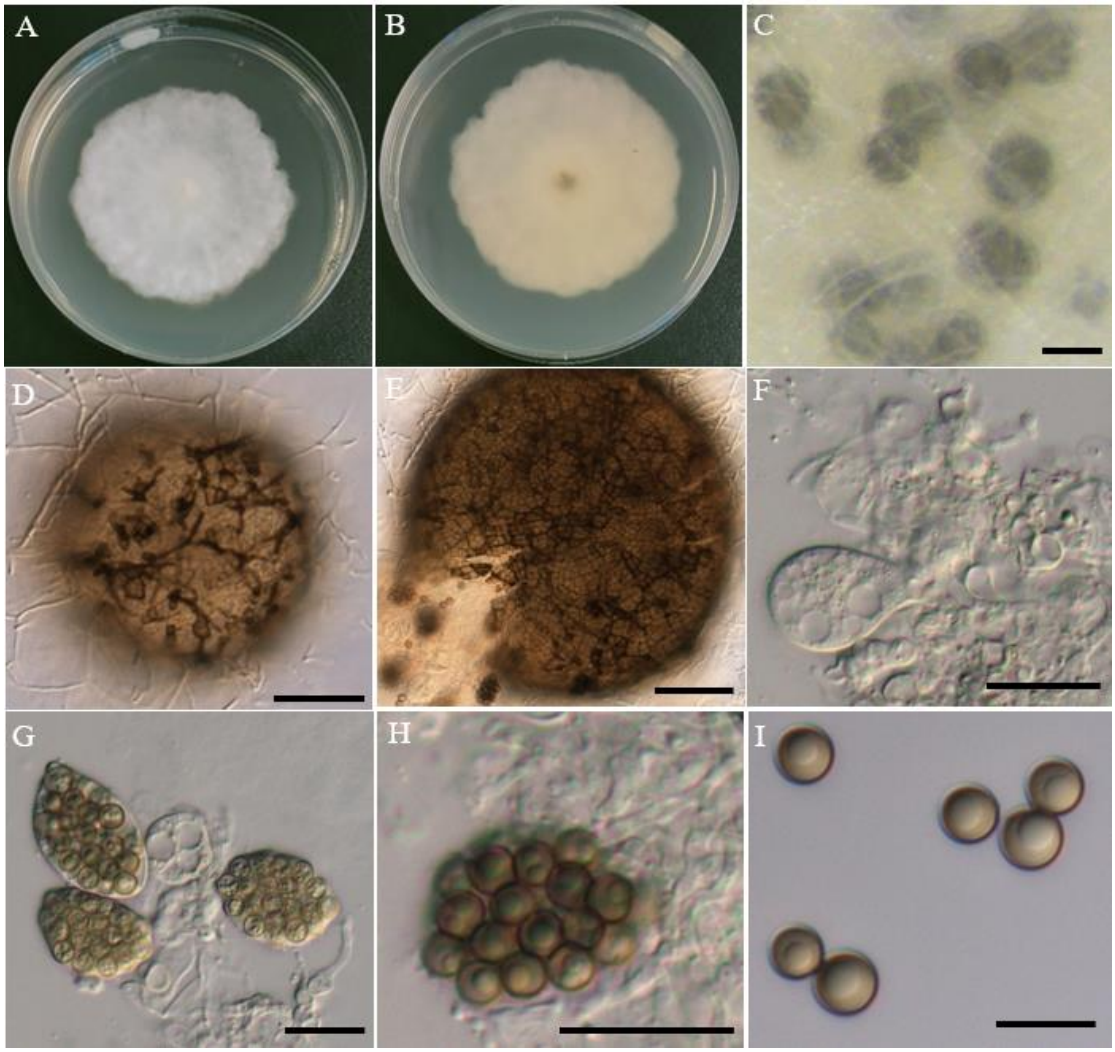

Figure 14. Morphology of *Westerdykella globosa* NTUPPMCC 22-246 (A)(B) 14-days-old colony on PDA (C) Ascomata (D) Immature ascomata (E) Squashed ascomata (F)(G) Immature asci (H) Ascus (I) Ascospores. Scale bars: C = 0.1 mm; D = 50 µm; F–H = 20 µm; I = 10 µm.

Westerdykella aquatica H.Y. Song and D.M. Hu (2020)

MycoBank: MB825645

Description: On PDA medium (NTUPPMCC 22-251). *Sexual morph*: *Cleistothecia* superficial or submerged on central region, 150–291 µm diam, globose to subglobose, glabrous, dirty gray when immature, black when mature. *Peridium* single-layered, brown, translucent, membranous, angular cells. *Asci* subglobose to ovoid, hyaline when immature, brown when mature, 32-spored, 10.7–14.7 µm × 12.2–16.3 µm ($\bar{x}$=14.3 × 12.6 µm, L/W ratio=1.15, n=30). *Ascospores* ellipsoidal, smooth, subhyaline to light brown, 1 to 2 guttules, no germ-slits, 2.2–3.3 µm × 4.7–5.9 µm ($\bar{x}$=2.8 × 5.1 µm, L/W ratio=1.87, n=50) (Fig. 15C–I). *Asexual morph*: undetermined.

Culture characteristics: NTUPPMCC 22-251 on PDA medium reached a diameter of 90 mm after 14 days at 25°C. The growth was radial with a slightly diffused edge, flat and fluffy, predominantly creamy white, with a central region transitioning to pale yellow, reverse yellow to dark yellow in the central region due to the presence of ascomata (Fig. 15A–B).

Material examined: Guanshan Township, Taitung County, Taiwan, 23°02'17.6"N, 121°11'26.3"E, serpentine soil in rice field, 3rd November 2022, K.W. Cheng, living culture NTUPPMCC 22-248 to 251.

Notes: *Westerdykella aquatica* has been reported from rice field mud and stems of *Acorus calamus* in China (Song et al. 2020), river sediment in Korea (Goh et al. 2021), and *Polygonum acuminatum* Kunth root in Brazil (Pietro-Souza et al. 2017; Senabio et al. 2023). In the present study, both single- and multi-gene phylogenies indicated that our strains NTUPPMCC 22-248 to 251 grouped with the clade representing *W. aquatica* (Fig. 12). Especially, similar to previous studies (Goh et al. 2021; Song et al. 2020), only the sexual stage was observed for all the strains identified as *W. aquatica* in the present study. Distinguishing *W. aquatica* from its phylogenetically closely related species, *W. purpurea* based solely on sexual-stage morphology can be challenging. This is the first report of *W. aquatica* in Taiwan.

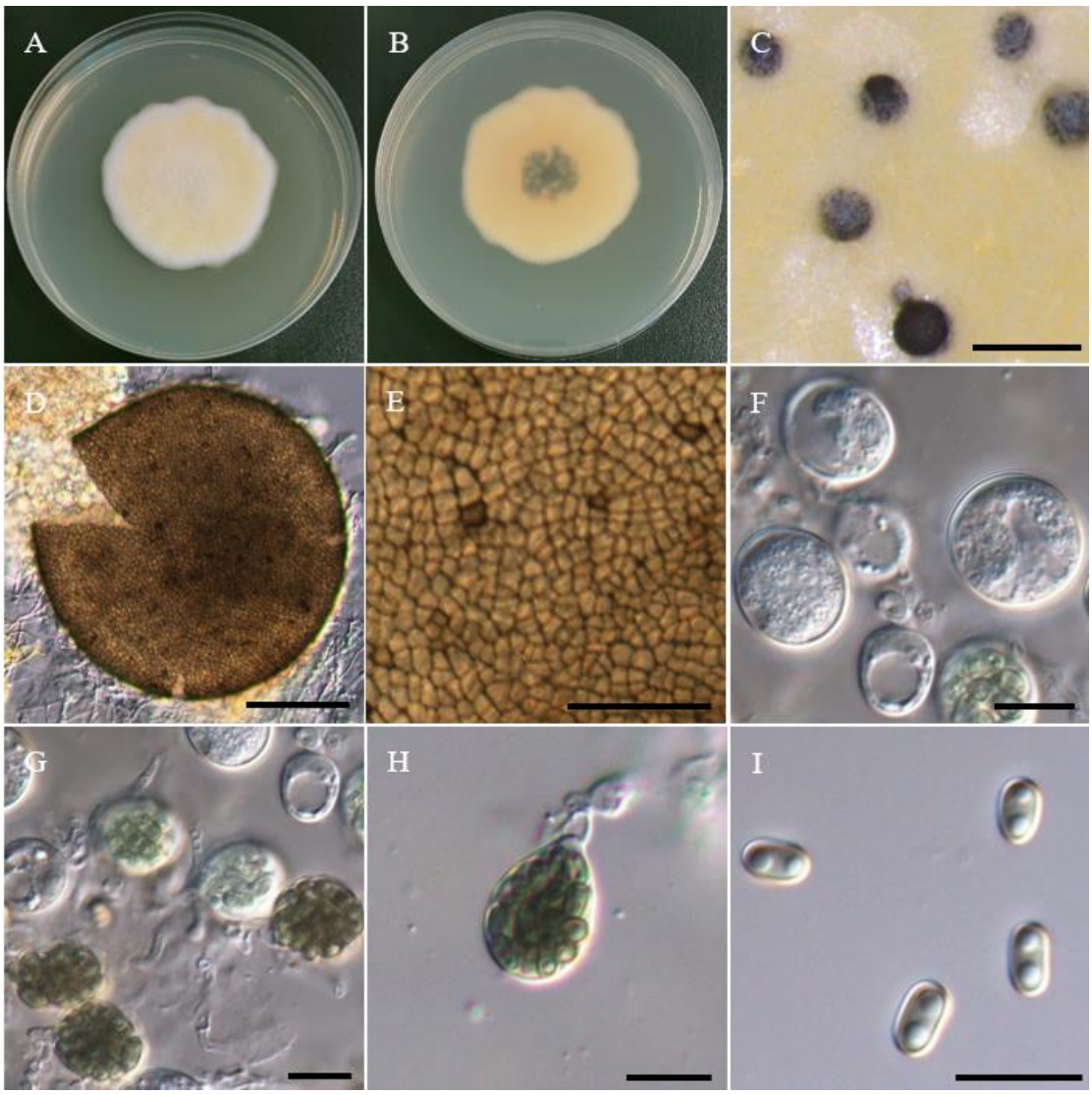

Figure 15. Morphology of *Westerdykella aquatica* NTUPPMCC 22-251 (A)(B) 14-days-old colony on PDA (C) Ascomata (D) Squashed ascomata (E) Peridium (F)(G) Immature asci (H) Ascus (I) Ascospores. Scale bars: C = 0.5 mm; D = 50 µm; E = 25 µm; F–I = 10 µm.

Westerdykella capitulum J.de Gruyter, M.M. Aveskamp, and J.Z. Groenewald (2012)

MycoBank: MB564801

Description: On PDA medium (NTUPPMCC 22-253). *Sexual morph*: undetermined. *Asexual morph*: *Conidiomata* 95–198 µm, globose, subglobose to irregular due to fusion of two or more, glabrous, dark brown, ostiolate, mostly superficial, some submerged. *Conidia* borne terminally in camel brown gelatinous mass, ellipsoidal, some globose, smooth, hyaline, 1 to 2 guttules, 2.4–3.4 µm × 3.0–4.1 µm ($\bar{x}$=2.8 × 3.5 µm, L/W ratio=1.3, n=50) (Fig. 16C–F).

Culture characteristics: NTUPPMCC 22-253 on PDA medium grows rapidly, reaching a diameter of 90 mm after 14 days at 25°C. The growth is radial with a uniform surface and smooth margins, forming a concentric pattern. The central region appears light grayish-brown due to dense conidiomata, while the edges exhibit a translucent beige hue (Fig. 16A–B).

Material examined: Wanrung Township, Hualien County, Taiwan, 23°42'40.3"N, 121°24'48.2"E, serpentine soil in rice field, 2nd November 2022, K.W. Cheng, living culture NTUPPMCC 22-253 and NTUPPMCC 22-254.

Notes: *Westerdykella capitulum* has been reported from various environments, including saline soil in India (Pawar et al. 1967), root of motherwort (*Leonurus cardiaca*) in Poland (Zimowska 2007), and mudflat in Korea (Genomic data) (Heo et al. 2019). The results of our phylogenetic analysis showed strains NTUPPMCC 22-253 and NTUPPMCC 22-254 were grouped with clade representing *W. capitulum* (Fig. 12). Morphological characters of the representative strain of *W. capitulum* NTUPPMCC 22-253 used in this study is similar to *W. capitulum* reported by de Gruyter et al. (2012). Similar to previous studies, only asexual stage was observed for strains identified as *W. capitulum* in the present study (Pawar et al. 1967; de Gruyter and Noordeloos 1992; Zimowska 2007). This is the first report of *W. capitulum* in Taiwan.

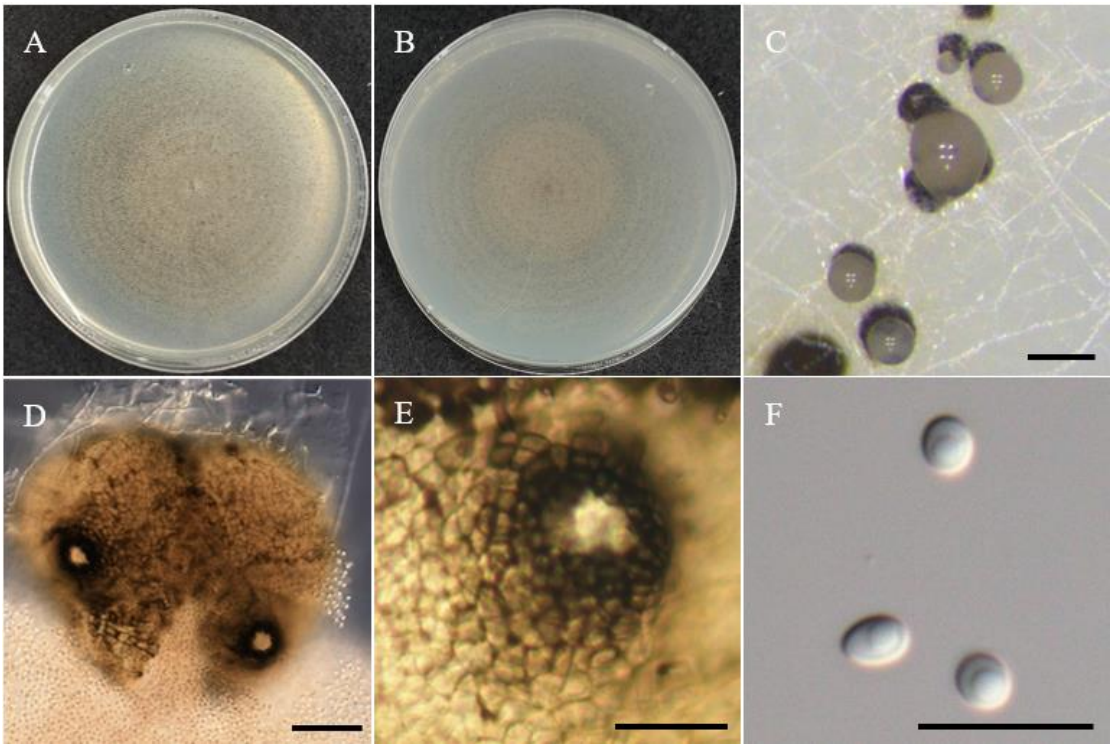

Figure 16. Morphology of *Westerdykella capitulum* NTUPPMCC 22-253 (A)(B) 14-days-old colony on PDA (C) Conidiomata (D) Squashed conidiomata (E) Ostiolate (F) Conidia. Scale bars: C = 0.2 mm; D–E = 20 µm; F = 10 µm.

Westerdykella dispersa K. Cejp & A.A. Milko (1964)

MycoBank: MB341019

Description: On PDA medium (NTUPPMCC 22-269). *Sexual morph*: *Cleistothecia* superficial or submerged, 187–296 µm diam, globose to subglobose, glabrous, dark brown to black when mature. *Peridium* single-layered, light brown, translucent, membranous, angular cells. *Asci* subglobose to ovoid, hyaline when immature, brown when mature, 32-spored, 9.7–11.8 µm × 11.0–13.6 µm ($\bar{x}$=10.8 × 12.3 µm, L/W ratio=1.14, n=30). *Ascospores* ellipsoidal, smooth, subhyaline to light brown, 2 guttules, no germ-slits, 1.8–2.7 µm × 3.7–4.5 µm ($\bar{x}$=2.3 × 4.0 µm, L/W ratio=1.82, n=50) (Fig. 17C, E, F–G, I–K). *Asexual morph*: *Conidiomata* abundant on PDA at 25°C, 7 days post-inoculation, 44–88 µm, globose, subglobose to irregular due to fusion of two or more, glabrous, brown, ostiolate, superficial. *Conidia* borne terminally in camel brown gelatinous mass, ellipsoidal, subglobose, some pyriform, smooth, hyaline, 0 to 2 guttules, 1.8–2.7 µm × 3.1–4.0 µm ($\bar{x}$=2.1 × 3.3 µm, L/W ratio=1.62, n=50) (Fig. 17C–D, H, L).

Culture characteristics: NTUPPMCC 22-269 on PDA medium grows rapidly, reaching a diameter of 90 mm after 14 days at 25°C. The growth is radial with smooth

margins. The abundant conidiomata caused the center to have numerous small, raised areas (Fig. 17A–B).

Material examined: Guanshan Township, Taitung County, Taiwan, 23°02'12.8"N, 121°11'22.6"E, serpentine soil in rice field, 3rd November 2022, K.W. Cheng, living culture NTUPPMCC 22-260 to 270.

Notes: *W. dispersa* have a global distribution and have been isolated from diverse substrates, including soil from the Netherlands and Nigeria (Arenal et al. 2007), freshwater ecosystem sediments in Brazil and Korea (da Silva et al. 2003; Goh et al. 2021), marine sediments in China and Spain (Xu et al. 2017; Guerra-Mateo et al. 2024), as an endophytes of *Phragmites australis* in Italy (Angelini et al. 2012), and in rare cases, isolated from a neutropenic patient (Clum 1955; Sue et al. 2014). In the multi-locus phylogenetic analysis, strains identified as *W. dispersa* were divided into two clusters (Fig. 12). Several strains (NTUPPMCC 22-260, 261, 263, 266) grouped with the ex-type strain of *W. dispersa*, while others (NTUPPMCC 22-262, 264, 265, 267 to 270) formed a separate clade sister to the main *W. dispersa* clade, making it difficult to define precise species boundaries. Although the PDA cultures showed differences between strains in the two clades, more phenotypic traits are needed to justify separating these clades into distinct species, as relying solely on culture characteristics is not a reliable method for defining fungal species (Fig. 17M–O). Therefore, based on these observations, we tentatively identified both clades as *W. dispersa*. The observed genetic variation may be related to their geographical origin or the specific habitats from which these strains were isolated. Consistent with previous studies (Sue et al. 2014), both sexual and asexual stages were observed in culture for *W. dispersa* in the present study. This report represents the first record of *W. dispersa* in Taiwan.

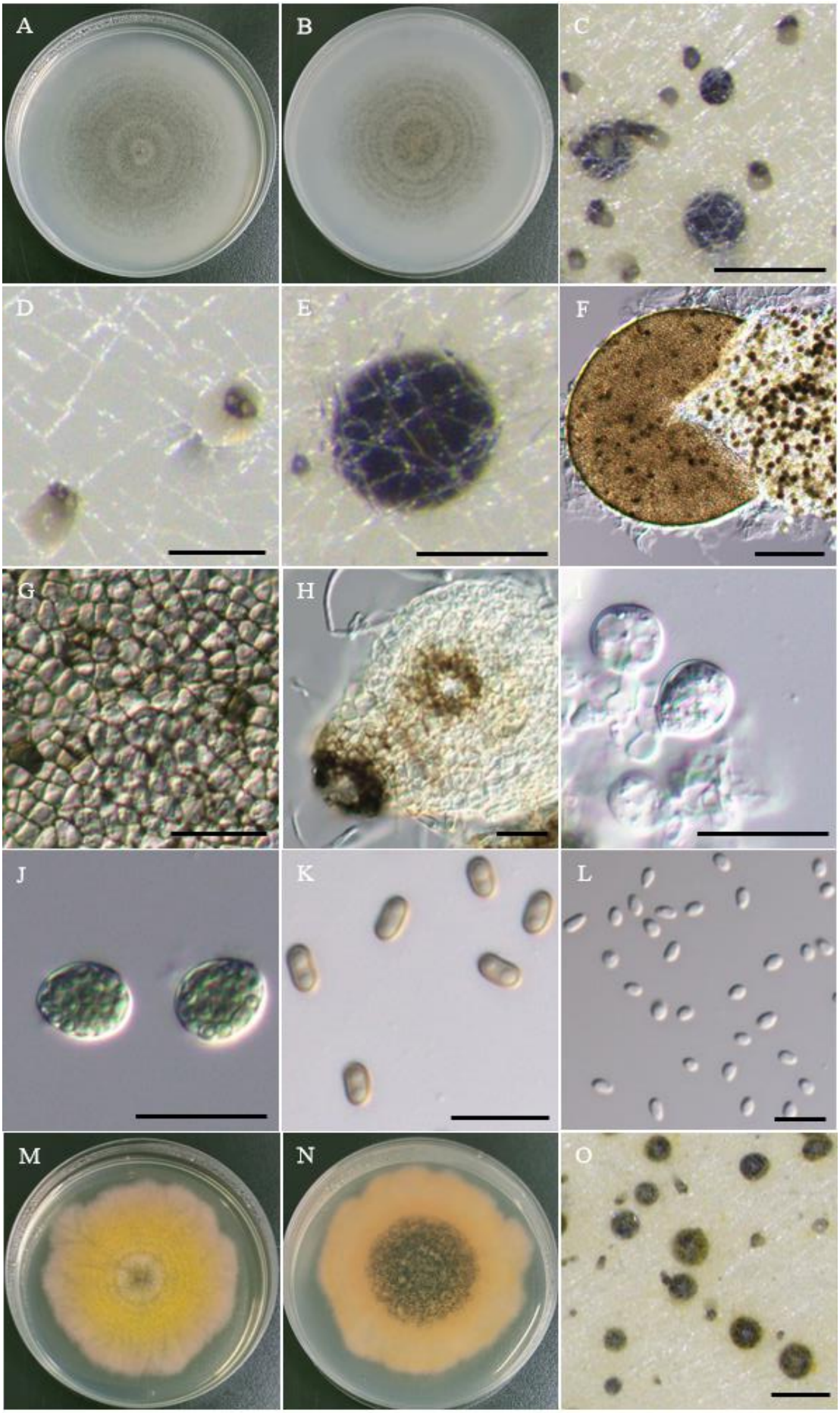
A
B
C
D
E
F
G
H
I
J
K
L
M
N
O

Figure 17. Morphology of *Westerdykella dispersa* NTUPPMCC 22-269 (A)(B) 14-days-old colony on PDA (C) Ascomata and conidiomata (D) Conidiomata (E) Ascomata (F) Squashed ascomata (G) Peridium (H) Conidiomata and ostiolate (I) Immature asci (J) Asci (K) Ascospores (L) Conidia. Morphology of *Westerdykella dispersa* NTUPPMCC 22-266 (M)(N) 14-days-old colony on PDA (O) Ascomata and conidiomata. Scale bars: C, O = 0.5 mm; D–E = 0.2 mm; F = 0.1 mm; G–J = 20 µm; K–L = 10 µm.

Eurotiomycetes

In total 15 strains clustered within Eurotiomycetes in this study categorized into one order, one family, one genus, and three species.

Talaromyces

The genus *Talaromyces* was first established by C.R. Benjamin (1955) and used to accommodate sexual stages of some *Penicillium* species. Currently, *Talaromyces* is the largest genera in the family Trichocomaceae, which is recorded over 170 accepted species classified into 8 sections in Mycobank (Accession date: February 15, 2025). *Talaromyces* has a global distribution and has been reported from a wide range of substrates including air, indoor environments, plant materials, food products, dungs, but mostly from soils (Hyde et al. 2024; Visagie et al. 2024). Some *Talaromyces* species play a key role as endophytes, helping plants against pathogens and promoting plant growth (Naraghi et al. 2012; Hashem et al. 2023; Nicoletti et al. 2023b). Additionally, while some species can cause diseases in humans, others can be utilized as drugs (Chan et al. 2016; Zhai et al. 2016; Nicoletti et al. 2023a).

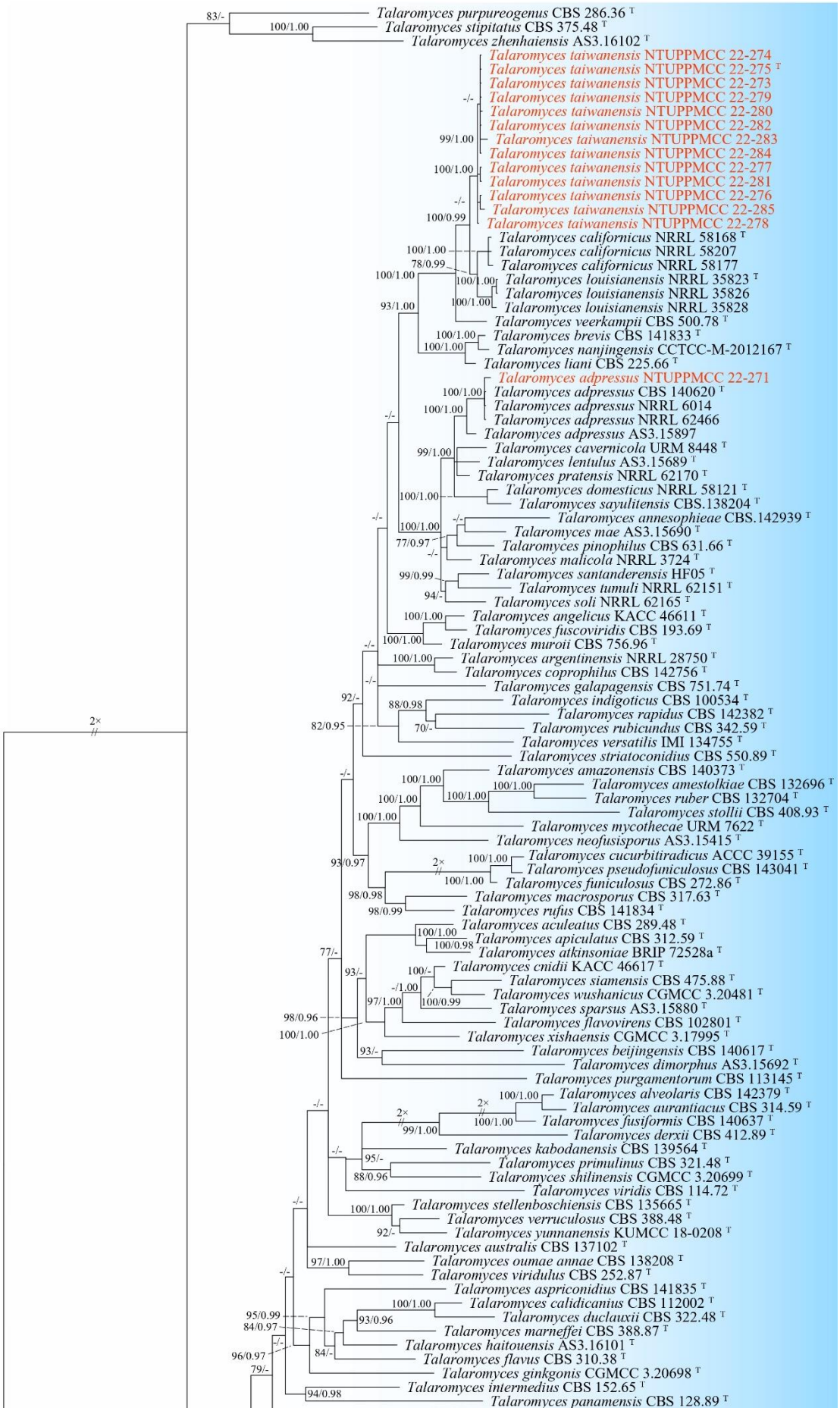

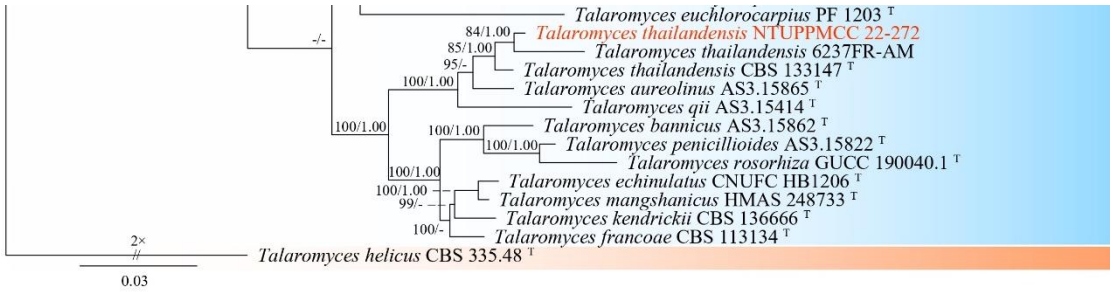

Figure 18. Maximum-likelihood phylogenetic tree based on concatenated sequences of ITS, *cmd*A, *rpb2*, and *tub2* for the genus *Talaromyces*. The tree was rooted with *Talaromyces helicus* CBS 335.48. MLB ≥ 70% and BPPs ≥ 0.95 were shown at each node; values lower than these thresholds are indicated by a hyphen (–). The scale bar indicates the number of estimated substitutions per site. The new strains are shown in red. The type strains are marked with ^{T}.

Talaromyces taiwanensis K.W. Cheng & H.A. Ariyawansa, sp. nov.

MycoBank: MB858707

Typification: Wanrung Township, Hualien County, Taiwan, 23°42'40.3"N, 121°24'48.2"E, serpentine soil in rice field, 2nd November 2022, K.W Cheng, holotype, NTUPPMH 22-219 (Permanently preserved in a metabolically inactive state), ex-holotype NTUPPMCC 22-275, ex-isotype NTUPPMCC 22-273 to 274, 276 to 285.

Etymology: Named after Taiwan, the country where the type specimen was collected.

Description: On PDA medium (NTUPPMCC 22-275). *Sexual Morph*: undetermined. *Asexual Morph*: *Conidiophores* arised from aerial hyphae, or roping hyphal aggregations, hyaline, smooth but some slightly rough, straight, and most bi-verticillate, occasionally formed subterminal side branches of mono-verticillate. *Metulae* 2.8–3.2 µm × 10.5–14.3µm. *Phialides* 3–5, flask-shaped, 2.0–2.8 µm × 8.2–18.2 µm. *Conidia* globose to subglobose, few pyriform, rough surfaces and walls, hyaline in immature, pale green to green in mature, 2.9–4.0 µm × 3.2–4.5 µm ($\bar{x}$=3.5 × 3.8 µm, L/W ratio=1.1, n=50) (Fig. 19C, F, G–I).

Culture characteristics: NTUPPMCC 22-275 on PDA medium reached a diameter of 70 mm after 14 days at 25°C. The colony exhibited a floccose to funiculose texture, with a compact central region displaying a light yellowish hue. Toward the margin, the colony transitioned into a dense greenish layer, indicating well-developed fungal growth with active sporulation, and had a whitish, smooth margin; reverse in salmon-buff (Fig. 19A–B). NTUPPMCC 22-275 on MEA medium grew rapidly, reaching a diameter of 85 mm after 14 days at 25°C. Similar characteristics to PDA, but colony color was grayish-green with slightly irregular margin (Fig. 19D–E).

Notes: *Talaromyces taiwanensis* NTUPPMCC 22-275 formed a distinct clade separate from its sister species *T. californicus* and *T. louisianensis* in the multi-gene phylogeny (Fig. 18). *T. taiwanensis* shares similar morphologies with other species of the genus in having, most bi-verticillate but occasionally subterminal of mono-verticillate conidiophores, and globose to subglobose, rough surfaces conidia. However, *T. taiwanensis* NTUPPMCC 22-275 formed smaller conidia to its phylogenetically closely related species *T. californicus* and *T. louisianensis* ($\bar{x}$= × 2.9–4.0 µm × 3.2–4.5 µm versus 4.0–6.0 µm × 4.0–7.0 µm and versus 3.5–5.0 µm × 3.5–5.0 µm) (Peterson and Jurjevic 2019). Furthermore, these two species were isolated from air in USA and our samples were from serpentine soil in Taiwan (Peterson and Jurjevic 2019).

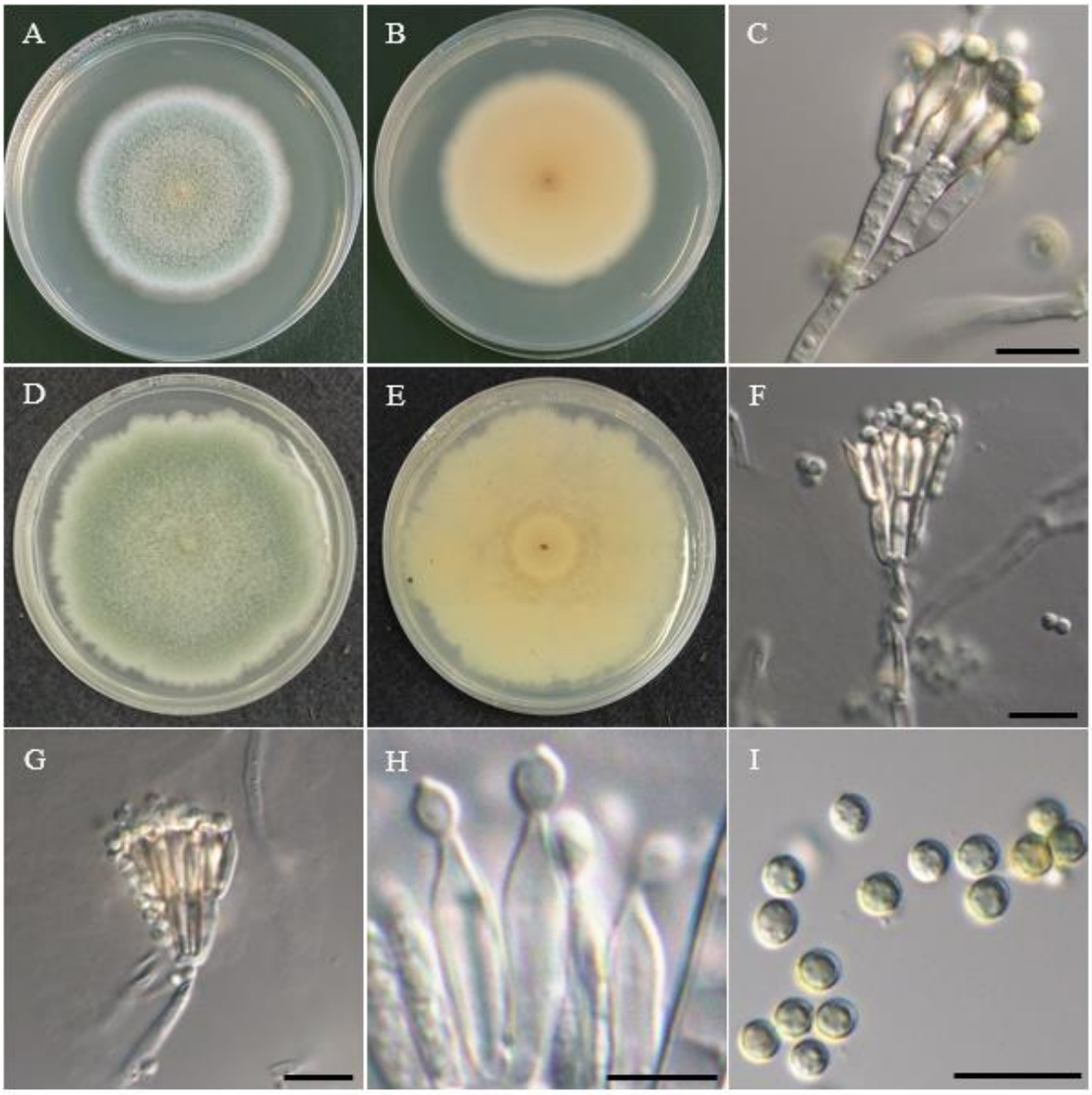

Figure 19. Morphology of *Talaromyces taiwanensis* NTUPPMCC 22-275 (A)(B) 14-days-old colony on PDA (D)(E) 14-days-old colony on MEA (C) Conidiophores (subterminal with mono-verticillate) (F)(G) Conidiophores (bi-verticillate) (H) Phialides and sporulating conidia (I) Conidia. Scale bars: C, F–G, I = 10 µm; H = 5 µm.

Talaromyces adpressus A.J. Chen, J.C. Frisvad & R.A. Samson (2016)

MycoBank: MB817397

Description: On PDA medium (NTUPPMCC 22-271). *Sexual Morph*: undetermined. *Asexual Morph*: *Conidiophores* arised from aerial hyphae, or roping hyphal aggregations, hyaline, straight, bi-verticillate. *Metulae* 2.6–3.0 µm × 9.6–11.5 µm. *Phialides* 3–5, flask-shaped, 2.1–2.7 µm × 8.2–10.7 µm. *Conidia* globose to subglobose, hyaline, few pale green, 1.6–2.1 µm × 2.2–2.5 µm ($\bar{x}$=1.9 × 2.3 µm, L/W ratio=1.20, n=25) (Fig. 20C, F).

Culture characteristics: NTUPPMCC 22-271 on PDA medium reached a diameter of 55 mm after 14 days at 25°C. The colony exhibited a floccose to funiculose texture, center dense sporulation exhibited grayish green, margin whitish, scalloped; reverse in salmon-buff (Fig. 20A–B). NTUPPMCC 22-271 on MEA medium grew rapidly, reaching a diameter of 80 mm after 14 days at 25°C. Similar characteristics to PDA, but colony color was olive green with slightly irregular margin; reverse yellowish brown (Fig. 20D–E).

Material examined: Guanshan Township, Taitung County, Taiwan, 23°02'12.8"N, 121°11'22.0"E, serpentine soil in rice field, 2nd November 2022, K.W Cheng, living culture NTUPPMCC 22-271.

Notes: In the present study, our strain (NTUPPMCC 22-271) clustered within the clade containing ex-type strain, along with other representative strains of *T. adpressus* with strong statistical support (Fig. 18). *T. adpressus* NTUPPMCC 22-271 exhibited similar asexual morph to the ex-type strain of *T. adpressus* (CBS 140620), with bi-verticillate conidiophores, phialides 3–5, and subglobose conidia (Chen et al. 2016). *T. adpressus* has been reported from a wide range of substrates including sea sand, indoor air, peanut, *Heterodera zeae* cysts, *Oryza coarctata* as endophytic fungi. (Chen et al. 2016; Peterson and Jurjevic 2019; Airin et al. 2023; Lee et al. 2023; Mo et al. 2024,). However, this study represents the first discovery of *T. adpressus* in Taiwan.

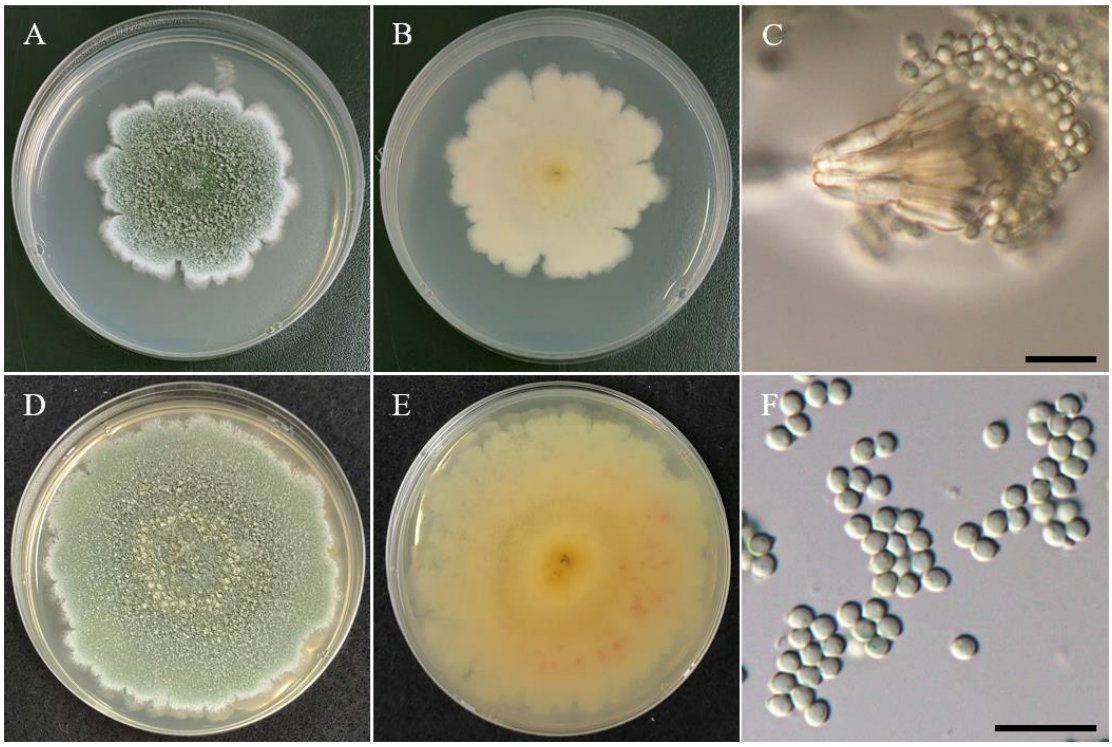

Figure 20. Morphology of *Talaromyces adpressus* NTUPPMCC 22-271 (A)(B) 14-days-old colony on PDA (D)(E) 14-days-old colony on MEA (C) Conidiophores, phialides, and conidiogenous cells (F) Conidia. Scale bars: C, F = 10 µm.

Talaromyces thailandensis L. Manoch, T. Dethoup & N. Yilmaz (2013)

MycoBank: MB801737

Description: On PDA medium (NTUPPMCC 22-272). *Sexual morph*: *Ascomata* solitary or clustered, superficial, globose to subglobose, yellow hyphae covered, 220–470 µm diam. *Asci* subglobose to ovoid, hyaline, 7.9–10.1 µm × 8.6–12.7 µm ($\bar{x}$=9.6 × 10.9 µm, L/W ratio=1.14, n=15). *Ascospores* ellipsoidal, spiny, thick walled, 2.8–3.5 µm × 4.2–5.0 µm ($\bar{x}$=3.2 × 4.6 µm, L/W ratio=1.47, n=25). *Asexual Morph*: *Conidiophores* straight, bi-verticillate, smooth walled and long stipes, up to 300 µm. *Metulae* 2.5–2.9 µm × 9.3–14.0 µm. *Phialides* 3–6, flask-shaped, 2.2–2.6 µm × 8.0–12.5 µm. *Conidia* globose to subglobose, smooth walled, hyaline to pale brownish green, 1.6–2.4 µm × 2.0–2.8 µm ($\bar{x}$=2.0 × 2.4 µm, L/W ratio=1.20, n=25) (Fig. 21C, F, G–K).

Culture characteristics: NTUPPMCC 22-272 on PDA medium reached a diameter of 70 mm after 14 days at 25°C. The colony exhibited a floccose texture, center dense sporulation exhibited grayish green and well-defined, smooth yellowish margin; reverse rajah orange (Fig. 21A–B). NTUPPMCC 22-272 on MEA medium reached a diameter of 70 mm after 14 days at 25°C. Texture of colony floccose, dominantly yellowish-orange but white, slightly irregular in margin, exudate clear droplets; reverse pale orange-brown (Fig. 21D–E).

Material examined: Guanshan Township, Taitung County, Taiwan, 23°02'17.6"N, 121°11'26.3"E, serpentine soil in rice field, 3rd November 2022, K.W. Cheng, living culture NTUPPMCC 22-272.

Notes: In the present study, our strain (NTUPPMCC 22-272) clustered within the clade containing ex-type strain, along with other representative strains of *T. thailandensis* with strong statistical support (Fig. 18). *T. thailandensis* (NTUPPMCC 22-272) displayed morphological features similar to the ex-type strain (CBS 133147) as reported by Manoch et al. (2013) and Yilmaz et al. (2014). These include ellipsoidal, spiny, thick-walled ascospores in the sexual stage and bi-verticillate conidiophores with 3–6 phialides, subglobose conidia, and clear exudate droplets on MEA in the asexual stage. *T. thailandensis* has been reported previously in Thailand as soil-derived fungus (Manoch et al. 2013, Ningsih et al. 2024). This study represents the first discovery of *T. thailandensis* in Taiwan.

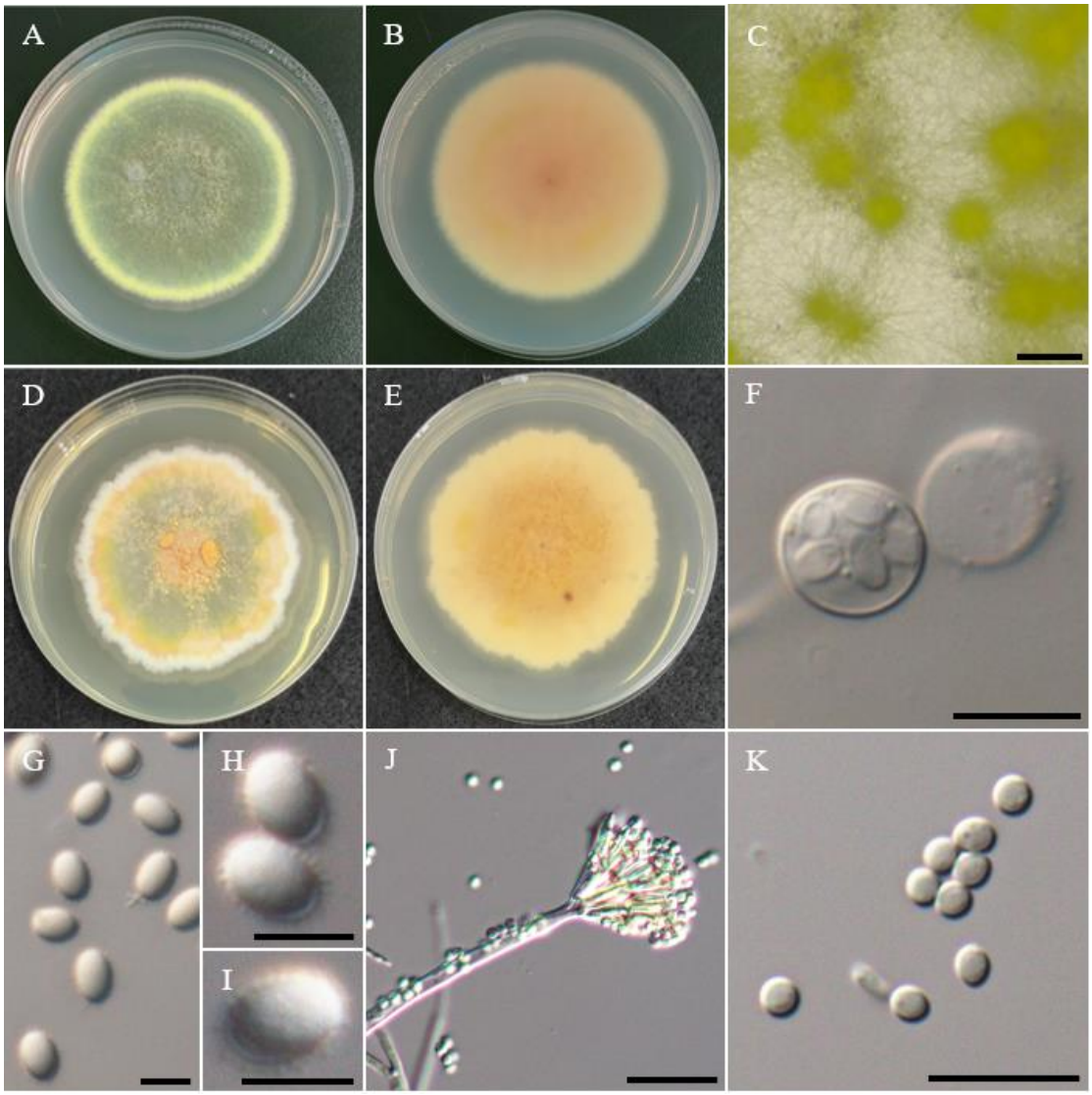

Figure 21. Morphology of *Talaromyces thailandensis* NTUPPMCC 22-272 (A)(B) 14-days-old colony on PDA (D)(E) 14-days-old colony on MEA (C) Ascomata and conidiophores (F) Asci (G)(H)(I) Ascospores (J) Conidiophores (K) Conidia. Scale bars: C = 0.5 mm; F, J, K = 10 µm; G–I = 5 µm.

Sordariomycetes

In total 16 strains clustered within class Sordariomycetes in this study categorized into four orders, six families, seven genera, and nine species.

Dimorphiseta

The genus *Dimorphiseta* was introduced to place *D. terrestris*, a strain originally isolated from soil habit in USA by Lombard and Crous (2016). Currently, three species are recognized in MycoBank (Accession date: February 15, 2025) for *Dimorphiseta.* The species of *Dimorphiseta* have been reported from China, Taiwan, and USA occurring on soil and also as saprobes in plant species belonging to Poaceae and Cannabaceae families (Lombard et al 2016; Liang et al. 2019; Tennakoon et al. 2021). *Dimorphiseta* exhibited sporodochial, stromatic, setae, conidiomata, macronematous, irregularly conidiophores, phialidic, hyaline, smooth, cylindrical conidia (Liang et al. 2019). In this study, two isolates (NTUPPMCC 22-291 and NTUPPMCC 22-292) were clustered within the genus *Dimorphiseta*, and these strains formed two distinct clades within the genus sperated from other known species (Fig. 22). Therefore, two new species are proposed to accommodate these new strains namely *Dimorphiseta formosana* and *Dimorphiseta serpentinicola*.

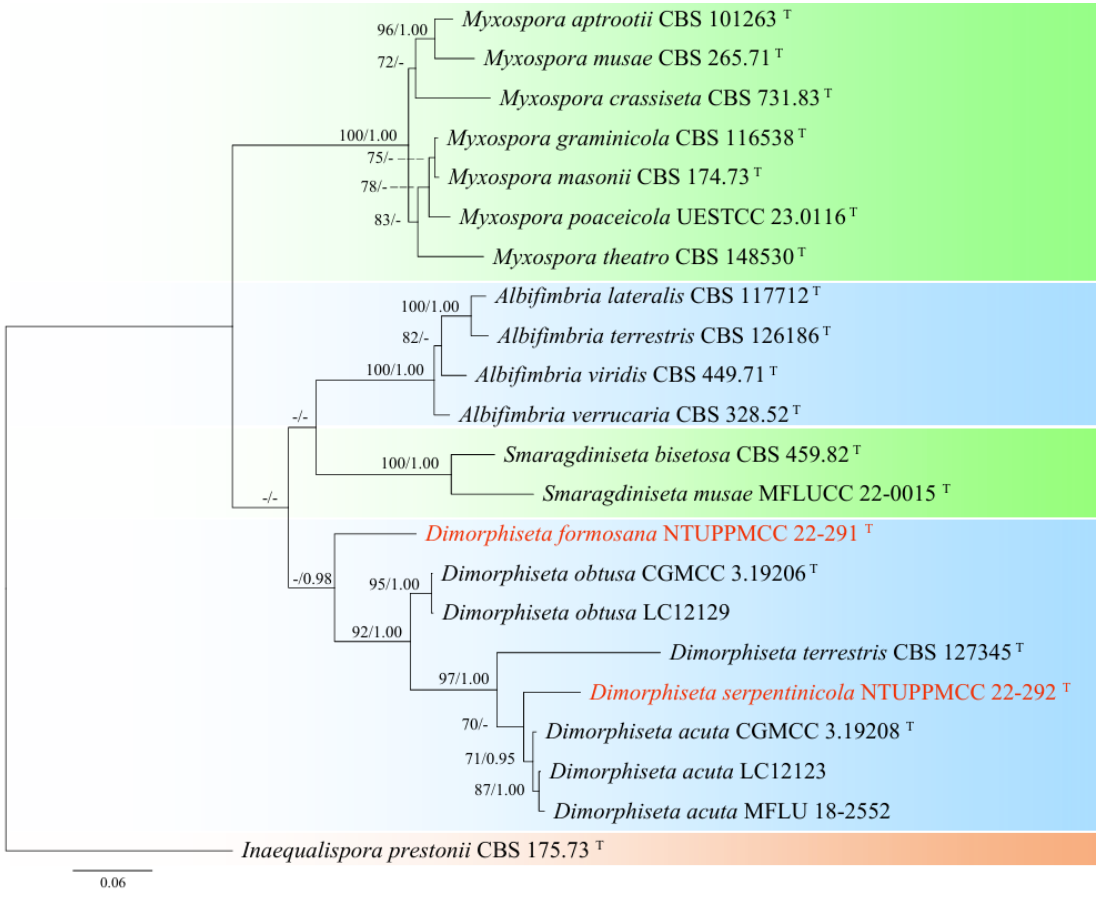

Figure 22. Maximum-likelihood phylogenetic tree based on concatenated sequences of ITS, *cmd*A, *rpb2*, and *tub2* for the genus *Dimorphiseta*. The tree was rooted with *Inaequalispora prestonii* CBS 175.73. MLB ≥ 70% and BPPs ≥ 0.95 were shown at each node; values lower than these thresholds are indicated by a hyphen (–). The scale bar indicates the number of estimated substitutions per site. The new strains are shown in red. The type strains are marked with ^{T}.

Dimorphiseta formosana K.W. Cheng & H.A. Ariyawansa, sp. nov.

MycoBank: MB 858708

Typification: Wanrung Township, Hualien County, Taiwan, 23°42'40.3"N, 121°24'48.2"E, serpentine soil in rice field, 2nd November 2022, K.W Cheng, holotype, NTUPPMH 22-224 (Permanently preserved in a metabolically inactive state), ex-holotype NTUPPMCC 22-291.

Etymology: Named after Formosa, the former name of Taiwan, where the type specimen was collected.

Description: On carnation leaves (*Dianthus caryophyllus*) supplanted on WA (NTUPPMCC 22-291). *Sexual morph*: undetermined. *Asexual morph*: *Setae* thick-walled, hyaline, smooth, septate, straight to slightly curved, tapering to sharp apices, 170–240 µm long, 4–6 µm wide at broadest part. *Conidiomata* 258–463 µm diam, randomly scattered, superficial, sporodochial, stromatic, subglobose to irregular in outline, dark green to black, agglutinated slimy mass of conidia. *Conidiophores* unbranched, hyaline to green, smooth to lightly verrucose, arising from basal stroma. *Conidiogenous cells* phialidic, hyaline, cylindrical, smooth, with collarette at tip, 17.2–22.7 µm × 1.7–2.3 µm ($\bar{x}$=20 × 1.9 µm, n=25). *Conidia* aseptate, hyaline, fusiform, smooth, few with funnel-shaped apical appendage, 7.8–9.0 µm × 2.1–3 µm ($\bar{x}$=8.4 × 2.6 µm, L/W ratio=3.32, n=50) (Fig. 23C–F).

Culture characteristics: NTUPPMCC 22-291 on PDA medium reaching 60 mm diam after 14 days at 25°C, with white, fluffy, cotton-like mycelium in center that gradually thinned toward the edges with a slightly irregular margin. A slight yellowish-green pigment diffused in PDA and the reverse side of the medium appeared canary yellow (Fig. 23A–B).

Notes: This study introduces *Dimorphiseta formosana* as a new fungal species, described from a single strain obtained from serpentine soil. While examining multiple strains is preferred when establishing a new species, obtaining additional isolates proved difficult due to this organism's specialized ecological niche and scarcity in the sampled habitat. Nevertheless, thorough morphological analysis and phylogenetic evidence strongly support the recognition of this fungus as a distinct species (Fig. 22). Phylogenetic analysis using multiple loci clearly separates *D. formosana* from its

closest relatives, *D. obtusa* (CGMCC 3.19206) with significant genetic divergence in four different loci, ITS sequences (identities = 491/516, 95.2% including gaps); *cmd*A sequences (identities = 501/572, 87.6% including gaps); *rpb2* sequences (identities = 608/721, 84.3%); *tub2* sequences (identities = 254/307, 82.7% including gaps). Furthermore, our new species can be differentiated from *D. obtusa* (CGMCC 3.19206) by its smaller conidia, measuring 8–9 µm × 2–3 µm compared to 9–11 µm × 2–4 µm as reported by Liang et al. (2019). Even though its conidiogenous cells and conidia closely resemble those of the ex-type strain of *D. terrestris* (CBS 127345), our species lacks any Type I setae—characterized as thin-walled, flexuous to circinate, and verrucose (Lombard et al. 2016). Additionally, while both *D. formosana* and *D. serpentinicola* were isolated from serpentine environments, *D. formosana* demonstrated a faster growth rate on PDA and produced a more vibrant yellow on the reverse side of the culture.. Though our research conclusively identifies *D. formosana* as a unique species, subsequent investigations should focus on obtaining additional specimens from comparable habitats to better understand its morphological diversity and ecological range.

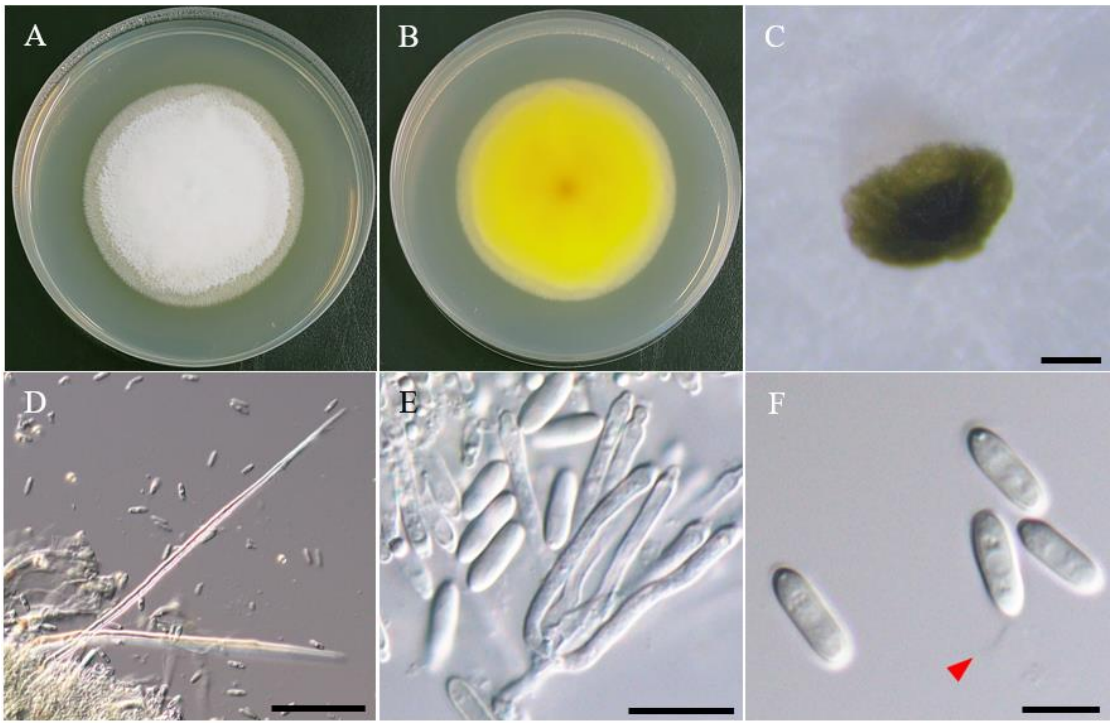

Figure 23. Morphology of *Dimorphiseta formosana* NTUPPMCC 22-291 (A)(B) 14-days-old colony on PDA (C) Conidiomata (D) Setae (E) Conidiophores and conidiogenous cells (F) Conidia (red arrow: funnel-shaped appendage). Scale bars: C = 0.2 mm; D = 50 µm E–F = 10 µm.

Dimorphiseta serpentinicola K.W. Cheng & H.A. Ariyawansa, sp. nov.

MycoBank: MB858710

Typification: Wanrung Township, Hualien County, Taiwan, 23°42'40.3"N, 121°24'48.2"E, serpentine soil in rice field, 2nd November 2022, K.W Cheng, holotype, NTUPPMH 22-225 (Permanently preserved in a metabolically inactive state), ex-holotype NTUPPMCC 22-292.

Etymology: Named for the serpentine soil from which the species was isolated.

Description: On carnation leaves (*Dianthus caryophyllus*) supplanted on WA (NTUPPMCC 22-292). *Sexual morph*: undetermined. *Asexual morph*: *Conidiomata* 258–548 µm diam, 70–225 µm deep, randomly scattered, superficial, sporodochial, stromatic, globose to subglobose, smooth outline, dark green to black, agglutinated slimy, mucoid mass of conidia. *Stroma* difficult to observe. *Setae* thick-walled, hyaline, smooth, septate, straight to slightly curved, tapering to sharp apices, 180–280 µm long, 5–7 µm wide at broadest part. *Conidiophores* unbranched, hyaline to green, smooth to lightly verrucose, arising from basal stroma. *Conidiogenous cells* phialidic, hyaline, cylindrical, smooth, with collarette at tip, 18.3–23.5 µm × 1.6–2.2 µm ($\bar{x}$=21.0 × 1.9 µm, n=25). *Conidia* aseptate, hyaline, fusiform, smooth, funnel-shaped apical appendage, 7.4–8.7 µm × 2.2–3.1 µm ($\bar{x}$=8.1 × 2.7 µm, L/W ratio=3.07, n=50) (Fig. 24C–H).

Culture characteristics: NTUPPMCC 22-292 on PDA medium reaching 38 mm diam after 14 days at 25°C, with abundant white, cotton-like mycelium and slightly irregular margin. A mustard pigment developed, and the reverse side of the medium appeared pale yellow (Fig. 24A–B).

Notes: This investigation presents *Dimorphiseta serpentinicola* as a previously undescribed fungal species, characterized from a single isolate recovered from serpentine soil. Although taxonomic best practices recommend analyzing multiple strains when establishing new species, additional specimens proved obscure, presumably due to the organism's specialized habitat requirements and relative scarcity within the sampling area. Nevertheless, extensive morphological examination and robust phylogenetic analysis strongly support the recognition of this fungus as a distinct taxonomic entity (Fig. 22). Phylogenetic analysis across multiple loci clearly separates *D. serpentinicola* from its closest relative species *D. acuta* (CGMCC 3.19208) with significant genetic divergence in three different loci, *cmd*A sequences (identities = 526/580, 90.7% including gaps); *rpb2* sequences (identities = 675/721, 93.6% including gaps); *tub2* sequences (identities = 286/293, 97.6%). The colony color and texture on PDA were similar to *D. acuta* CGMCC 3.19208, but pigment diffusion into the medium was observed in PDA and MEA (Liang et al. 2019). *D. acuta* was previous recorded in Taiwan, isolated from the dead leaves of *Celtis formosana* by (Tennakoon

et al. 2021) . However, our species exhibited smaller conidia (8.1 × 2.7 µm versus 10.5 × 2.5 µm) and longer setae (up to 280 µm versus 150 µm) compared to *D. acuta* (Tennakoon et al. 2021). Although our investigation confirms *D. serpentinicola* as a valid taxonomic entity, further research should focus on collecting additional specimens from comparable serpentine habitats to enhance our understanding of its morphological variability and environmental distribution patterns.

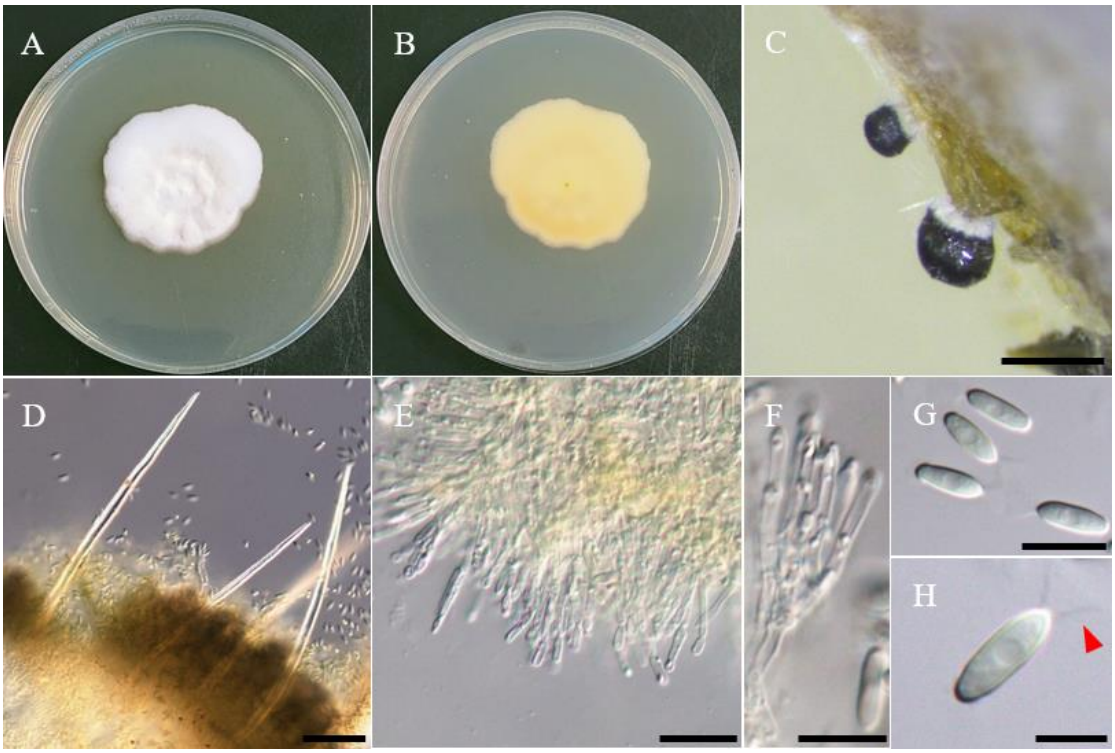

Figure 24. Morphology of *Dimorphiseta serpentinicola* NTUPPMCC 22-292 (A)(B) 14-days-old colony on PDA (C) Conidiomata (D) Setae (E)(F) Conidiophores and conidiogenous cells (G)(H) Conidia (red arrow: funnel-shaped appendage). Scale bars: C = 0.5 mm; D = 50 µm; E = 20 µm; F–G = 10 µm H = 5 µm.

Parasarocladium

The genus *Parasarocladium* was first introduced by Summerbell et al. (2018) to accommodate three soilborne, acremonium-like species, and is typified by *Parasarocladium radiatum*, which was isolated from soil in India. Currently, 13 species epithets are recognized for *Parasarocladium* in Mycobank (Accession date: February 15, 2025). *Parasarocladium* has a global distribution and has been isolated from soil and plants as a soil borne fungus, plant pathogen, and endophyte. (Summerbell et al. 2018; Hou et al. 2023). In this study, single isolate (NTUPPMCC 22-288) was clustered within the genus *Parasarocladium* and formed a distinct clade within the genus (Fig. 25). Therefore, new species is proposed to accommodate this strain in the genus *Parasarocladium*.

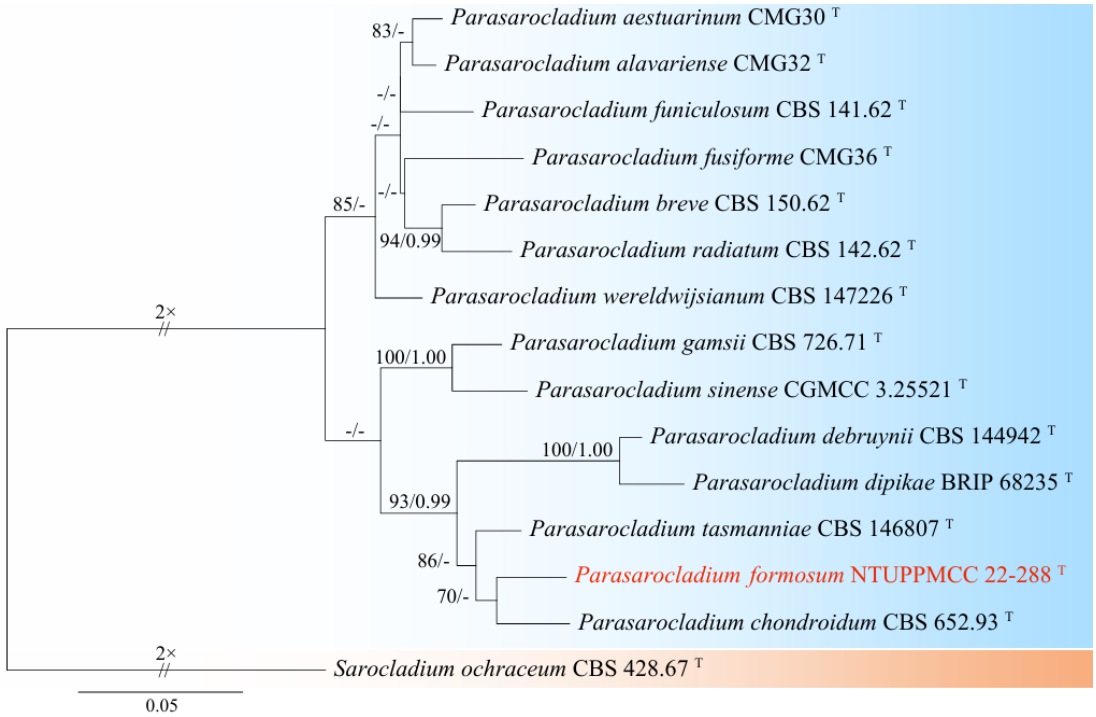

Figure 25. Maximum-likelihood phylogenetic tree based on concatenated sequences of ITS, LSU, *rpb2*, and *tef*-1 for the genus *Parasarocladium*. The tree was rooted with *Sarocladium ochraceum* CBS 428.67. MLB ≥ 70% and BPPs ≥ 0.95 were shown at each node; values lower than these thresholds are indicated by a hyphen (–). The scale bar indicates the number of estimated substitutions per site. The new strain is shown in red. The type strains are marked with ^{T}.

Parasarocladium formosum K.W. Cheng & H.A. Ariyawansa, sp. nov.

MycoBank: MB858711

Typification: Guanshan Township, Taitung County, Taiwan, 23°02'17.6"N, 121°11'26.3"E, serpentine soil in rice field, 3rd November 2022, K.W. Cheng, holotype, NTUPPMH 22-221 (Permanently preserved in a metabolically inactive state), ex-holotype NTUPPMCC 22-288.

Etymology: Named after Formosa, the former name of Taiwan, where the type specimen was collected.

Description: On WA medium (NTUPPMCC 22-288). *Sexual morph*: undetermined. *Asexual morph*: *Conidiophores* most solitary, straight, arising directly from aerial or substratal hyphe, unbranched, mono-phialides or adelophialides predominant, usually reduced to phialides, 7–18 × 2–3 µm. C*onidia* ellipsoidal, sometimes fusoid, hyaline, aseptate, smooth-walled, 1-celled, several tiny guttules, arranged in slimy heads, 2.0–3.9 µm × 3.7–7.4 µm ($\bar{x}$=2.6 × 4.9 µm, L/W ratio=1.94, n=50) (Fig. 26C–F).

Culture characteristics: NTUPPMCC 22-288 on PDA medium, reaching a diameter of 35 mm after 14 days at 25°C. The colony was creamy white, radially folded, slightly rugose at center region, smooth margin, reverse pale yellow (Fig. 26A–B).

Notes: This investigation introduces *Parasarocladium formosum* as a previously undescribed fungal species, characterized from a single isolate obtained from serpentine soil. Although examining multiple strains is preferred when establishing new species, additional specimens proved difficult to obtain, presumably due to this organism's specialized habitat requirements and limited prevalence in the sampled environment. Nevertheless, robust morphological assessment and phylogenetic analysis strongly support its designation as a distinct taxon (Fig. 25). Multi-locus phylogenetic evaluation definitively distinguishes *P. formosum* from its nearest relatives, particularly the ex-type strain of *P. chondroidum* (CBS 652.93), with notable genetic differentiation in two key loci: *rpb2* sequences (showing 93.0% identity, 588/632 bases including gaps) and *tef*-1α sequences (showing 93.1% identity, 758/814 bases including gaps).Furthermore, the sister species *P. chondroidum* has been reported as an endophyte in Gramineae, whereas *P. formosum* NTUPPMCC 22-288, although isolated from a paddy field, was recovered from soil and has not been identified as an endophyte (Hou et al. 2023). Moreover, the conidia of our new species are slightly larger and straighter compared to the original description of *P. chondroidum* CBS 652.93, which exhibited relatively smaller and curved conidia. (2.0–3.9 µm × 3.7–7.4 µm versus 1.2–2.5 µm × 3.4–8 µm) (Hou et al. 2023). While this study establishes *P. formosum* as a distinct species, future studies should aim to recover additional isolates from similar environments to further validate its phenotypic variation and ecological

distribution.

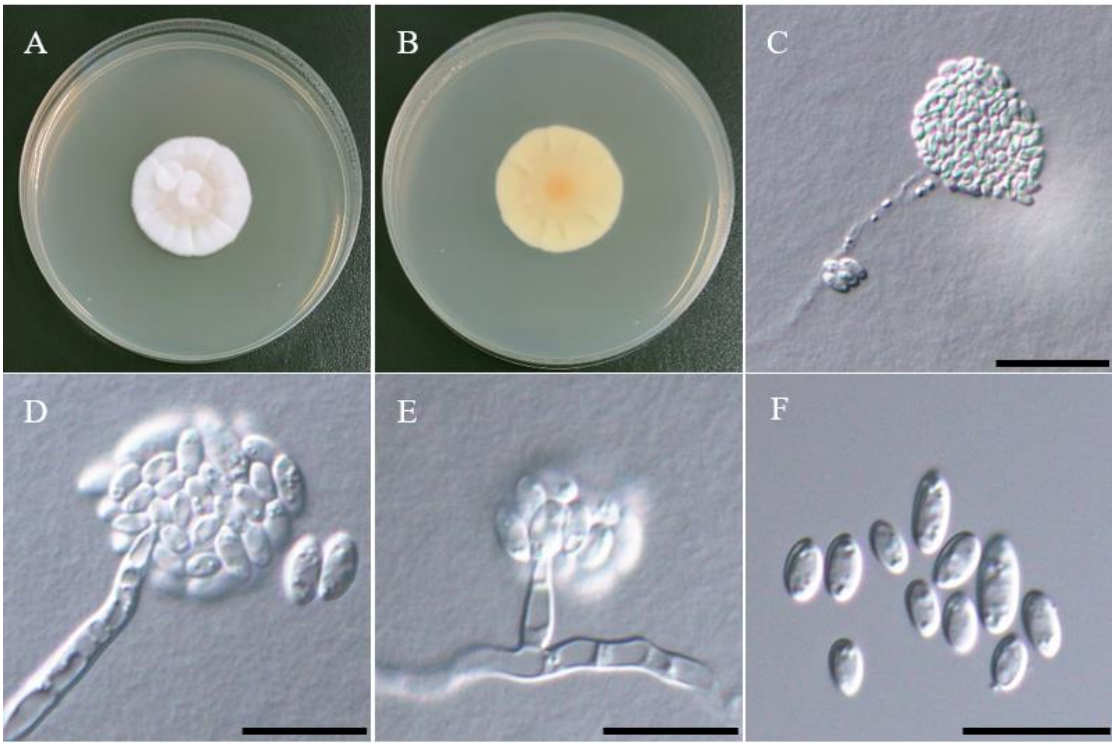

Figure 26. Morphology of *Parasarocladium formosum* NTUPPMCC 22-288 (A)(B) 14-days-old colony on PDA (C)(D)(E) Conidiophores, phialides, and conidiogenous cells (F) Conidia. Scale bars: C = 20 µm D–F = 10 µm.

Phialoparvum

The genus *Phialoparvum* was introduced by Giraldo and Crous (2019) to place *Phialoparvum bifurcatum*, which was isolated from soil habitat in Belgium. Up to date, three species are recognized in MycoBank (Accession date: February 15, 2025) for *Phialoparvum*. The genus was introduced only based in the asexual morph and characterized by its erect, originating directly from vegetative hyphae or hyphal ropes, either unbranched or poorly branched conidiophores (Giraldo and Crous 2019). Conidiogenous cell of this genus is enteroblastic, hyaline, mono-, poly-, and adelophialides, subulate to ampulliform while forming conspicuous collarette. Conidia are cylindrical, hyaline, unicellular, smooth walled, and aggregated in slimy heads (Giraldo et al. 2019). In this study, single strain isolated from Taitung county was clustered within the genus *Phialoparvum* and formed a distinct clade within the genus (Fig. 27). Therefore, new species *Phialoparvum formosana* is proposed to accommodate this strain.

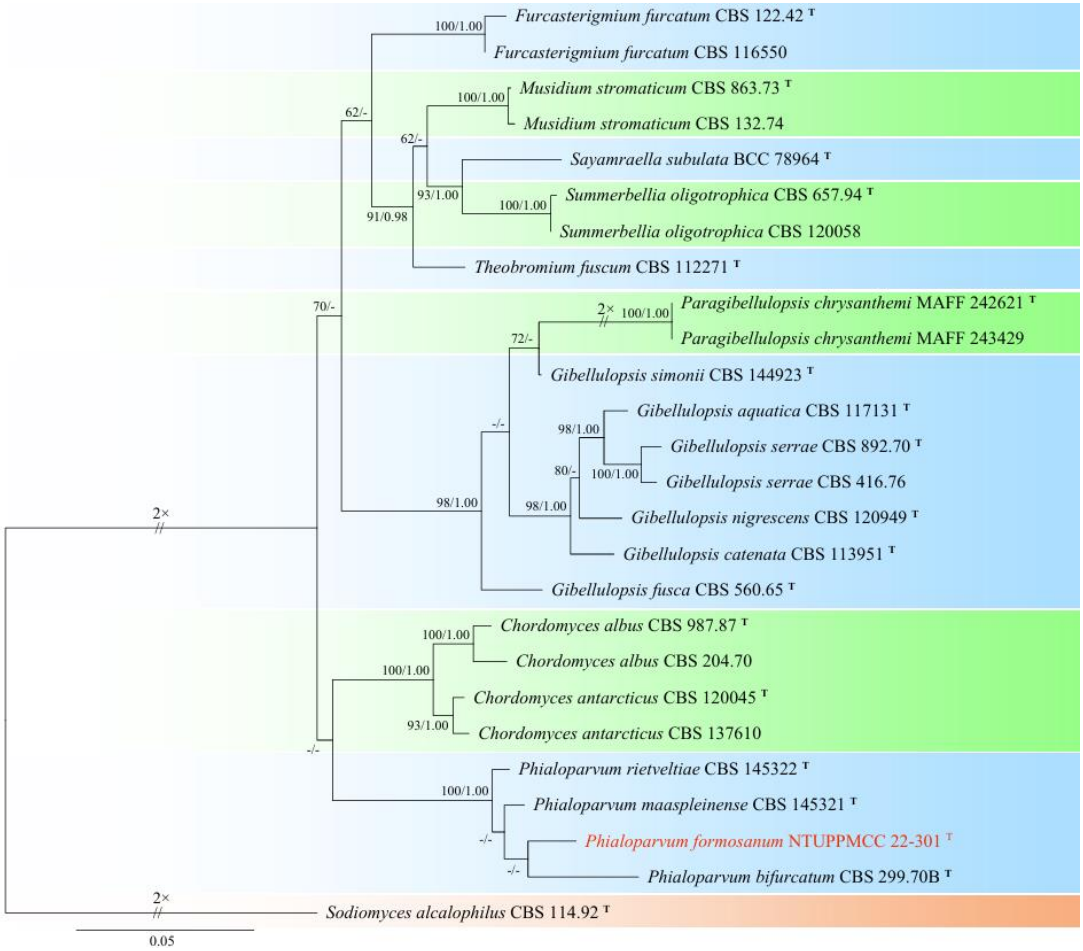

Figure 27. Maximum-likelihood phylogenetic tree based on concatenated sequences of ITS, LSU, *rpb2*, and *tef*-1 for the genus *Phialoparvum*. The tree was rooted with *Sodiomyces alcalophilus* CBS 114.92. MLB ≥ 70% and BPPs ≥ 0.95 were shown at each node; values lower than these thresholds are indicated by a hyphen (–). The scale

bar indicates the number of estimated substitutions per site. The new strain is shown in red. The type strains are marked with ^{T}.

Phialoparvum formosanum K.W. Cheng & H.A. Ariyawansa, sp. nov.

MycoBank: MB858712

Typification: Guanshan Township, Taitung County, Taiwan, 23°02'14.8"N, 121°11'22.6"E, serpentine soil in rice field, 3rd November 2022, K.W. Cheng, holotype, NTUPPMH 227 (Permanently preserved in a metabolically inactive state), ex-holotype NTUPPMCC 22-301.

Etymology: Named after Formosa, the former name of Taiwan, where the type specimen was collected.

Description: On WA medium (NTUPPMCC 22-301). *Sexual morph*: undetermined. *Asexual morph*: *Conidiophores* solitary, hyaline, straight to slightly flexuous, arising from hyphal ropes or vegetative hyphae. *Phialides* subulate to ampulliform, hyaline, terminal or lateral, with conspicuous periclinal thickening and cylindrical collarette, 4–18 µm long. Mono-phialides or adelophialides predominant, few poly-phialides with two conidiogenous loci. *Conidia* cylindrical, hyaline, smooth, thick-walled, 1-celled, with 1 to 2 guttules, sometimes aggregated in clusters forming a slimy head, 1.7–2.4 µm × 3.6–4.6 µm ($\bar{x}$=2.1 × 4.2 µm, L/W ratio=2.04, n=50) (Fig. 28C–F).

Culture characteristics: NTUPPMCC 22-301 exhibited slow growth on PDA medium, reaching a diameter of 30 mm after 14 days at 25°C. The colony was flat, creamy white, and velvety to powdery at the center, gradually thinning toward the edges with a smooth margin. The reverse side of the colony displayed similar characteristics (Fig. 28A–B).

Notes: This investigation presents *Phialoparvum formosanum* as a previously uncharacterized fungal species, identified from a solitary isolate recovered from serpentine soil. Although taxonomic convention favors the examination of multiple strains when establishing new species, obtaining additional specimens proved difficult, presumably due to the organism's specialized ecological requirements and sparse distribution within the sampling area. Nevertheless, extensive morphological evaluation, comprehensive phylogenetic analysis, and genomic characterization robustly support its classification as a distinct taxon (Fig. 27). Multi-locus phylogenetic assessment conclusively differentiates *P. formosanum* from its nearest evolutionary relatives, particularly the ex-type strain of *P. bifurcatum* (CBS 299.70B), with substantial genetic divergence across three critical loci: ITS sequences (showing 96.7% identity, 440/455 bases including gaps), *rpb2* sequences (showing 92.8% identity, 259/279 bases including gaps), and *tef*-1α sequences (showing 96.7% identity, 761/787

bases including gaps). *P. formosanum* NTUPPMCC 22-301 shares typical characteristics of the genus *Phialoparvum*, including hyaline, solitary, arising from hyphal ropes or vegetative hyphae of conidiophores and subulate to ampulliform phialides. However, the conidia of *P. formosanum* NTUPPMCC 22-301 are larger than the type strain of *P. bifurcatum* CBS 299.70B (1.7–2.4 µm × 3.6–4.6 µm versus 1.2–1.8 µm × 2.8–4.4 µm) (Giraldo and Crous, 2019). Additionally, *P. formosanum* exhibits prominent guttules in its conidia, a feature that differentiates it from the other three *Phialoparvum* species (Giraldo and Crous 2019; Giraldo et al. 2019). While this study establishes *P. formosanum* as a distinct species, future studies should aim to recover additional isolates from similar environments to further validate its phenotypic variation and ecological distribution.

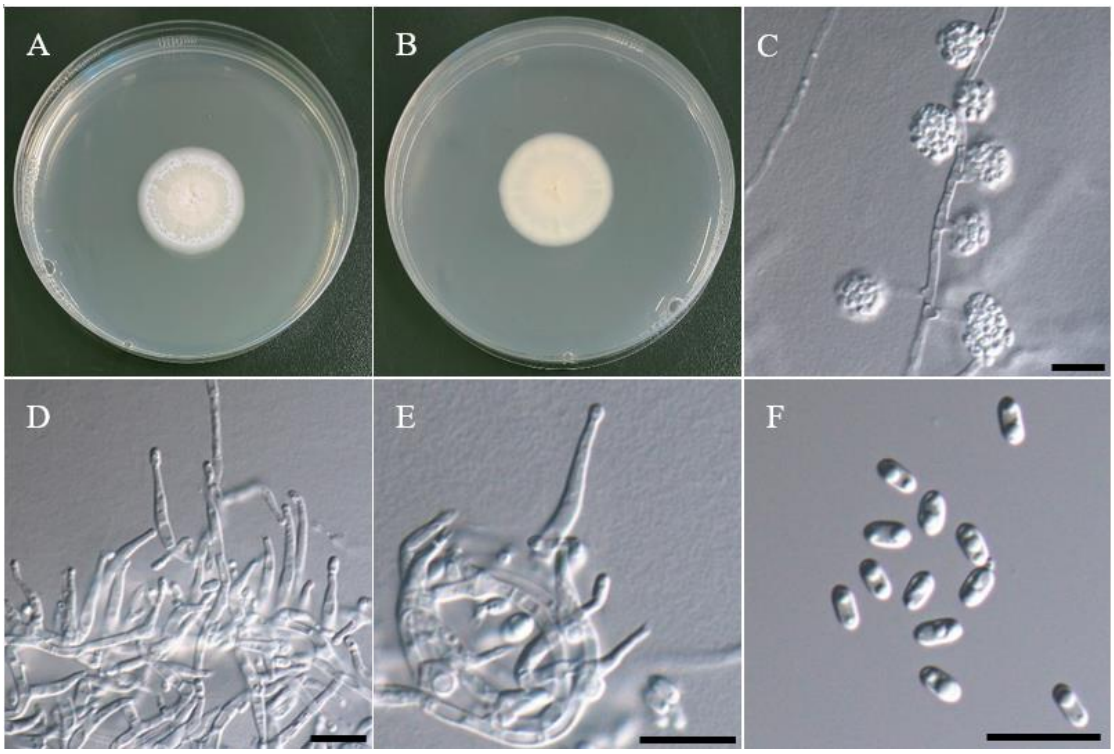

Figure 28. Morphology of *Phialoparvum formosanum* NTUPPMCC 22-301 (A)(B) 14-days-old colony on PDA (C–E) Conidiophores, phialides, and conidiogenous cells (F) Conidia. Scale bars: C–F = 10 µm.

Pseudorhypophila

The genus *Pseudorhypophila* was proposed accommodate four *Zopfiella* species namely, *Zopfiella mangenotii*, *Z. marina*, *Z. pilifera*, and *Z. submersa*, which form a well-supported monophyletic clade within the family Navicularisporaceae in Harms et al. (2021). *Pseudorhypophila* has been reported from Egypt, France, Iraq, Japan, and Taiwan, occurring on substrates such as freshwater, plant debris, soil, and mud (Guarro et al. 1997; Chang et al. 2010; Marin-Felix et al. 2020; Hussien et al. 2023). In this study, six isolates were clustered within the genus *Pseudorhypophila*, and these isolated strain (NTUPPMCC 22-295 to 300) formed a separate clade to other known species (Fig. 29). Therefore, new species *Pseudorhypophila formosana* is proposed to accommodate these strains within the genus.

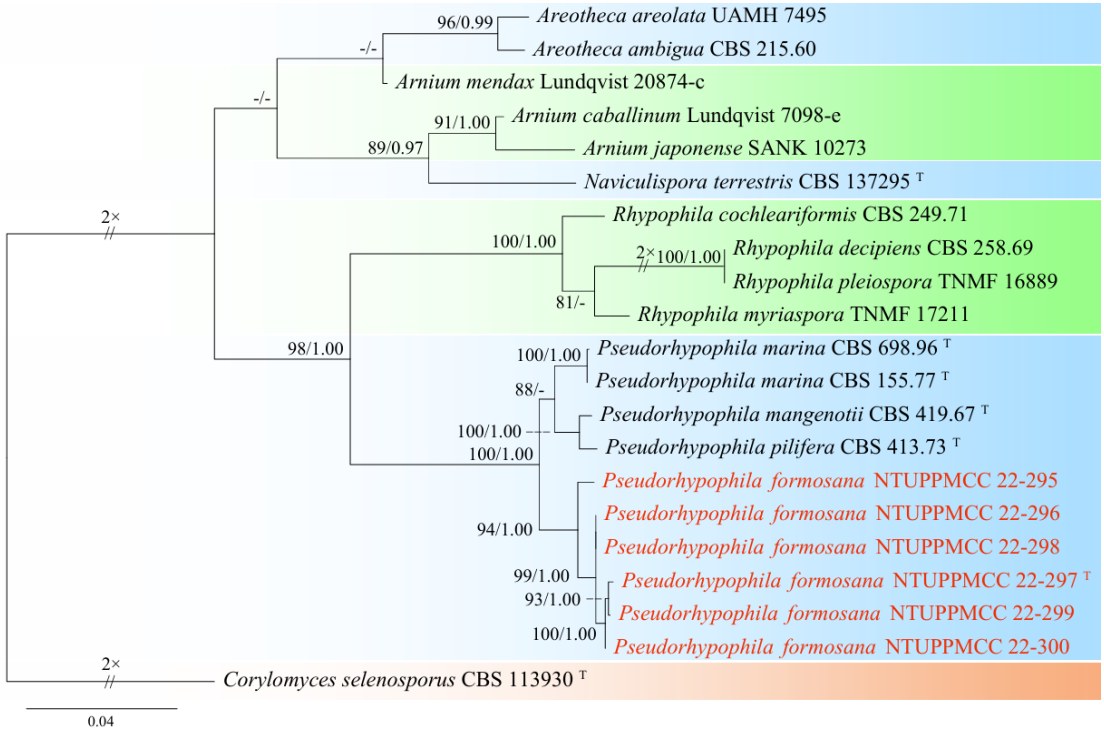

Figure 29. Maximum-likelihood phylogenetic tree based on concatenated sequences of ITS, LSU, and *rpb2* for the genus *Pseudorhypophila*. The tree was rooted with *Corylomyces selenosporus* CBS 113930. MLB ≥ 70% and BPPs ≥ 0.95 were shown at each node; values lower than these thresholds are indicated by a hyphen (–). The scale bar indicates the number of estimated substitutions per site. The new strains are shown in red. The type strains are marked with ^{T}.

Pseudorhypophila formosana K.W. Cheng & H.A. Ariyawansa, sp. nov.

MycoBank: MB858713

Typification: Guanshan Township, Taitung County, Taiwan, 23°02'14.8"N, 121°11'22.6"E, serpentine soil in rice field, 3rd November 2022, K.W. Cheng, holotype, NTUPPMH 22-226 (Permanently preserved in a metabolically inactive state), ex-holotype NTUPPMCC 22-297, ex-isotype NTUPPMCC 22-295, 296, 298 to 300.

Etymology: Named after Formosa, the former name of Taiwan, where the type specimen was collected.

Description: On PDA medium (NTUPPMCC 22-297). *Sexual morph*: *Ascomata* 342–504 µm diam, non-ostiolate, globose, submerged, dirty gray when immature, black when mature. *Peridium* multi-layered, brown, translucent, membranous, angular cells. *Asci* clavate to cylindrical, hyaline when immature, 8-spored, 14.2–20.9 µm × 74.3–111.0 µm ($\bar{x}$=17.8 × 90.9 µm, L/W ratio=5.13, n=20). *Ascospores* two-celled; *upper cell* ellipsoidal to slightly fusiform, smooth, brown, multiple guttules, subapical germ pore, 8.8–12.5 µm × 18.3–24.6 µm ($\bar{x}$=11.0 × 21.3 µm, L/W ratio=1.95, n=50). *Lower cell* cylindrical with slightly tapering or rounded end, hyaline to pale brown, thin-walled, 3.1–5.8 µm × 4.0–8.0 µm ($\bar{x}$=4.3 × 5.8 µm, L/W ratio=1.36, n=50) (Fig. 30C–L). *Asexual morph*: undetermined.

Culture characteristics: NTUPPMCC 22-297 expanded rapidly on PDA medium reaching 80 mm diam after 14 days at 25°C, with flat, sparse aerial mycelium, white, surface and margins slight smooth. The reverse exhibited blackish-gray center, with a gradient radiating outward into lighter gray tones (Fig. 30A–B).

Notes: In the present study, six *Pseudorhypophila* isolates (NTUPPMCC 22-295 to 300) formed a distinct clade separate from known *Pseudorhypophila* species in both single- and multi-locus phylogenies (Fig. 29). In line with earlier research on *P. marina* and *P. pilifera*, our isolate produces ascomata lacking ostioles and bearing 2-celled ascospores, a distinctive trait of the *Pseudorhypophila* (Harms et al. 2021). However, *P. formosana* NTUPPMCC 22-297 is distinguished by its lower cell lengths, which are noticeably smaller than those of the type species, *P. marina* CBS 698.96 (4–8 µm × 3–6 µm versus 6–13 µm × 3–5 µm) (Guarro et al. 1997). Notably, the other representative strain of *P. marina* (*Zopfiella marina* CBS 155.77) was previously reported from Taiwan. However, it also differs from *P. formosana* NTUPPMCC 22-297 in morphology, phylogeny and habitat (marine mud versus terrestrial serpentine soil) (Overy et al. 2014; Harms et al. 2021).

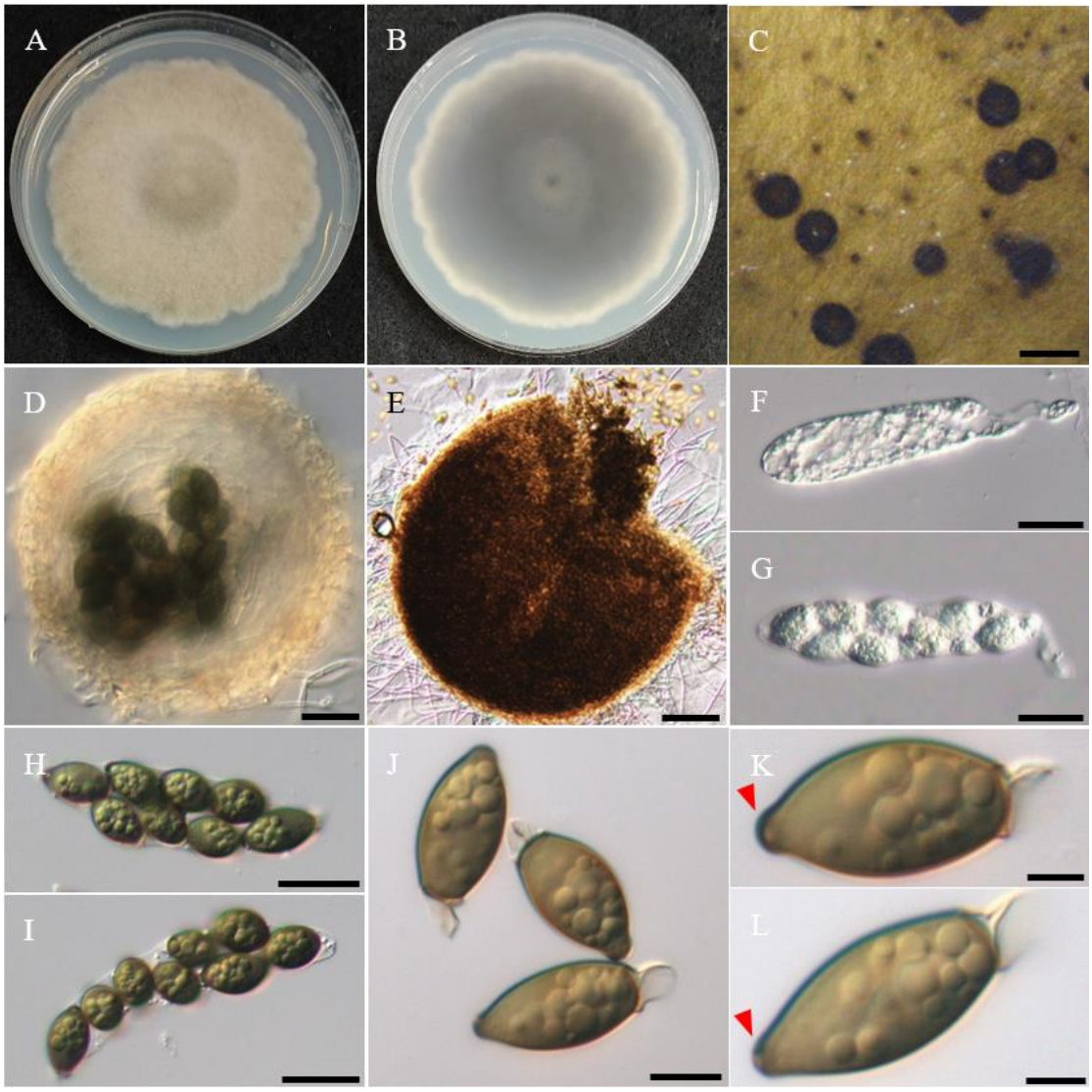

Figure 30. Morphology of *Pseudorhypophila* NTUPPMCC 22-297 (A)(B) 14-days-old colony on PDA (C) Ascomata (D) Immature ascomata (E) Squashed ascomata (F)(G) Immature ascus (H)(I) Ascus (J) Ascospores (K)(L) Ascospores (red arrows: subapical germ pores). Scale bars: C = 0.5 mm; E = 100 µm; D, F–I = 20 µm; J = 10 µm K–L = 5 µm.

Pseudothielavia

The genus *Pseudothielavia* was initially proposed by Wang and Houbraken (2019), to placed *Coniothyrium terricola*, which is initially isolated from soil habitat. In recent years several species were introduced in this genus and currently four species epithets are listed in MycoBank (Accession date: February 15, 2025) for *Pseudothielavia.* Species reported for *Pseudothielavia* are widely distributed and have been reported from Chile, China, Egypt, Japan, Papua New Guinea, and USA mainly from soil habitats (Wang et al. 2019; Zhang et al. 2021; Noguchi et al. 2022; Hussien et al. 2023). In this study, two isolates (NTUPPMCC 22-293 and NTUPPMCC 22-294) were clustered within the genus *Pseudothielavia* and grouped within the clade (Fig. 31).

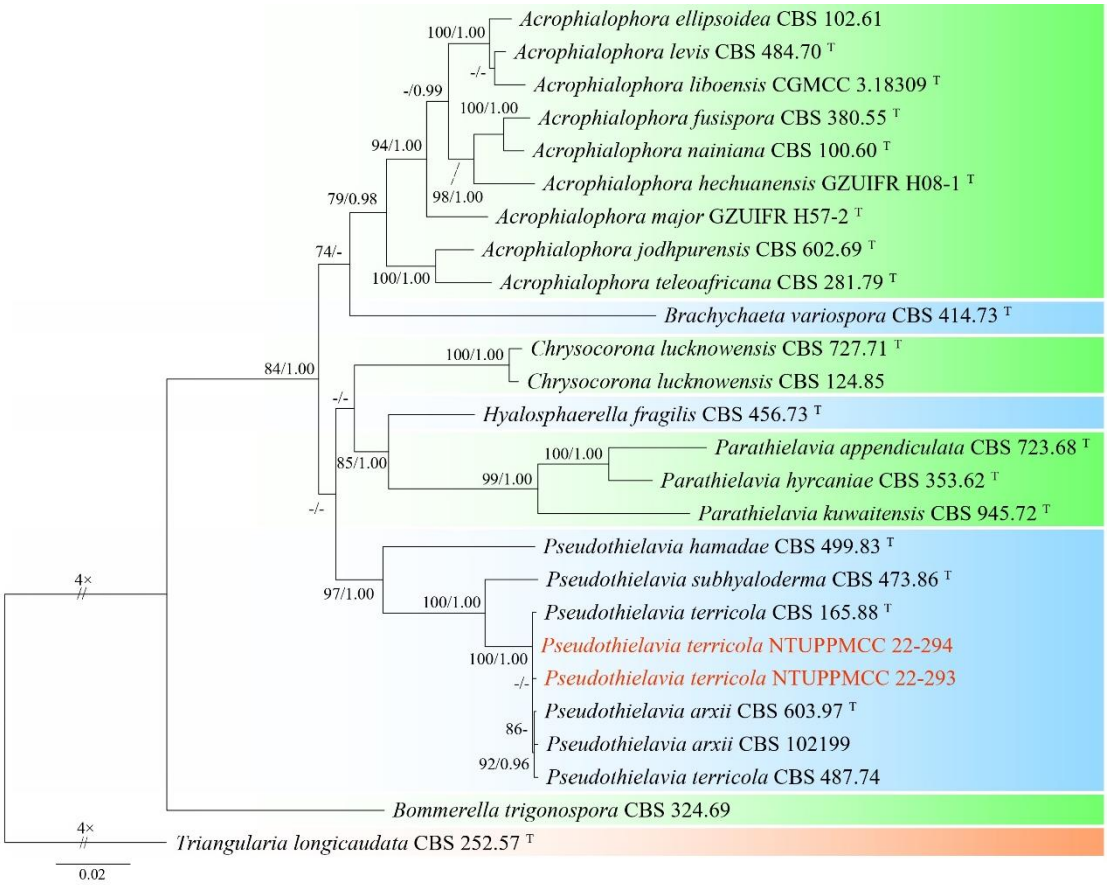

Figure 31. Maximum-likelihood phylogenetic tree based on concatenated sequences of ITS, LSU, *rpb2*, and *tub2* for the genus *Pseudothielavia*. The tree was rooted with *Triangularia longicaudata* CBS 252.57. MLB ≥ 70% and BPPs ≥ 0.95 were shown at each node; values lower than these thresholds are indicated by a hyphen (–). The scale bar indicates the number of estimated substitutions per site. The new strains are shown in red. The type strains are marked with ^{T}.

Pseudothielavia terricola X.W. Wang & Houbraken (2019)

MycoBank: MB829876

Description: On PDA medium (NTUPPMCC 22-294). *Sexual morph*: *Cleistothecia* 105–145 µm diam, non-ostiolate, globose, glabrous, black when mature, solitary to aggregated, mostly superficial, some submerged, aerial mycelium covered. *Peridium* brown, semi-translucent, membranous, *textura epidermoidea*. *Asci* subglobose to pyriform, hyaline when immature, 8-spored, 23.7–27.0 µm × 20.5–23.5 µm ($\bar{x}$=22.5 × 25.5 µm, L/W ratio=1.13, n=10). *Ascospores* 1 celled, olivaceous brown when mature, subglobose to ellipsoidal, some smooth, apical germ pore, 9.3–11.7 µm × 6.7–9.0 µm ($\bar{x}$=7.6 × 10.5 µm, L/W ratio=1.39, n=20) (Fig. 32C–F). *Asexual morph*: undetermined.

Culture characteristics: NTUPPMCC 22-294 on PDA medium reaching 50 mm diam after 14 days at 25°C, predominantly white with thick white aerial mycelium, fluffy, edge irregularly, wavy margin, and similar to reverse side of the colony (Fig. 32A–B).

Material examined: Guanshan Township, Taitung County, Taiwan, 23°02'12.8"N, 121°11'22.0"E, serpentine soil in rice field, 2nd November 2022, K.W Cheng, living culture NTUPPMCC 22-293 and NTUPPMCC 22-294.

Notes: Two strains (NTUPPMCC 22-293 and NTUPPMCC 22-294) isolated in this study clustered within the clade containing ex-type strains, along with other representative strains of *P. arxii* and *P. terricola*, with strong statistical support (Fig. 31). Although both *P. arxii* and *P. terricola* exhibited no clear phylogenetic variation in our tree or in previous studies, they can be distinguished by differences in ascospore morphology (Wang et al. 2019). The morphology of our strain (NTUPPMCC 22-294) exhibited an apical germ pore, similar to that of *P. terricola* (CBS 165.88). According to its original description (Wang et al. 2019; Noguchi et al. 2022), *P. arxii* lacks an apical germ pore and instead possesses an oblique to lateral germ pore.Therefore, based solely on morphological similarity, we identified our strain as *P. terricola*. However, further studies are required to determine whether *P. arxii* and *P. terricola* represent two distinct species or a single species. This study represents the first discovery of a *Pseudothielavia* species in Taiwan.

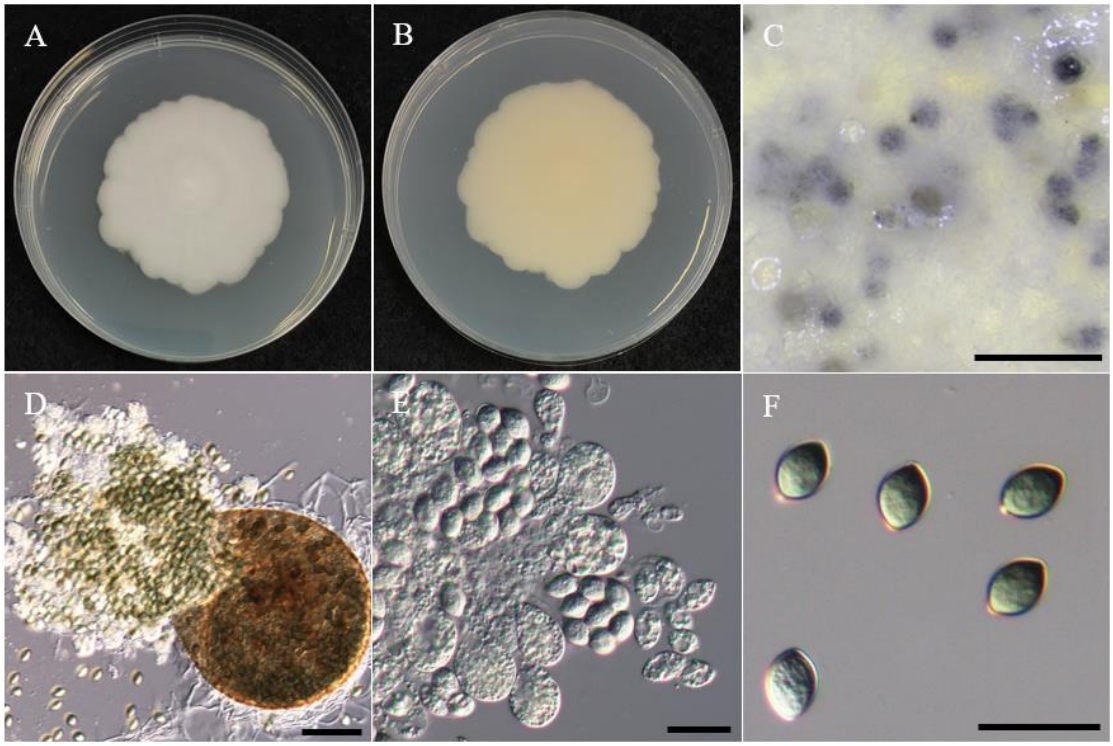

Figure 32. Morphology of *Pseudothielavia terricola* NTUPPMCC 22-294 (A)(B) 14-days-old colony on PDA (C) Ascomata (D) Squashed ascomata (E) Immature ascus (F) Ascospores. Scale bars: C = 1 mm; D = 50 µm E–F = 20 µm.

Reticulascus

Reticulascus tulasneorum originally isolated from *Sambucus nigra* in Czech Republic was used by Réblová and Gams (2011) to establish the genus *Reticulascus*. Up to date, three species are recognized for *Reticulascus* in MycoBank (Accession date: February 15, 2025). *Reticulascus* strains has been reported from Czech Republic, France, Germany, and Netherlands as a saprobe on dead wood (Réblová et al. 2011; Crous et al. 2022). In this study, two isolates (NTUPPMCC 22-286 and NTUPPMCC 22-287) were clustered within the genus *Reticulascus* and formed a separate clade to other known species (Fig. 33). Thus, *Reticulascus formosana* is proposed to accommodate these strains within the genus.

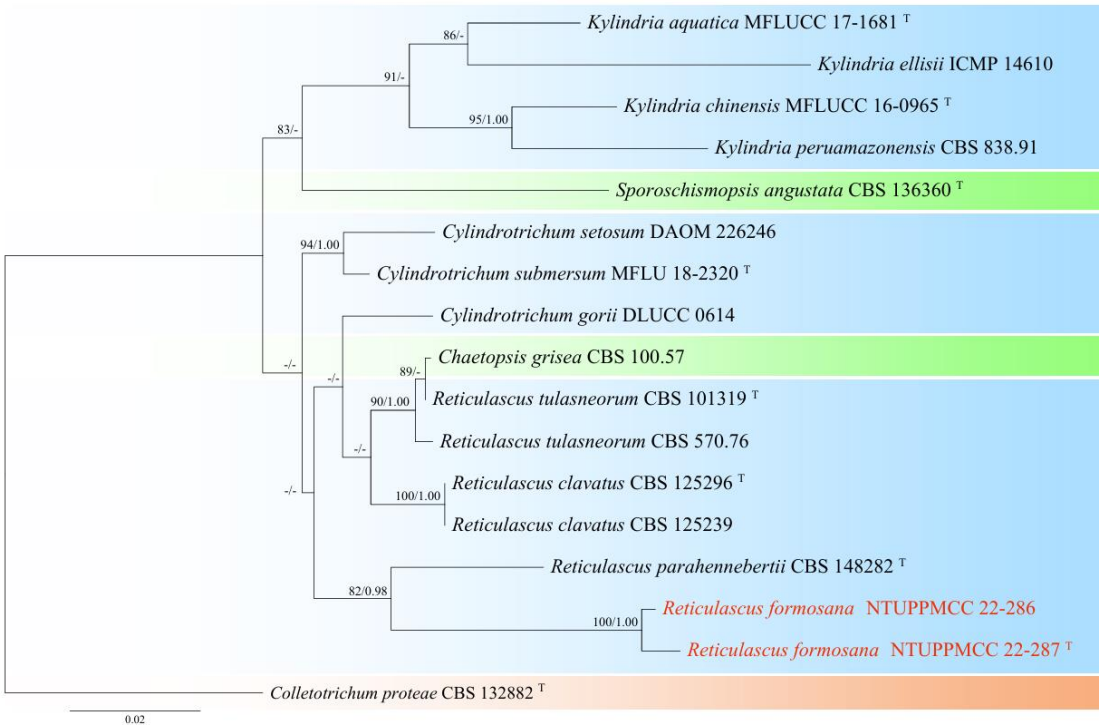

Figure 33. Maximum-likelihood phylogenetic tree based on concatenated sequences of ITS and LSU for the genus *Reticulascus*. The tree was rooted with *Colletotrichum proteae* CBS 132882. MLB ≥ 70% and BPPs ≥ 0.95 were shown at each node; values lower than these thresholds are indicated by a hyphen (–). The scale bar indicates the number of estimated substitutions per site. The new strains are shown in red. The type strains are marked with ^{T}.

Reticulascus formosana K.W. Cheng & H.A. Ariyawansa, sp. nov.

MycoBank: MB858714

Typification: Guanshan Township, Taitung County, Taiwan, 23°02'12.8"N, 121°11'22.0"E, serpentine soil in rice field, 2nd November 2022, K.W Cheng, holotype, NTUPPMH 22-220 (Permanently preserved in a metabolically inactive state), ex-holotype NTUPPMCC 22-287, ex-isotype NTUPPMCC 22-286.

Etymology: Named after Formosa, the former name of Taiwan, where the type specimen was collected.

Description: On carnation leaves (*Dianthus caryophyllus*) supplanted on WA (NTUPPMCC 22-287). *Sexual morph*: undetermined. *Asexual Morph*: *Conidiophores* solitary, subcylindrical, light brown, unbranched, straight to slightly flexuous, and thick-walled. *Conidiogenous cells* subcylindrical, light brown to light gray, terminal or intercalary, with flared collarettes. *Conidia* solitary or aggregated in clusters, subcylindrical to slightly curved, with an obtuse apex, guttules, hyaline, smooth-walled, and 0 to 3-septate, 3.8–6.1 µm × 13.4–19.9 µm ($\bar{x}$=4.6 × 16.3 µm, L/W ratio=3.6, n=50). *Chlamydospores* rusty copper-brown, circular to slightly elliptical, clustered 1–3 on PDA and 1.5% WA. Single chlamydospores 6.1–8.9 µm × 5.9–8.4 µm ($\bar{x}$=7.3 × 7.2 µm, L/W ratio=3.6, n=50) (Fig. 34C–L).

Culture characteristics: NTUPPMCC 22-287 on PDA medium reaching 60 mm diam after 30 days at 25°C, with flat, spreading, gray margin and dark gray blue in the center, reverse similar (Fig. 34A–B).

Notes: *Reticulascus formosana* NTUPPMCC 22-287 is typical of *Reticulascus* in having straight to flexuous, brown, subcylindrical conidiophores, terminal or intercalary conidiogenous cells with flared collarettes, and subcylindrical, smooth, hyaline conidia (Réblová et al. 2011; Crous et al. 2022). However, our strains (NTUPPMCC 22-286 and NTUPPMCC 22-287) can be easily differentiated from its closely related species based on both morphology and phylogeny (Fig. 33). *R. formosana* NTUPPMCC 22-287 forme larger conidia compared to *R. parahennebertii* ($\bar{x}$=16.3 × 4.6 µm versus 13.5 × 3.8 µm). Moreover, *R. formosana* NTUPPMCC 22-287 forms 0 to 3-septate conidia but *R. parahennebertii* is known to form distinct 3-septate (Crous et al. 2022).

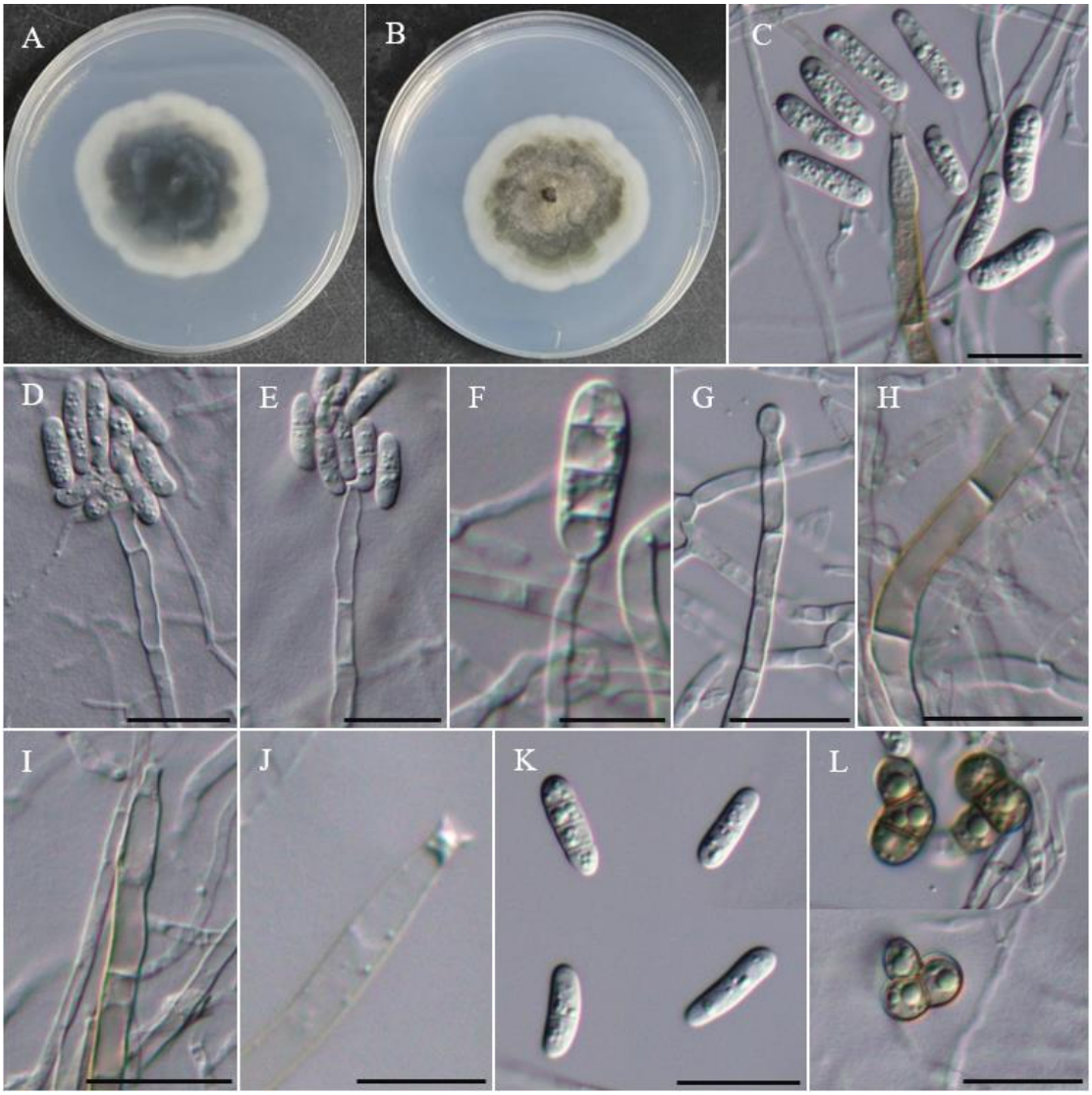

Figure 34. Morphology of *Reticulascus formosana* NTUPPMCC 22-287 (A)(B) 14-days-old colony on PDA (C–G) Conidiophores and conidiogenous cells giving rise to conidia (H)(I) Conidiophore (J) Conidiogenous cells (K) Conidia (L) Chlamydospores. Scale bars: C–E, G–I, K–L = 20 µm; F, J = 10 µm.

Sarocladium

The genus *Sarocladium* was introduced by Gams and Hawksworth (1975) to accommodate two rice (*Oryza sativa*) pathogens, *S. oryzae* and *S. attenuatum*, with the former as type species. Currently, 37 species epithets are recognized for *Sarocladium* in Mycobank (Accession date: February 15, 2025). *Sarocladium* has a global distribution (Ou et al. 2020). Species in *Sarocladium* have been reported as plant pathogens of rice and apple fruit and some species reported as opportunistic human pathogens, and saprophytic fungi in soil or plant debris. Furtheremore, recent studies have reported them as endophytes in tropical grasses, coastal grass, and crops (Yeh and Kirschner 2014; Giraldo et al. 2015; Gonzáles-Teuber et al. 2017; Hou et al. 2019; Anjos et al. 2020; Ou et al. 2020). In this study, two isolates namely, NTUPPMCC 22-289 and NTUPPMCC 22-290 clustered within the genus *Sarocladium* and formed a two distinct clades within the genus (Fig. 35). Therefore, two novel taxa are proposed to accommodate these strains in the genus *Sarocladium*.

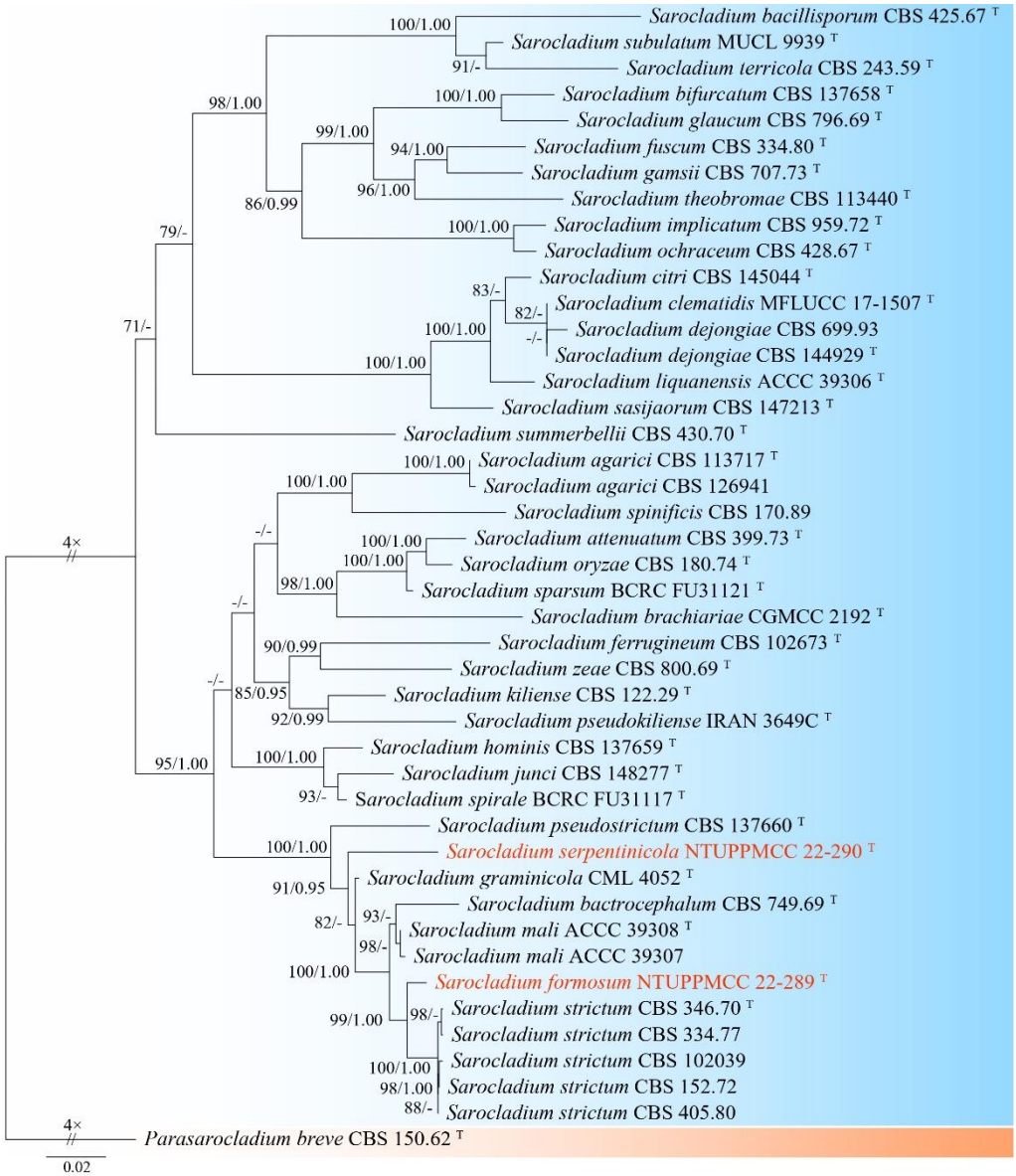

Figure 35. Maximum-likelihood phylogenetic tree based on concatenated sequences of ITS, LSU, *rpb2*, and *tef*-1 for the genus *Sarocladium*. The tree was rooted with *Parasaroocladium breve* CBS 150.62. MLB ≥ 70% and BPPs ≥ 0.95 were shown at each node; values lower than these thresholds are indicated by a hyphen (–). The scale bar indicates the number of estimated substitutions per site. The new strains are shown in red. The type strains are marked with ^{T}.

Sarocladium formosum K.W. Cheng & H.A. Ariyawansa, sp. nov.

MycoBank: MB858715

Typification: Guanshan Township, Taitung County, Taiwan, 23°02'17.6"N, 121°11'26.3"E, serpentine soil in rice field, 3rd November 2022, K.W. Cheng, holotype, NTUPPMH 22-222 (Permanently preserved in a metabolically inactive state), ex-holotype NTUPPMCC 22-289.

Etymology: Named after Formosa, the former name of Taiwan, where the type specimen was collected.

Description: On WA medium (NTUPPMCC 22-289). *Sexual morph*: undetermined. *Asexual morph*: *Conidiophores* solitary, hyaline, straight to slightly flexuous, smooth-walled, arising from hyphal ropes or vegetative hyphae. *Phialides* subulate, hyaline, wide at the base, with, 13–30 µm long. *Adelophialides* and *schizophialides* not observed. *Conidia* unicellular, cylindrical with rounded ends, hyaline, smooth-walled, 1-celled, few with inconspicuous 1 to 2 guttules on the end(s), sometimes aggregated in clusters forming a slimy head, 1.1–2.1 µm × 3.5–5.3 µm ($\bar{x}$=1.5 × 4.4 µm, L/W ratio=3.08, n=50) (Fig. 36C–F).

Culture characteristics: NTUPPMCC 22-289 exhibited slow growth on PDA medium, reaching a diameter of 35 mm after 14 days at 25°C. The colony was flat, pale orange, wrinkled in the center, slimy, and smooth margin. The reverse side of the colony displayed similar characteristics (Fig. 36A–B).

Notes: This study describes *Sarocladium formosum* as a novel species based on a single strain isolated from serpentine soil. While it is ideal to check multiple strains when introducing a new species, isolating additional strains of this fungus demonstrated challenging due to its ecological niche and low abundance in the sampled environment. However, the species is well-supported as distinct, based on comprehensive morphological and phylogenetic evidence (Fig. 35). A multi-locus phylogenetic analysis clearly separates *S. formosum* from its closest relative, *S. strictum* (CBS 346.70), showing significant genetic divergence in two loci: *rpb2* (identities = 677/710, 95.4% including gaps) and *tef-1* (identities = 799/808, 98.9% including gaps). *S.*

formosum shares typical characteristics to the sister species *S. strictum*, with pale orange culture on PDA, producing conidia in slimy heads and lacking scyzophialides (Giraldo et al. 2015). However, guttules on conidia was observed in *S. formosum* NTUPPMCC 22-289. Several *Sarocladium* species have been recorded in Taiwan. *S. spinificis* was reported as an endophyte of the coastal grass *Spinifex littoreus* (Yeh and Kirschner 2014), while *S. attenuatum*, *S. oryzae*, *S. sparsum*, and *S. spirale* were isolated from rice grains and leaf sheaths (Ou et al. 2020). However, our species, *S. formosum* and *S. serpentinicola*, were isolated from serpentine environments and formed distinct clades from these previously reported species in the phylogeny. While this study establishes *S. formosum* as a distinct species, future studies should aim to recover additional isolates from similar environments to further validate its phenotypic variation and ecological distribution.

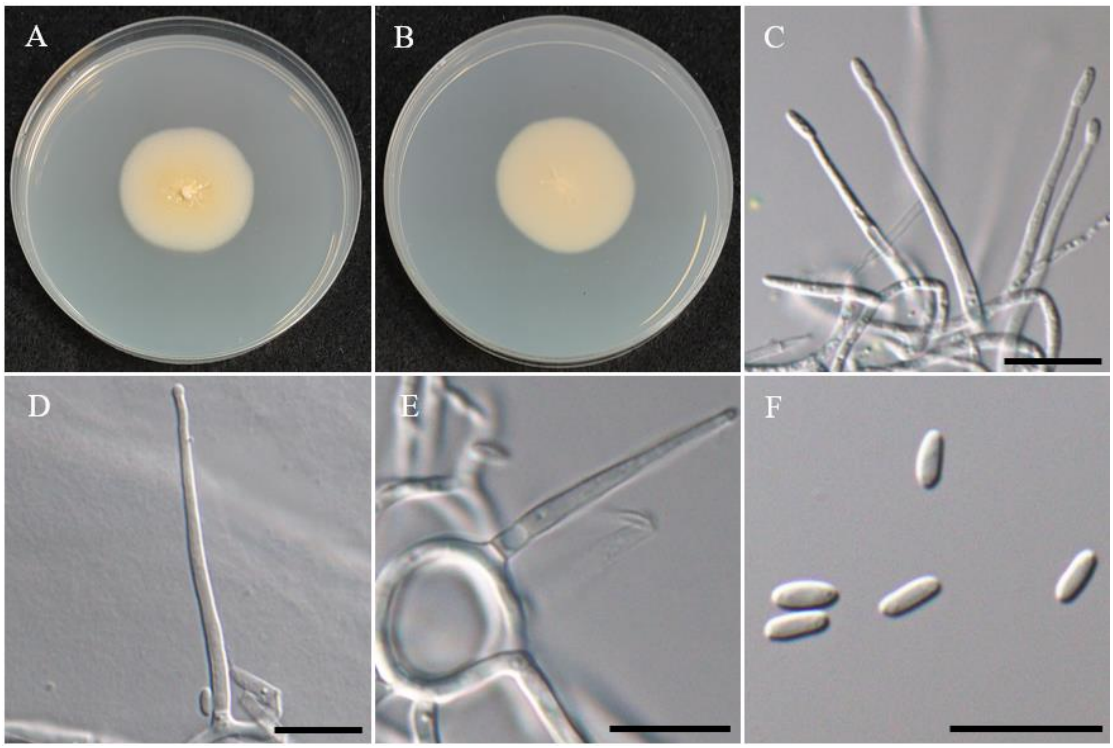

Figure 36. Morphology of *Sarocladium formosum* NTUPPMCC 22-289 (A)(B) 14-days-old colony on PDA (C)(D) Conidiophores and phialides (E)(F) Adelophialides (G) Conidia. Scale bars: C–G = 10 µm.

Sarocladium serpentinicola K.W. Cheng & H.A. Ariyawansa, sp. nov.

MycoBank: MB858716

Typification: Guanshan Township, Taitung County, Taiwan, 23°02'14.8"N, 121°11'22.6"E, serpentine soil in rice field, 3rd November 2022, K.W. Cheng, holotype, NTUPPMH 22-223 (Permanently preserved in a metabolically inactive state), ex-holotype NTUPPMCC 22-290.

Etymology: Named after the serpentine soil from which the species was isolated.

Description: On WA medium (NTUPPMCC 22-290). *Sexual morph*: undetermined. *Asexual morph*: *Conidiophores* solitary, hyaline, straight to slightly flexuous, smooth-walled, arising from hyphal ropes or vegetative hyphae. *Phialides* subulate, hyaline, wide at the base, with, 23–32 µm long. *Schizophialides* not observed. *Conidia* unicellular, cylindrical with rounded ends, hyaline, smooth-walled, 1-celled, few with inconspicuous 1 to 2 guttules on the end(s), sometimes aggregated in clusters forming a slimy head, 1.2–1.8 µm × 3.2–5.5 µm ($\bar{x}$=1.5 × 4.3 µm, L/W ratio=2.92, n=30). *Adelophialides* observed, 3.6–8.8 µm long and sporulated obvious guttules and larger conidia, 1.6–2.5 µm × 3.8–7.0 µm ($\bar{x}$=2.0 × 5.3 µm, L/W ratio=2.73, n=30) (Fig. 37C–G).

Culture characteristics: NTUPPMCC 22-290 exhibited slow growth on PDA medium, reaching a diameter of 30 mm after 14 days at 25°C. The colony was flat, pale orange, slightly wrinkled in the center, slimy, and smooth margin. The reverse side of the colony displayed similar characteristics (Fig. 37A–B).

Notes: This investigation introduces *Sarocladium serpentinicola* as a previously undescribed fungal species, characterized from a single isolate recovered from serpentine soil. Although taxonomic best practices recommend analyzing multiple strains when establishing new species, additional specimens proved elusive, presumably due to the organism's specialized habitat requirements and relative scarcity within the sampling area. Nevertheless, thorough morphological assessment and multi-locus phylogenetic analysis strongly support its recognition as a distinct taxon (Fig. 35). Phylogenetic evaluation across multiple genetic markers clearly distinguishes *S. serpentinicola* from its nearest relative, *S. pseudostrictum* (CBS 137660), with notable genetic differentiation in three key loci: ITS sequences (showing 97.1% identity, 464/478 bases including gaps), LSU sequences (showing 98.8% identity, 506/512 bases), and *tef*-1α sequences (showing 96.0% identity, 776/808 bases including gaps). *S. formosum* NTUPPMCC 22-289 can be distinguished from its close relatives *S. pseudostrictum* and *S. graminicola* by the absence of adelophialides, which are present in the latter (Giraldo et al. 2015; Anjos et al. 2020). Although our research confirms *S. serpentinicola* as a valid taxonomic entity, subsequent investigations should target additional specimens from comparable serpentine habitats to better characterize its

morphological diversity and environmental distribution patterns.

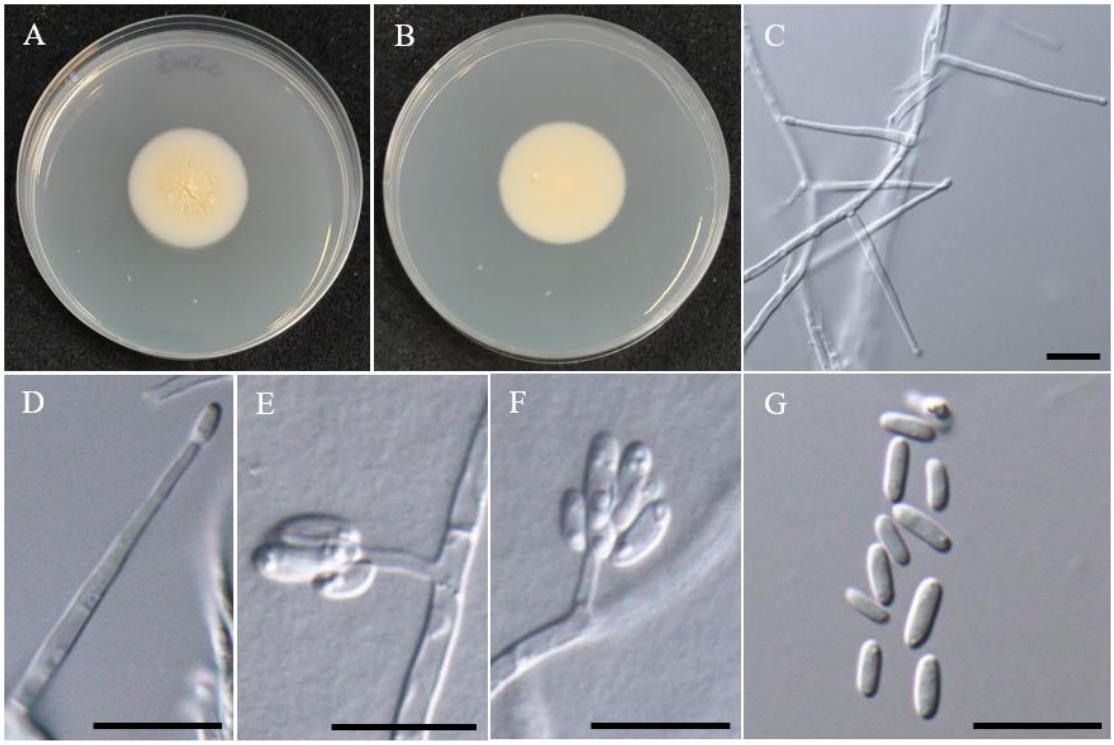

Figure 37. Morphology of *Sarocladium serpentinicola* NTUPPMCC 22-290 (A)(B) 14-days-old colony on PDA (C)(D) Conidiophores and phialides (E)(F) Adelophialides (G) Conidia. Scale bars: C–G = 10 µm.

Discussion

The present study delivers the first comprehensive analysis of culturable fungal flora in serpentine-characterized paddy soils of eastern Taiwan. Thes results of the present study reveal a unique mycobiota dominated by Dothideomycetes (60% of isolates), with *Westerdykella*, *Pyrenochaetopsis*, and *Talaromyces* as the most frequently isolated genera. This contrasts with previous studies of serpentine soils, where *Aspergillus*, *Cladosporium*, and *Penicillium* were frequently isolated as dominant taxa (Pal et al. 2007; Daghino et al. 2012). The lack of these genera in our study may reveal ecological specialization tied to agricultural practices. For example, paddy soils are periodically flooded, creating anaerobic conditions that favor fungal group such as *Westerdykella* and *Pyrenochaetopsis*, which are frequently reported from waterlogged or plant-associated environments (Goh et al. 2021; Surono et al. 2023). Moreover, the use of half-strength media to suppress fast-growing fungi may have selectively enriched slower-growing, stress-adapted species, further shaping community composition (Su et al. 2012). Especially, 12 genera mainly including *Dimorphiseta*, *Parasarocladium*, and *Poaceascoma* are reported for the first time in serpentine environments, highlighting the ecological uniqueness of these metal-rich soils. It is noteworthy that *Poaceascoma serpentinum* represents the first documented asexual morph within its genus, suggesting adaptive strategies such as reduced sexual reproduction in response to heavy metal stress (Ali 2007; Gajewska et al. 2022; Zhang et al. 2024). The discovery of 11 novel species and 11 new records for Taiwan highlights serpentine ecosystems as reservoirs of fungal diversity and endemism, consistent with the high species abundance observed in other extreme environments (Oze et al. 2008).

Notably, in our study, 35% of the strains belong to *Westerdykella*. It is worth conducting further research to understand the role this genus plays in serpentine paddy fields. In a previous study, *Westerdykella aquatica* P71, a phylogenetically close relative of the strains isolated in this study, demonstrated mercury phytotoxicity mitigation in maize (Senabio et al. 2023). This suggests that the isolates identified in our study could serve as promising candidates for bioremediation, particularly in agricultural systems impacted by serpentine-derived heavy metals. Future studies should quantify their metal uptake capacities and evaluate their symbiotic potential with crops to enhance phytostabilization. The genus *Sarocladium* is commonly associated with rice pathogens (Pramunadipta et al. 2020). Several *Sarocladium* species, including *S. attenuatum*, *S. oryzae*, *S. sparsum*, and *S. spirale*, have been reported in Taiwan paddy fields prior to this study (Ou et al. 2020). In our study, we have identified two novel species of *Sarocladium*. However, since our strains were isolated from soil, further examination is needed to determine whether these species have pathogenicity towards rice. Additionally, *Sarocladium* species have been isolated from coal mine soil

and have exhibited high levels of resistance to cadmium (Zhang et al. 2024). Thus, further research is essential to investigate whether these strains have the ability to develop as a potential bio-remediation agent against cadmium.

Phylogenetic analyses discovered significant genetic divergence in novel species represented by a single isolate, such as *Poaceascoma serpentinum* nov. sp. (ITS sequence identity <89% with closest relatives), supporting their classification as distinct taxa as proposed in this study. However, the reliance on single strain for some species descriptions (e.g., *Dimorphiseta formosana* nov. sp.) highlights a limitation common in studies of rare environmental fungi (Crous et al. 2018a; Hurdeal et al. 2022). Although polyphasic taxonomy offers initial taxonomic insights, systematic sampling across different seasonal contexts and microhabitats represents a critical next step in resolving species delimitations and characterizing their ecological potential.

A key limitation of this study is its focus on culturable fungi, which likely underestimates the total fungal diversity. Metagenomic approaches, such as ITS amplicon sequencing, could uncover non-culturable taxa and provide comprehensive insights into community functional profiles (Koner et al. 2023). Additionally, linking fungal diversity to soil physicochemical parameters (e.g., Ni/Cr concentrations, pH) would help elucidate the relative impacts of metal toxicity and edaphic factors in shaping microbial community structure. In conclusion, our research expands the frontiers of fungal ecology by uncovering the remarkable adaptive capabilities of microorganisms in serpentine ecosystems. The predominance of asexual morphs and exceptional metal tolerance reveal the significant evolutionary strategies of fungal communities under extreme stress. By integrating fundamental research with multi-omics approaches and targeted field trials, we open promising avenues for understanding microbial adaptation with potential applications in phytoremediation, sustainable agriculture, and ecosystem management.

References

Absalan S, Armand A, Jayawardena RS, McKenzie EH, Hyde KD, Lumyong S (2024) Diversity of Pleosporalean Fungi Isolated from Rice (*Oryza sativa* L.) in Northern Thailand and Descriptions of Five New Species. Journal of Fungi 10(11): 763. https://doi.org/10.3390/jof10110763

Airin AA, Arafat MI, Begum RA, Islam MR, Seraj ZI (2023) Plant growth-promoting endophytic fungi of the wild halophytic rice *Oryza coarctata*. Annals of Microbiology 73(1): 36. https://doi.org/10.1186/s13213-023-01738-3

Alexander EB (2004) Serpentine soil redness, differences among peridotite and serpentinite materials, Klamath Mountains, California. International Geology

Review 46(8): 754–764. https://doi.org/10.2747/0020-6814.46.8.754

Ali EH (2007) Comparative study of the effect of stress by the heavy metals Cd, Pb, and Zn on morphological characteristics of *Saprolegnia delica* Coker and *Dictyuchus carpophorus* Zopf. Polish Journal of Microbiology 56(4): 257–264.

Angelini P, Rubini A, Gigante D, Reale L, Pagiotti R, Venanzoni R (2012) The endophytic fungal communities associated with the leaves and roots of the common reed (*Phragmites australis*) in Lake Trasimeno (Perugia, Italy) in declining and healthy stands. Fungal Ecology 5(6): 683–693. https://doi.org/10.1016/j.funeco.2012.03.001

Anjos RM, Moreira SI, Costa SS, Abreu LM, Alves E, Cardoso PG (2020) *Sarocladium graminicola*, a new endophytic species from tropical grasses. Mycological Progress 19(6): 605–614. https://doi.org/10.1007/s11557-020-01585-5

Arenal F, Platas G, Pelaez F (2007) A new endophytic species of *Preussia* (Sporormiaceae) inferred from morphological observations and molecular phylogenetic analysis. Fungal Diversity 25: 1-17.

Ariyawansa HA, Tsai I, Thambugala KM, Chuang WY, Lin SR, Hozzein WN, Cheewangkoon R (2020) Species diversity of Pleosporalean taxa associated with *Camellia sinensis* (L.) Kuntze in Taiwan. Scientific Reports 10(1): 12762. https://doi.org/10.1038/s41598-020-69718-0

Benjamin CR (1955) Ascocarps of *Aspergillus* and *Penicillium*. Mycologia 47(5): 669-687. https://doi.org/10.1080/00275514.1955.12024485

Bonifacio E, Zanini E, Boero V, Franchini-Angela M (1997) Pedogenesis in a soil catena on serpentinite in north-western Italy. Geoderma 75(1-2): 33–51. https://doi.org/10.1016/S0016-7061(96)00076-6

Boonmee S, Wanasinghe DN, Calabon MS, Huanraluek N, Chandrasiri SKU, Jones EBG, Rossi W, Leonardi M, Singh SK, Rana S, Singh PN, Maurya DK, Lagashetti AC, Choudhary D, Dai Y-C, Zhao C-L, Mu Y-H, Yuan H-S, He S-H, Phookamsak R, Jiang H-B, Martín MP, Dueñas M, Telleria MT, Kałucka IL, Jagodziński AM, Liimatainen K, Pereira DS, Phillips AJL, Suwannarach N, Kumla J, Khuna S, Lumyong S, Potter TB, Shivas RG, Sparks AH, Vaghefi N, Abdel-Wahab MA, Abdel-Aziz FA, Li G-J, Lin W-F, Singh U, Bhatt RP, Lee HB, Nguyen TTT, Kirk PM, Dutta AK, Acharya K, Sarma VV, Niranjan M, Rajeshkumar KC, Ashtekar N, Lad S, Wijayawardene NN, Bhat DJ, Xu RJ, Wijesinghe SN, Shen HW, Luo ZL, Zhang JY, Sysouphanthong P, Thongklang N, Bao DF, Aluthmuhandiram JVS, Abdollahzadeh J, Javadi A, Dovana F, Usman M, Khalid AN, Dissanayake AJ, Telagathoti A, Probst M, Peintner U, Garrido-Benavent I, Bóna L, Merényi Z, Boros L, Zoltán B, Stielow JB, Jiang N, Tian CM, Shams E, Dehghanizadeh F, Pordel A, Javan-Nikkhah M, Denchev TT, Denchev CM, Kemler M, Begerow D, Deng CY,

Harrower E, Bozorov T, Kholmuradova T, Gafforov Y, Abdurazakov A, Xu JC, Mortimer PE, Ren GC, Jeewon R, Maharachchikumbura SSN, Phukhamsakda C, Mapook A, Hyde KD (2021) Fungal diversity notes 1387–1511: taxonomic and phylogenetic contributions on genera and species of fungal taxa. Fungal Diversity 111: 1–335. https://doi.org/10.1007/s13225-021-00489-3

Botha D, Barnard S, Claassens S, Rajakaruna N, Venter A, Ismail A, Allam M, Siebert SJ (2024) Soil type and precipitation level have a greater influence on fungal than bacterial diversity in serpentine and non-serpentine biological soil crusts. Ecological Research 39(6): 862–878. https://doi.org/10.1111/1440-1703.12500

Chan JF, Lau SK, Yuen KY, Woo PC (2016) *Talaromyces* (*Penicillium*) *marneffei* infection in non-HIV-infected patients. Emerging Microbes and Infections 5(1): 1–9. https://doi.org/10.1038/emi.2016.18

Chang JH, Kao HW, Wang YZ (2010) Molecular phylogeny of *Cercophora*, *Podospora*, and *Schizothecium* (Lasiosphaeriaceae, Pyrenomycetes). Taiwania 55(2): 110–116.

Carbone I, Kohn LM (1999) A method for designing primer sets for speciation studies in filamentous ascomycetes. Mycologia 91(3): 553–556. https://doi.org/10.1080/00275514.1999.12061051

Chen AJ, Sun BD, Houbraken J, Frisvad JC, Yilmaz N, Zhou YG, Samson RA (2016) New *Talaromyces* species from indoor environments in China. Studies in Mycology 84(1): 119–144. https://doi.org/10.1016/j.simyco.2016.11.003

Chen Z, Wang Q, Ma J, Zou P, Yu Q, Jiang L (2020) Fungal community composition change and heavy metal accumulation in response to the long-term application of anaerobically digested slurry in a paddy soil. Ecotoxicology and Environmental Safety 196: 110453. https://doi.org/10.1016/j.ecoenv.2020.110453

Cheng CH, Jien SH, Tsai H, Chang YH, Chen YC, Hseu ZY (2009) Geochemical element differentiation in serpentine soils from the ophiolite complexes, eastern Taiwan. Soil Science 174(5): 283–291. https://doi.org/10.1097/SS.0b013e3181a4bf68

Chethana KWT, Niranjan M, Dong W, Samarakoon MC, Bao DF, Calabon MS, Chaiwan N, Chuankid B, Dayarathne MC, De Silva NI, Devadatha B, Dissanayake AJ, Goonasekara ID, Huanraluek N, Jayawardena RS, Karunarathna A, Luo ZL, Marasinghe DS, Ma X, Norphanphoun C, Pem D, Perera RH, Rathnayaka AR, Raspé O, Samarakoon BC, Senwanna C, Sun YR, Tang X, Thiyagaraja V, Tennakoon DS, Zeng M, Zeng XY, Zhang JY, Zhang SN, Bulgakov TS, Camporesi E, Sarma VV, Wang Y, Bhat DJ, Hyde KD (2021) AJOM new records and collections of fungi: 101–150. Asian Journal of Mycology 4: 113–260. https://doi.org/10.5943/ajom/4/1/8

Choi YJ, Eom H, Park J, Park J, Cheon S, Ro HS (2024) Fungal diversity in Nam River and their biodegradative activities. Mycobiology 52(2): 102–110.

https://doi.org/10.1080/12298093.2024.2324575

Chuang WY, Lin YC, Shrestha B, Luangsa-Ard JJ, Stadler M, Tzean SS, Wu S, Ko CC, Hsieh SY, Wu ML, Wang SC, Shen TL, Ariyawansa HA (2024) Phylogenetic diversity and morphological characterization of cordycipitaceous species in Taiwan. Studies in Mycology 109(1): 6-61. https://doi.org/10.3114/sim.2024.109.01

Clum FM (1955) A New Genus in the Aspergillaceae. Mycologia 47(6): 899–901. https://doi.org/10.1080/00275514.1955.12024505

Crous PW, Shivas RG, Quaedvlieg W, van der Bank M, Zhang Y, Summerell BA, Guarro J, Wingfeld MJ, Wood AR, Alfenas AC, Braun U, Cano-Lira JF, García D, Marin-Felix Y, Alvarado P, Andrade JP, Armengol J, Assefa A, den Breeÿen A, Camele I, Cheewangkoon R, De Souza JT, Duong TA, Esteve-Raventós F, Fournier J, Frisullo S, García-Jiménez J, Gardiennet A, Gené J, Hernández-Restrepo M, Hirooka Y, Hospenthal DR, King A, Lechat C, Lombard L, Mang SM, Marbach PAS, Marincowitz S, Marin-Felix Y, Montaño-Mata NJ, Moreno G, Perez CA, Pérez Sierra AM, Robertson JL, Roux J, Rubio E, Schumacher RK, Stchigel AM, Sutton DA, Tan YP, Thompson EH, van der Linde E, Walker AK, Walker DM, Wickes BL, Wong PTW, Groenewald JZ (2014) Fungal planet description sheets: 214–280. Persoonia 32: 184–306. https://doi.org/10.3767/003158514X682395

Crous PW, Wingfield MJ, Burgess TI, Carnegie AJ, Hardy GESJ, Smith D, Summerell BA, Cano-Lira JF, Guarro J, Houbraken J, Lombard L, Martín MP, Sandoval-Denis M, Alexandrova A, Barnes CW, Baseia IG, Bezerra JDP, Guarnaccia V, May TW, Hernández-Restrepo M, Stchige AM, Miller AN, Ordoñez ME, Abreu VP, Accioly T, Agnello C, Colmán AA, Albuquerque CC, Alfredo DS, Alvarado P, Araújo-Magalhães GR, Arauzo S, Atkinson T, Barili A, Barreto RW, Bezerra JL, Cabral TS, Rodríguez FC, Cruz RHSF, Daniëls PP, da Silva BDB, de Almeida DAC, Carvalho Júnior AA, Decock CA, Delgat L, Denman S, Dimitrov RA, Edwards J, Fedosova AG, Ferreira RJ, Firmino AL, Flores JA, García D, Gené J, Giraldo A, Góis JS, Gomes AAM, Gonçalves CM, Gouliamova DE, Groenewald M, Guéorguiev BV, Guevara-Suarez M, Gusmão LFP, Hosaka K, Hubka V, Huhndorf SM, Jadan M, Jurjević Ž, Kraak B, Kučera V, Kumar TKA, Kušan I, Lacerda SR, Lamlertthon S, Lisboa WS, Loizides M, Luangsa-ard JJ, Lysková P, Mac Cormack WP, Macedo DM, Machado AR, Malysheva EF, Marinho P, Matočec N, Meijer M, Mešić A, Mongkolsamrit S, Moreira KA, Morozova OV, Nair KU, Nakamura N, Noisripoom W, Olariaga I, Oliveira RJV, Paiva LM, Pawar P, Pereira OL, Peterson SW, Prieto M, RodríguezAndrade E, Blas CRD, Roy M, Santos ES, Sharma R, Silva GA, Souza-Motta CM, Takeuchi-Kaneko Y, Tanaka C, Thakur A, Smith MT, Tkalčec Z, Valenzuela-Lopez N, van der Kleij P, Verbeken A, Viana MG, Wang XW, Groenewald JZ (2017) Fungal planet description sheets: 625–715. Persoonia 39:

270–467. https://doi.org/10.3767/persoonia.2017.39.11

Crous PW, Luangsa-Ard JJ, Wingfield MJ, Carnegie AJ, HernándezRestrepo M, Lombard L, Roux J, Barreto RW, Baseia IG, CanoLira JF, Martín MP, Morozova OV, Stchigel AM, Summerell BA, Brandrud TE, Dima B, García D, Giraldo A, Guarro J, Gusmão LFP, Khamsuntorn P, Noordeloos ME, Nuankaew S, Pinruan U, Rodríguez-Andrade E, Souza-Motta CM, Thangavel R, van Iperen AL, Abreu VP, Accioly T, Alves JL, Andrade JP, Bahram M, Baral HO, Barbier E, Barnes CW, Bendiksen E, Bernard E, Bezerra JDP, Bezerra JL, Bizio E, Blair JE, Bulyonkova TM, Cabral TS, Caiafa MV, Cantillo T, Colmán AA, Conceição LB, Cruz S, Cunha AOB, Darveaux BA, da Silva AL, da Silva GA, da Silva GM, da Silva RMF, de Oliveira RJV, Oliveira RL, De Souza JT, Dueñas M, Evans HC, Epifani F, Felipe MTC, Fernández-López J, Ferreira BW, Figueiredo CN, Filippova NV, Flores JA, Gené J, Ghorbani G, Gibertoni TB, Glushakova AM, Healy R, Huhndorf SM, Iturrieta-González I, Javan-Nikkhah M, Juciano RF, Jurjević Ž, Kachalkin AV, Keochanpheng K, Krisai-Greilhuber I, Li YC, Lima AA, Machado AR, Madrid H, Magalhães OMC, Marbach PAS, Melanda GCS, Miller AN, Mongkolsamrit S, Nascimento RP, Oliveira TGL, Ordoñez ME, Orzes R, Palma MA, Pearce CJ, Pereira OL, Perrone G, Peterson SW, Pham THG, Piontelli E, Pordel A, Quijada L, Raja HA, Rosas de Paz E, Ryvarden L, Saitta A, Salcedo SS, SandovalDenis M, Santos TAB, Seifert KA, Silva BDB, Smith ME, Soares AM, Sommai S, Sousa JO, Suetrong S, Susca A, Tedersoo L, Telleria MT, Thanakitpipattana D, Valenzuela-Lopez N, Visagie CM, Zapata M, Groenewald JZ (2018a) Fungal Planet description sheets: 785–867. Persoonia 41: 238–417. https://doi.org/10.3767/persoonia.2018.41.12

Crous PW, Schumacher RK, Wingfield MJ, Akulov A, Denman S, Roux J, Braun U, Burgess TI, Carnegie AJ, Váczy KZ, Guatimosim E, Schwartsburd PB, Barreto RW, Hernández-Restrepo M, Lombard L, Groenewald JZ (2018b) New and interesting fungi. 1. Fungal Systematics and Evolution 1: 169–215. https://doi.org/10.3114/fuse.2018.01.08

Crous PW, Wingfield MJ, Chooi YH, Gilchrist CLM, Lacey E, Pitt JI, Roets F, Swart WJ, Cano-Lira JF, Valenzuela-Lopez N, Hubka V, Shivas RG, Stchigel AM, Holdom DG, Jurjević Z, Kachalkin AV, Lebel T, Lock C, Martín MP, Tan YP, Tomashevskaya MA, Vitelli JS, Baseia IG, Bhatt VK, Brandrud TE, De Souza JT, Dima B, Lacey HJ, Lombard L, Johnston PR, Morte A, Papp V, Rodríguez A, Rodríguez-Andrade E, Semwa KC, Tegart L, Abad ZG, Akulov A, Alvarado P, Alves A, Andrade JP, Arenas F, Asenjo C, Ballarà J, Barrett MD, Berná LM, Berraf-Tebba A, Bianchinotti MV, Bransgrove K, Burgess TI, Carmo FS, Chávez R, Čmoková A, Dearnaley JDW, de Santiago ALCM, Freitas-Neto JF, Denman S, Douglas B, Dovana F, Eichmeier A, Esteve-Raventós F, Farid A, Fedosova AG, Ferisin G, Ferreira RJ, Ferrer A,

Figueiredo CN, Figueiredo YF, ReinosoFuentealba CG, Garrido-Benavent I, Cañete-Gibas CF, Gil-Durán C, Glushakova AM, Gonçalves MFM, González M, Gorczak M, Gorton C, Guard FE, Guarnizo AL, Guarro J, Gutiérrez M, Hama P, Hien LT, Hocking AD, Houbraken J, Hunter GC, Inácio CA, Jourdan M, Kapitonov VI, Kelly L, Khan TN, Kisło K, Kiss L, Kiyashko A, Kolařík M, Kruse J, Kubátová A, Kučera V, Kučerová I, Kušan I, Lee HB, Levicán G, Lewis A, Liem NV, Liimatainen K, Lim HJ, Lyons MN, Maciá-Vicente JG, MagañaDueñas V, Mahiques R, Malysheva EF, Marbach PAS, Marinho P, Matočec N, McTaggart AR, Mešić A, Morin L, Muñoz-Mohedano JM, Navarro-Ródenas A, Nicolli CP, Oliveira RL, Otsing E, Ovrebo CL, Pankratov TA, Paños A, Paz-Conde A, Pérez-Sierra A, Phosri C, Pintos Á, Pošta A, Prencipe S, Rubio E, Saitta A, Sales LS, Sanhueza L, Shuttleworth LA, Smith J, Smith ME, Spadaro D, Spetik M, Sochor M, Sochorová Z, Sousa JO, Suwannasai N, Tedersoo L, Thanh HM, Thao LD, Tkalčec Z, Vaghefi N, Venzhik AS, Verbeken A, Vizzini A, Voyron S, Wainhouse M, Whalley AJS, Wrzosek M, Zapata M, Zeil-Rolfe I, Groenewald JZ (2020) Fungal planet description sheets: 1042–1111. Persoonia 44: 301–459. https://doi.org/10.3767/persoonia.2020.44.11

Crous PW, Begoude BAD, Boers J, Braun U, Declercq B, Dijksterhuis J, Elliott TF, Garay-Rodriguez GA, Jurjević Ž, Kruse J, Linde CC, Loyd A, Mound L, Osieck ER, Rivera-Vargas LI, Quimbita AM, Rodas CA, Roux J, Schumacher RK, Starink-Willemse M, Thangavel R, Trappe JM, van Iperen AL, Van Steenwinkel C, Wells A, Wingfield MJ, Yilmaz N, Groenewald JZ (2022) New and interesting fungi. 5. Fungal Systematics and Evolution 10: 19–90. https://doi.org/10.3114/fuse.2022.10.02

da Silva M, Umbuzeiro GA, Pfenning LH, Canhos VP, Esposito E (2003) Filamentous fungi isolated from estuarine sediments contaminated with industrial discharges. Soil and Sediment Contamination 12(3): 345-356. https://doi.org/10.1080/713610976

Daghino S, Murat C, Sizzano E, Girlanda M, Perotto S (2012) Fungal diversity is not determined by mineral and chemical differences in serpentine substrates. PLoS ONE 7(9): e44233. https://doi.org/10.1371/journal.pone.0044233

de Gruyter J, and Noordeloos ME (1992) Contributions towards a monograph of *Phoma* (Coelomycetes)-I. 1. Section *Phoma*: Taxa with very small conidia *in vitro*. Persoonia 15: 71–92.

de Gruyter J, Woudenberg JH, Aveskamp MM, Verkley GJ, Groenewald JZ, Crous PW (2010) Systematic reappraisal of species in *Phoma* section *Paraphoma*, *Pyrenochaeta* and *Pleurophoma*. Mycologia 102(5): 1066–1081. https://doi.org/10.3852/09-240

de Gruyter J, Woudenberg JHC, Aveskamp MM, Verkley GJM, Groenewald JZ, Crous PW (2013) Redisposition of *Phoma*-like anamorphs in Pleosporales. Studies in

Mycology 75(1): 1–36. https://doi.org/10.3114/sim0004

Dong W, Wang B, Hyde KD, McKenzie EHC, Raja HA, Tanaka K, Abdel-Wahab MA, Abdel-Aziz FA, Doilom M, Phookamsak R, Hongsanan S, Wanasinghe DN, Yu XD, Wang GN, Yang H, Yang J,Thambugala KM, Tian Q, Luo ZL, Yang JB, Miller AN, Fournier J, Boonmee S, Hu DM, Nalumpang S, Zhang H (2020) Freshwater Dothideomycetes. Fungal Diversity 105: 319–575. https://doi.org/10.1007/s13225-020-00463-5

Ebead GA, Overy DP, Berrué F, Kerr RG (2012) *Westerdykella reniformis* sp. nov., producing the antibiotic metabolites melinacidin IV and chetracin B. IMA Fungus 3: 189–201. https://doi.org/10.5598/imafungus.2012.03.02.11

Ellegaard-Jensen L, Aamand J, Kragelund BB, Johnsen AH, Rosendahl S (2013) Strains of the soil fungus *Mortierella* show different degradation potentials for the phenylurea herbicide diuron. Biodegradation 24: 765–774. https://doi.org/10.1007/s10532-013-9624-7

Fisher NL, Burgess LW, Toussoun TA, Nelson PE (1982) Carnation leaves as a substrate and for preserving cultures of *Fusarium* species. Phytopathology 72(1): 151–153.

Gadd GM. (2007) Geomycology: biogeochemical transformations of rocks, minerals, metals and radionuclides by fungi, bioweathering and bioremediation. Mycological Research 111(1): 3–49. https://doi.org/10.1016/j.mycres.2006.12.001

Gajewska J, Floryszak-Wieczorek J, Sobieszczuk-Nowicka E, Mattoo A, Arasimowicz-Jelonek M (2022) Fungal and oomycete pathogens and heavy metals: an inglorious couple in the environment. IMA fungus 13(1): 6. https://doi.org/10.1186/s43008-022-00092-4

Gams W (1975) *Cephalosporium*-like Hyphomycetes: some tropical species. Transactions of the British Mycological Society 64(3): 389–404 IN3. https://doi.org/10.1016/S0007-1536(75)80138-0

Giraldo A, Gené J, Sutton DA, Madrid H, De Hoog GS, Cano J, Decock C, Crous PW, Guarro J (2015) Phylogeny of *Sarocladium* (Hypocreales). Persoonia 34(1): 10–24. http://dx.doi.org/10.3767/003158515X685364

Giraldo A, Crous PW (2019) Inside Plectosphaerellaceae. Studies in Mycology 92(1): 227–286. https://doi.org/10.1016/j.simyco.2018.10.005

Giraldo A, Hernández-Restrepo M, Crous PW (2019) New plectosphaerellaceous species from Dutch garden soil. Mycological Progress 18(9): 1135–1154. https://doi.org/10.1007/s11557-019-01511-4

Glass NL, Donaldson GC (1995) Development of primer sets designed for use with the PCR to amplify conserved genes from filamentous ascomycetes. Applied and Environmental Microbiology 61(4): 1323–1330. https://doi.org/10.1128/aem.61.4.1323-1330.1995

Goh TK, Ho WH, Hyde KD, Tsui KM (1997) Four new species of *Xylomyces* from submerged wood. Mycological Research 101(11): 1323–1328. https://doi.org/10.1017/S0953756297004164

Goh J, Jeon YJ, Mun HY, Chung N, Park YH, Park S, Hwang H, Cheon W (2020) Isolation and characterization of eleven unrecorded *Pezizomycotina* species from freshwater ecosystems in Korea. The Korean Journal of Mycology 48(4): 423–443. https://doi.org/10.4489/KJM.20200042

Goh J, Mun HY, Oh Y (2021) Seven previously unrecorded fungal species isolated from freshwater ecosystems in Korea. The Korean Journal of Mycology 49(2): 183–197. https://doi.org/10.4489/KJM.20210018

Gonçalves SC, Martins-Loução MA, Freitas H (2009) Evidence of adaptive tolerance to nickel in isolates of *Cenococcum geophilum* from serpentine soils. Mycorrhiza 19: 221–230. https://doi.org/10.1007/s00572-008-0211-4

González-Teuber M, Vilo C, Bascuñán-Godoy L (2017) Molecular characterization of endophytic fungi associated with the roots of *Chenopodium quinoa* inhabiting the Atacama Desert, Chile. Genomics Data 11: 109–112. https://doi.org/10.1016/j.gdata.2016.12.015

Groenewald JZ, Nakashima C, Nishikawa J, Shin HD, Park JH, Jama AN, Groenewald M, Braun U, Crous PW (2013) Species concepts in *Cercospora*: spotting the weeds among the roses. Studies in Mycology 75(1): 115–170. https://doi.org/10.3114/sim0012

Guarro J, Al-Saadoon AH, Gene J, Abdullah SK (1997) Two new cleistothecial Ascomycetes from Iraq. Mycologia 89(6): 955–961. https://doi.org/10.1080/00275514.1997.12026867

Guerra-Mateo D, Cano-Lira JF, Fernández-Bravo A, Gené J (2024) Sunken riches: Ascomycete diversity in the Western Mediterranean Coast through direct plating and flocculation, and description of four new taxa. Journal of Fungi 10(4): 281. https://doi.org/10.3390/jof10040281

Harms K, Milic A, Stchigel AM, Stadler M, Surup F, Marin-Felix Y (2021) Three New Derivatives of Zopfinol from *Pseudorhypophila Mangenotii* gen. et comb. nov. Journal of Fungi 7(3): 181. https://doi.org/10.3390/jof7030181

Hashem AH, Attia MS, Kandil EK, Fawzi MM, Abdelrahman AS, Khader MS, Khodaira MA, Emam AE, Goma MA, Abdelaziz AM (2023) Bioactive compounds and biomedical applications of endophytic fungi: a recent review. Microbial Cell Factories 22(1): 107. https://doi.org/10.1186/s12934-023-02131-0

Heo YM, Lee H, Kim K, Kwon SL, Park MY, Kang JE, Kim GH, Kim BS, Kim JJ (2019) Fungal diversity in intertidal mudflats and abandoned solar salterns as a source for biological resources. Marine Drugs 17(11): 601.

https://doi.org/10.3390/md17110601

Hong SB, Cho HS, Shin HD, Frisvad JC, Samson RA (2006) Novel *Neosartorya* species isolated from soil in Korea. International Journal of Systematic and Evolutionary Microbiology 56(2): 477–486. https://doi.org/10.1099/ijs.0.63980-0

Hou D, O'Connor D, Igalavithana AD, Alessi DS, Luo J, Tsang DCW, Sparks DL, Yamauchi Y, Rinklebe J, Ok, YS (2020) Metal contamination and bioremediation of agricultural soils for food safety and sustainability. Nature Reviews Earth and Environment 1(7): 366–381. https://doi.org/10.1038/s43017-020-0061-y

Hou LW, Giraldo A, Groenewald JZ, Rämä T, Summerbell RC, Huang GZ, Crous PW (2023) Redisposition of acremonium-like fungi in Hypocreales. Studies in Mycology 105: 23–203. https://doi.org/10.3114/sim.2023.105.02

Hou YM, Zhang X, Zhang NN, Naklumpa W, Zhao WY, Liang XF, Zhang R, Sun GY, Gleason ML (2019) Genera *Acremonium* and *Sarocladium* cause brown spot on bagged apple fruit in China. Plant Disease 103(8): 1889–1901. https://doi.org/10.1094/PDIS-10-18-1794-RE

Hseu ZY, Lai YJ (2017) Nickel accumulation in paddy rice on serpentine soils containing high geogenic nickel contents in Taiwan. Environmental Geochemistry and Health 39(6): 1325–1334. https://doi.org/10.1007/s10653-017-9925-6

Hseu, ZY, Zehetner F, Ottner F, Iizuka Y (2015) Clay-mineral transformations and heavy-metal release in Paddy soils formed on serpentinites in eastern Taiwan. Clays and Clay Minerals 63: 119-131. https://doi.org/10.1346/CCMN.2015.0630204

Hsieh MS (2020) Effects of nickel and chromium on microbial communities and root-knot nematode in serpentine soil. Master thesis. National Taiwan University, Taipei, Taiwan. http://doi:10.6342/NTU202004110

Hsu SY, Xu YC, Lin YC, Chuang WY, Lin SR, Stadler M, Tangthirasunun N, Cheewangkoon R, AL-Shwaiman HA, Elgorban AM, Ariyawansa HA (2024) Hidden diversity of *Pestalotiopsis* and *Neopestalotiopsis* (Amphisphaeriales, Sporocadaceae) species allied with the stromata of entomopathogenic fungi in Taiwan. MycoKeys 101: 275. https://doi.org/10.3897/mycokeys.101.113090

Hurdeal VG, Jones EBG, Santiago ALCMDA, Hyde KD, Gentekaki E (2022) Expanding the diversity of mucoralean fungi from northern Thailand: novel *Backusella* species from soil. Phytotaxa 559(3): 275–284. https://doi.org/10.11646/phytotaxa.559.3.5

Hussien AKE, Hussein NAG, El-Nagdy MA (2023) Biodiversity of *Chaetomium*-like genera in the Nile River, at Assiut, Egypt. Assiut University Journal of Multidisciplinary Scientific Research 52(3) 295–321.

Hyde KD, Chaiwan N, Norphanphoun C, Boonmee S, Camporesi E, Chethana KWT, Dayarathne MC, de Silva NI, Dissanayake AJ, Ekanayaka AH, Hongsanan S, Huang

SK, Jayasiri SC, Jayawardena R, Jiang HB, Karunarathna A, Lin CG, Liu JK, Liu NG, Lu YZ, Luo ZL, Maharachchimbura SSN, Manawasinghe IS, Pem D, Perera RH, Phukhamsakda C, Samarakoon MC, Senwanna C, Shang QJ, Tennakoon DS, Thambugala KM, Tibpromma S, Wanasinghe DN, Xiao YP, Yang J, Zeng XY, Zhang JF, Zhang SN, Bulgakov TS, Bhat DJ, Cheewangkoon R, Goh TK, Jones EBG, Kang JC, Jeewon R, Liu ZY, Lumyong S, Kuo CH, McKenzie EHC, Wen TC, Yan JY, Zhao Q (2018) Mycosphere notes 169–224. Mycosphere 9(2): 271–430. https://doi.org/10.5943/mycosphere/9/2/8

Hyde KD, Wijesinghe SN, Afshari N, Aumentado HD, Bhunjun CS, Boonmee S, Camporesi E, Chethana KWT, Doilom M, Dong W, Du T, Farias A, Gao Y, Jayawardena RS, Karimi O, Karunarathna SC, Kularathnage ND, Lestari AS, Li CJY, Li YX, Liao C, Liu XF, Lu L, Lu YZ, Luo ZL, Ma J, Mamarabadi M, Manawasinghe IS, Mapook A, Mi LX, Niranjan M, Senanayake IC, Shen HW, Su HL, Tibpromma S, Xu RJ, Yan JY, Yang YH, Yang YY, Yu FQ, Kang JC, Zhang JY (2024) Mycosphere notes 469–520. Mycosphere 15: 1294–1454.

Imrefi I, Knapp DG, Kovács GM (2024) *Poaceascoma zborayi* sp. nov. and *Agrorhizomyces patris* gen. et spec. nov.–Two novel dark septate endophytes colonizing wheat (*Triticum aestivum*) roots from a cropland in Hungary. Mycological Progress 23(1): 35. https://doi.org/10.1007/s11557-024-01970-4

Ito T, Nakagiri A (1995) *Westerdykella globosa*, a proposal for a new combination. Mycoscience 36: 361–363. https://doi.org/10.1007/BF02268614

Khan I, Ali M, Aftab M, Shakir S, Qayyum S, Haleem KS, Tauseef I (2019) Mycoremediation: a treatment for heavy metal-polluted soil using indigenous metallotolerant fungi. Environmental Monitoring and Assessment 191: 1–15. https://doi.org/10.1007/s10661-019-7781-9

Koner S, Chen JS, Rathod J, Hussain B, Hsu BM (2023) Unravelling the ultramafic rock-driven serpentine soil formation leading to the geo-accumulation of heavy metals: An impact on the resident microbiome, biogeochemical cycling and acclimatized eco-physiological profiles. Environmental Research 216: 114664. https://doi.org/10.1016/j.envres.2022.114664

Kumar RS, Koner S, Tsai HC, Chen JS, Huang SW, Hsu BM (2023) Deciphering endemic rhizosphere microbiome community's structure towards the host-derived heavy metals tolerance and plant growth promotion functions in serpentine geo-ecosystem. Journal of Hazardous Materials 452: 131359. https://doi.org/10.1016/j.jhazmat.2023.131359

Kumarathilaka P, Dissanayake CB, Vithanage MA (2014) Geochemistry of serpentinite soils: A brief overview. Journal of Geological Society of Sri Lanka 16: 53–63.

Kumari R, Jayachandran LE, Ghosh AK (2019) Investigation of diversity and

dominance of fungal biota in stored wheat grains from governmental warehouses in West Bengal, India. Journal of the Science of Food and Agriculture 99(7): 3490–3500. https://DOI/10.1002/jsfa.9568

Latz MA, Jensen B, Collinge DB, Jørgensen HJL (2020) Identification of two endophytic fungi that control Septoria tritici blotch in the field, using a structured screening approach. Biological Control 141: 104128. https://doi.org/10.1016/j.biocontrol.2019.104128

Lee JW, Seo CW, Lee W, Kim JS, Park KH, Cho Y, Lim YW (2023) Diversity and dynamics of marine arenicolous fungi in three seasides of the Korean peninsula. Journal of Microbiology 61(1): 63–82. https://doi.org/10.1007/s12275-023-00011-1

Li X, Wang H, Li X, Li X, Zhang H (2020) Distribution characteristics of fungal communities with depth in paddy fields of three soil types in China. Journal of Microbiology 58: 279–287. https://doi.org/10.1007/s12275-020-9409-8

Li Z, Xu J, Teng HH, Liu L, Chen J, Chen Y, Ji J (2015) Bioleaching of lizardite by magnesium-and nickel-resistant fungal isolate from serpentinite soils–implication for carbon capture and storage. Geomicrobiology Journal 32(2): 181–192. https://doi.org/10.1080/01490451.2013.835888

Liang J, Li G, Zhou S, Zhao M, Cai L (2019) Myrothecium-like new species from turfgrasses and associated rhizosphere. MycoKeys 51: 29–53. https://doi.org/10.3897/mycokeys.51.31957

Lipovy B, Kocmanova I, Holoubek J, Hanslianova M, Bezdicek M, Rihova H, Suchanek I, Brychta P (2018) The first isolation of *Westerdykella dispersa* in a critically burned patient. Folia Microbiologica 63: 479–482. https://doi.org/10.1007/s12223-018-0590-7

Liu SL, Zhao P, Cai L, Shen S, Wei HW, Na Q, Han M, Wei R, Ge Y, Ma H, Karunarathna SC, Tibprommab S, Zhang B, Dai D, Lin L, Fan XL, Luo ZL, Shen HW, Lu L, Lu W, Xu RF, Tohtirjap A, Wu F, Zhou LW (2024) Catalogue of fungi in China 1. New taxa of plant-inhabiting fungi. Mycology 1–58. https://doi.org/10.1080/21501203.2024.2316066

Liu TS, Guo HY, Chu JL, Lian S (2007) Preliminary study on heavy metal characteristics in serpentinite-developed soil regions in eastern Taiwan. Journal of Taiwan Agricultural Research 56:65–78.

Liu YJ, Whelen S, Hall BD (1999) Phylogenetic relationships among ascomycetes: evidence from an RNA polymerse II subunit. Molecular Biology and Evolution 16(12): 1799–1808. https://doi.org/10.1093/oxfordjournals.molbev.a026092

Lombard L, Houbraken J, Decock C, Samson RA, Meijer M, Réblová M, Groenewald JZ, Crous PW (2016) Generic hyper-diversity in Stachybotriaceae. Persoonia 36(1): 156–246. https://doi.org/10.3767/003158516X691582

Luo ZL, Bahkali AH, Liu XY, Phookamsak R, Zhao YC, Zhou DQ, Su HY, Hyde KD (2016) *Poaceascoma aquaticum* sp. nov. (Lentitheciaceae), a new species from submerged bamboo in freshwater. Phytotaxa 253(1): 71–80. http://dx.doi.org/10.11646/phytotaxa.253.1.5

Manoch L, Dethoup T, Yilmaz N, Houbraken J, Samson RA (2013) Two new *Talaromyces* species from soil in Thailand. Mycoscience 54(5): 335–342. https://doi.org/10.1016/j.myc.2012.12.002

Marin-Felix Y, Miller AN, Cano-Lira GJ, Garcia D, Stadler M, Huhndorf SM, Stchigel AM (2020) Re-evaluation of the order sordariales: delimitation of Lasiosphaeriaceae s. str., and Introduction of the New Families Diplogelasinosporaceae, Naviculisporaceae, and Schizotheciaceae. Microorganisms 8(1430): 1–41. https://doi.org/10.3390/microorganisms8091430

McGahan DG, Southard RJ, Claassen VP (2008) Tectonic inclusions in serpentinite landscapes contribute plant nutrient calcium. Soil Science Society of America Journal 72(3): 838-847. https://doi.org/10.2136/sssaj2007.0159

Miller AN, Huhndorf SM (2005) Multi-gene phylogenies indicate ascomal wall morphology is a better predictor of phylogenetic relationships than ascospore morphology in the Sordariales (Ascomycota, Fungi). Molecular Phylogenetics and Evolution 35(1): 60–75. https://doi.org/10.1016/j.ympev.2005.01.007

Mo YX, Kan YZ, Jia LM, Cao XT, Sikandar A, Wu HY (2024) Characterization and effect of a nematophagous fungus *Talaromyces cystophila* sp. nov. for the biological control of corn cyst nematode. Phytopathology 114(3): 618–629. https://doi.org/10.1094/PHYTO-02-23-0045-R

Naraghi L, Heydari A, Rezaee S, Razavi M (2012) Biocontrol agent *Talaromyces flavus* stimulates the growth of cotton and potato. Journal of Plant Growth Regulation 31: 471–477. https://doi.org/10.1007/s00344-011-9256-2

Nicoletti R, Bellavita R, Falanga A (2023a) The outstanding chemodiversity of marine-derived *Talaromyces*. Biomolecules 13(7): 1021. https://doi.org/10.3390/biom13071021

Nicoletti R, Zimowska B (2023b) Endophytic fungi of hazelnut (*Corylus avellana*). Plant Protection Science 59(2). https://doi.org/10.17221/133/2022-PPS

Ningsih BNS, Rukachaisirikul V, Phongpaichit S, Muanprasat C, Preedanon S, Sakayaroj J, Intayot S, Jungsuttiwong S (2024) Talarostatin, a vermistatin derivative from the soil-derived fungus *Talaromyces thailandensis* PSU-SPSF059. Natural Product Research 38(15): 2535–2542. https://doi.org/10.1080/14786419.2023.2188209

Noguchi MT, Nagase H, Yamauchi N, Mimuro G, Sakai H, Furusawa A, Miki S, Yoshida S (2022) Taxonomical identification of Chinese cabbage yellows inhibitory

fungus isolated from disease suppressive soil. Journal of General Plant Pathology 88(4): 239–245. https://doi.org/10.1007/s10327-022-01058-5

Ou JH, Lin GC, Chen CY (2020) *Sarocladium* species associated with rice in Taiwan. Mycological Progress 19(1): 67–80. https://doi.org/10.1007/s11557-019-01543-w

Overy DP, Bayman P, Kerr RG, Bills GF (2014) An assessment of natural product discovery from marine (*sensu strictu*) and marine-derived fungi. Mycology 5(3): 145–167. https://doi.org/10.1080/21501203.2014.931308

Oze C, Skinner C, Schroth AW, Coleman RG (2008) Growing up green on serpentine soils: Biogeochemistry of serpentine vegetation in the Central Coast Range of California. Applied Geochemistry 23(12): 3391–3403. https://doi.org/10.1016/j.apgeochem.2008.07.014

Pal A, Wauters G, Paul AK (2007) Nickel tolerance and accumulation by bacteria from rhizosphere of nickel hyperaccumulators in serpentine soil ecosystem of Andaman, India. Plant and Soil 293: 37–48. https://doi.org/10.1007/s11104-007-9195-7

Panaccione DG, Sheets NL, Miller SP, Cumming JR (2001) Diversity of *Cenococcum geophilum* isolates from serpentine and non-serpentine soils. Mycologia 93(4): 645–652. https://doi.org/10.1080/00275514.2001.12063196

Pawar VH, Mathur PN, Thirumalachar MJ (1967) Species of *Phoma* isolated from marine soils in India. Transactions of the British Mycological Society 50(2): 259–265.

Peterson SW, Jurjević Ž (2019) The *Talaromyces pinophilus* species complex. Fungal Biology 123(10): 745–762. https://doi.org/10.1016/j.funbio.2019.06.007

Phookamsak R, Manamgoda DS, Li WJ, Dai DQ, Singtripop C, Hyde KD (2015) *Poaceascoma helicoides* gen et sp. nov., a new genus with scolecospores in Lentitheciaceae. Cryptogamie, Mycologie 36(2): 225–236. http://doi/10.7872/crym/v36.iss2.2015.225

Pietro-Souza W, Mello IS, Vendruscullo SJ, Silva GFD, Cunha CND, White JF, Soares MA (2017) Endophytic fungal communities of *Polygonum acuminatum* and *Aeschynomene fluminensis* are influenced by soil mercury contamination. PloS One, 12(7): e0182017. https://doi.org/10.1371/journal.pone.0182017

Pramunadipta S, Widiastuti A, Wibowo A, Suga H (2020) *Sarocladium oryzae* associated with sheath rot disease of rice in Indonesia. Biodiversitas Journal of Biological Diversity 21(3): 1243–1249.

Rai JN, Tewari JP (1963) On some isolates of the genus *Preussia Fuckel* from Indian soils. Proceedings/Indian Academy of Sciences 57(1): 45–55. https://doi.org/10.1007/BF03053881

Réblová M, Gams W, Seifert KA (2011) Monilochaetes and allied genera of the Glomerellales, and a reconsideration of families in the Microascales. Studies in

Mycology 68(1): 163–191. https://doi.org/10.3114/sim.2011.68.07

Rehner SA, Samuels GJ (1994) Taxonomy and phylogeny of *Gliocladium* analysed from nuclear large subunit ribosomal DNA sequences. Mycological Research 98(6): 625–634. https://doi.org/10.1016/S0953-7562(09)80409-7

Rehner SA, Buckley E (2005) A *Beauveria* phylogeny inferred from nuclear ITS and EF1-α sequences: evidence for cryptic diversification and links to *Cordyceps* teleomorphs. Mycologia 97(1): 84–98. https://doi.org/10.1080/15572536.2006.11832842

Roccotiello E, Manfredi A, Drava G, Minganti V, Mariotti MG, Berta G, Cornara L (2010) Zinc tolerance and accumulation in the ferns *Polypodium cambricum* L. and *Pteris vittata* L. Ecotoxicology and Environmental Safety 73(6): 1264–1271. https://doi.org/10.1016/j.ecoenv.2010.07.019

Ronquist F, Teslenko M, van der Mark P, Ayres DL, Darling A, Höhna S, Larget B, Liu L, Suchard MA, Huelsenbeck JP (2012) MrBayes 3.2: efficient Bayesian phylogenetic inference and model choice across a large model space. Systematic Biology 61(3): 539–542. https://doi.org/10.1093/sysbio/sys029

Senabio JA, Pereira FDC, Pietro-Souza W, Sousa TF, Silva GF, Soares MA (2023) Enhanced mercury phytoremediation by *Pseudomonodictys pantanalensis* sp. nov. A73 and *Westerdykella aquatica* P71. Brazilian Journal of Microbiology 54(2): 949–964. https://doi.org/10.1007/s42770-023-00924-4

Solano-Arguedas AF, Boothman C, Newsome L, Pattrick RA, Arguedas-Quesada D, Robinson CH, Lloyd JR (2022) Geochemistry and microbiology of tropical serpentine soils in the Santa Elena Ophiolite, a landscape-biogeographical approach. Geochemical Transactions 23(1): 2. https://doi.org/10.1186/s12932-022-00079-5

Song HY, El Sheikha AF, Zhong PA, Liao JL, Wang ZH, Huang YJ, Hu DM (2020) *Westerdykella aquatica* sp. nov., producing phytase. Mycotaxon 135(2): 281–292. https://doi.org/10.5248/135.281

Stolk AC (1955) *Emericellopsis minima* sp. nov. and *Westerdykella ornata* gen. nov., sp. nov. Transactions of the British Mycological Society 38(4): 419–424. https://doi.org/10.1016/S0007-1536(55)80046-0

Su YY, Qi YL, Cai L (2012) Induction of sporulation in plant pathogenic fungi. Mycology 3(3): 195–200. https://doi.org/10.1080/21501203.2012.719042

Sue PK, Gurda GT, Lee R, Watkins T, Green R, Memon W, Milstone AM, Zelazny AM, Fahle GA, Pham TA, Gibas CF, Sutton DA, Wickes BL, Wiederhold NP, Zhang SX (2014) First report of *Westerdykella dispersa* as a cause of an angioinvasive fungal infection in a neutropenic host. Journal of Clinical Microbiology 52(12): 4407–4411. https://doi.org/10.1128/jcm.02012-14

Summerbell RC, Gueidan C, Guarro J, Eskalen A, Crous PW, Gupta AK, Gené J, Cano-

Lira JF, van Iperen A, Starink M, Scott JA (2018) The protean *Acremonium*. *A. sclerotigenum/egyptiacum*: revision, food contaminant, and human disease. Microorganisms 6(3): 88. https://doi.org/10.3390/microorganisms6030088

Sung GH, Sung JM, Hywel-Jones NL, Spatafora JW (2007) A multi-gene phylogeny of Clavicipitaceae (Ascomycota, Fungi): Identification of localized incongruence using a combinational bootstrap approach. Molecular Phylogenetics and Evolution 44(3): 1204–1223. https://doi.org/10.1016/j.ympev.2007.03.011

Surono S, Zaffan ZR, Soekarno BPW, Munif A, Nurdebyandaru N (2023) The first report of *Pyrenochaetopsis terricola* as a dark septate endophytic fungus antagonistic to *Fusarium oxysporum* f. sp. Lycopersici, a pathogen causing wilt disease in tomato plants. Research Square. https://doi.org/10.21203/rs.3.rs-2823666/v1

Tanaka K, Hirayama K, Yonezawa H, Sato G, Toriyabe A, Kudo H, Hashimoto A, Matsumura M, Harada Y, Kurihara Y, Shirouzu T, Hosoya T (2015) Revision of the massarineae (Pleosporales, Dothideomycetes). Studies in Mycology 82: 75–136. https://doi.org/10.1016/j.simyco.2015.10.002

Tennakoon DS, Kuo CH, Maharachchikumbura SSN, Thambugala KM, Gentekaki E, Phillips AJL, Bhat DJ, Wanasinghe DN, de Silva NI, Promputtha I, Hyde KD (2021) Taxonomic and phylogenetic contributions to *Celtis formosana*, *Ficus ampelas*, *F. septica*, *Macaranga tanarius* and *Morus australis* leaf litter inhabiting microfungi. Fungal Diversity 108: 1–215

Trifinopoulos J, Nguyen LT, von Haeseler A, Minh BQ (2016) W-IQ-TREE: a fast online phylogenetic tool for maximum likelihood analysis. Nucleic Acids Research 44(W1): W232-W235. https://doi.org/10.1093/nar/gkw256

Tsai I, Chung CL, Lin SR, Hung TH, Shen TL, Hu CY, Hozzein WN, Ariyawansa HA (2021) Cryptic diversity, molecular systematics, and pathogenicity of genus *Pestalotiopsis* and allied genera causing gray blight disease of tea in Taiwan, with a description of a new *Pseudopestalotiopsis* species. Plant Disease 105(2): 425–443. https://doi.org/10.1094/PDIS-05-20-1134-RE

Valenzuela-Lopez N, Cano-Lira JF, Guarro J, Sutton DA, Wiederhold N, Crous PW, Stchigel AM (2018) Coelomycetous Dothideomycetes with emphasis on the families Cucurbitariaceae and Didymellaceae. Studies in Mycology 90(1): 1–69. https://doi.org/10.1016/j.simyco.2017.11.003

Vilgalys R, Hester M (1990) Rapid genetic identification and mapping of enzymatically amplified ribosomal DNA from several Cryptococcus species. Journal of Bacteriology 172(8): 4238-4246. https://doi.org/10.1128/jb.172.8.4238-4246.1990

Visagie CM, Yilmaz N, Kocsubé S, Frisvad JC, Hubka V, Samson RA, Houbraken J (2024) A review of recently introduced *Aspergillus*, *Penicillium*, *Talaromyces* and other Eurotiales species. Studies in Mycology 107(1): 1–66.

https://doi.org/10.3114/sim.2024.107.01

Wang XW, Bai FY, Bensch K, Meijer M, Sun BD, Han YF, Crous PW, Samson RA, Yang FY, Houbraken J (2019) Phylogenetic re-evaluation of *Thielavia* with the introduction of a new family Podosporaceae. Studies in Mycology 93: 155–252. https://doi.org/10.1016/j.simyco.2019.08.002

White TJ, Bruns TD, Lee S, Taylor J (1990) Amplification and direct sequencing of fungal ribosomal RNA genes for phylogenetics. PCR Protocols: a Guide to Methods and Applications 18(1): 315–322.

Woudenberg JHC, Aveskamp MM, De Gruyter J, Spiers AG, Crous PW (2009) Multiple *Didymella* teleomorphs are linked to the *Phoma clematidina* morphotype. Persoonia 22(1): 56–62. https://doi.org/10.3767/003158509X427808

Xu D, Luo M, Liu F, Wang D, Pang X, Zhao T, Xu L, Wu X, Xia M, Yang X (2017) Cytochalasan and tyrosine-derived alkaloids from the marine sediment-derived fungus *Westerdykella dispersa* and their bioactivities. Scientific Reports 7(1): 11956. https://doi.org/10.1038/s41598-017-12327-1

Yeh YH, Kirschner R (2014) *Sarocladium spinificis*, a new endophytic species from the coastal grass *Spinifex littoreus* in Taiwan. Botanical Studies 55: 1–6. https://doi.org/10.1186/1999-3110-55-25

Yilmaz N, López-Quintero CA, Vasco-Palacios AM, Frisvad JC, Theelen B, Boekhout T, Samson RA, Houbraken J (2016) Four novel *Talaromyces* species isolated from leaf litter from Colombian Amazon rain forests. Mycological Progress, 15, 1041–1056. https://doi.org/10.1007/s11557-016-1227-3

Zaheer A, Tang C, Yang Y, Zhang J, Zhou S (2024) The changes of microbial diversity and isolation of microorganism in soil for alleviating the production decreasing after continuous cultivation of *Ganoderma lucidum*. Current Microbiology 81(10): 321. https://doi.org/10.1007/s00284-024-03852-0

Zhai MM, Li J, Jiang CX, Shi YP, Di DL, Crews P, Wu QX (2016) The bioactive secondary metabolites from *Talaromyces* species. Natural Products and Bioprospecting 6: 1–24. https://doi.org/10.1007/s13659-015-0081-3

Zhang H, Wei TP, Li LZ, Luo MY, Jia WY, Zeng Y, Jiang YL, Tao GC (2021) Multigene phylogeny, diversity and antimicrobial potential of endophytic Sordariomycetes from *Rosa roxburghii*. Frontiers in Microbiology 12: 755919. https://doi.org/10.3389/fmicb.2021.755919

Zhang JF, Liu JK, Hyde KD, Chen YY, Ran HY, Liu ZY (2023) Ascomycetes from karst landscapes of Guizhou Province, China. Fungal Diversity 122(1): 1–160. https://doi.org/10.1007/s13225-023-00524-5

Zhang L, Wang C, Guo B, Yuan Z, Zhou X (2024) Reproductive strategy response of the fungi *Sarocladium* and the evaluation for remediation under stress of heavy metal

Cd (II). Ecotoxicology and Environmental Safety 271: 115967. https://doi.org/10.1016/j.ecoenv.2024.115967

Zhang ZF, Zhou SY, Eurwilaichitr L, Ingsriswang S, Raza M, Chen Q, Zhao P, Liu F, Cai L (2020) Culturable mycobiota from Karst caves in China II, with descriptions of 33 new species. Fungal Diversity 106: 29–136. https://doi.org/10.1007/s13225-020-00453-7

Zimowska B (2007) New *Phoma* species on *Leonurus cardiaca*. Acta Mycologica 42(1): 119–123. https://doi.org/10.5586/am.2007.012